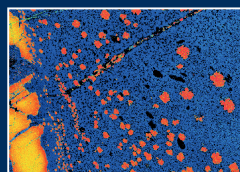# TSK15 Potsdam 2014

15th Symposium on Tectonics, Structural Geology and Geology of Crystalline Rocks
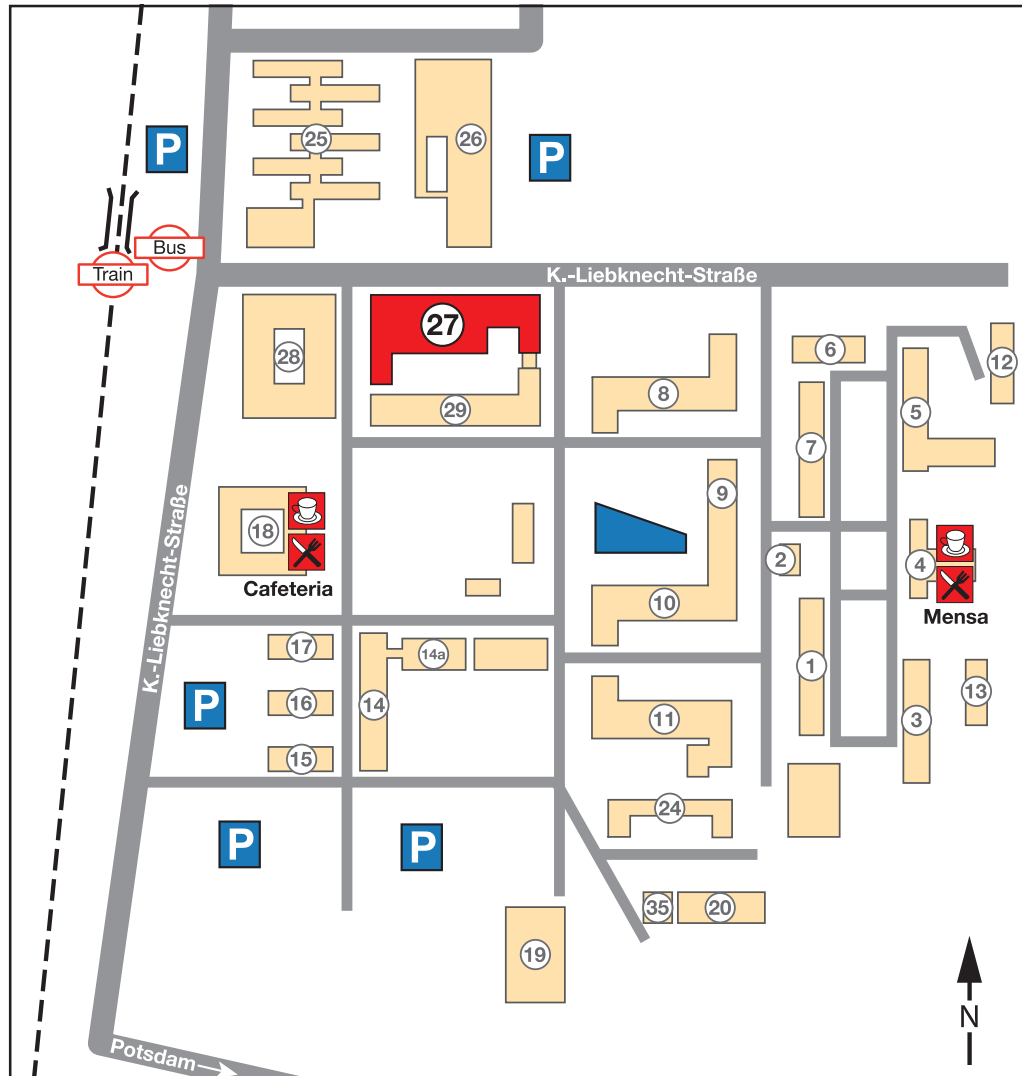
31st March to 4th April

Contact:
apl. Prof. Dr. U. Altenberger
Universität Potsdam
Institut für Erd-und Umweltwissenschaften
Karl-Liebknechtsraße 24-25
14476 Potsdam OT Golm
tsk15-potsdam@geo.uni-potsdam.de

TSK15 - Campus Golm

Universität Potsdam - Institut für Erd- und Umweltwissenschaften
Karl-Liebknecht-Str. 24-25 - Haus 27 - 14476 Potsdam-Golm

P

25
26

P

Bus
Train

K.-Liebknecht-Straße

28
27
29

6
12
8
5
7
9
2
4
Mensa
18
Cafeteria
1
10
3
13
17
14a
16
14
15
11
24
P
P
35
20
19
N

K.-Liebknecht-Straße

Potsdam →

Ice-Breaker - WIS im Bildungsforum
Am Kanal 47 - 14467 Potsdam

Gregor-Mendel-Str.
Weinbergstr.
Jägerallee
Nauener Tor
Holländisches Viertel
Hegelallee
Zentrum
Brandenburger Tor
Gutenbergstr.
Fr.-Ebert-Str.
Str. Bassinplatz
Brandenburger
Charlottenstr.
Platz der Einheit
Am Kanal
Luisenplatz
Berliner Str.
Nuthestr.
Humboldt-brücke
Bildungsforum
Am Neuen Markt
Nikolai-Kirche
Freundschafts-insel
Moschee
Breite Str.
Kiezstr.
Dortustr.
Landtag
Lange Brücke
Potsdam Hauptbahnhof
P+R
Havel
Bahn
Friedrich-Engels-Str.

© terra press 2014
0   250 m

Tram-Linie
Bus-Linie

Cover picture: Aluminum concentration map of a deep crustal pseudotachylyte showing layering of the fossil frictional melt(s). Left and right side represent the less deformed mafic protolith. Orange grains are plagioclase clasts Yellow and blue colours represent layers of different melt compositions: yellow = melt that predominantly originated from feldspars; blue = melt that predominatly originated from pyroxenes and amphiboles. Calabria, Southern Italy. *Photo U. Altenberger, University of Potsdam*

Montag, 31. März 2014
Workshop: **Introduction to thermodynamic modelling (how to build a P-T-e path)**
Workshop: **Experimental deformation**
Workshop: **Neotectonics**

		Dienstag, 1. April 2014
		Workshop: **Geodynamics - at the crossroads between nature and model**
18:00	21:00	**Ice-Breaker** and **registration** in the Bildungsforum, Am Kanal 47 (Platz der Einheit, Westseite)

Mittwoch, 2. April 2014

08:00	09:00	**Registration** in the Foyer of Haus 27 (Institute of Earth and Environmental Sciences)
09:00	09:20	**Introduction** by organizing commitee
09:20	09:40	**Welcome note** by Roland Oberhänsli, President of the International Union of Geological Sciences (IUGS)
09:40	10:00	Stünitz, H., Thust, A., Kilian, R., Heilbronner, R. **H₂O weakening in experimentally deformed quartz single crystals**
10:00	10:20	Walter, J.M., Randau, C., Stipp, M., Leiss, B., Ullemeyer, K., Klein, H., Hansen, B.T., Kuhs, W.F. **Quantifying the Experimental Deformation and Recrystallisation Path at POWTEX Neutron Diffractometer, FRM II Garching, Germany**
10:20	10:40	**Kaffeepause / coffee break**
10:40	11:00	Yilmaz, T.I., Prosser, G., Liotta, D., Kruhl, J.H., Gilg, H.A., Ord, A. **Quartz formation during hydrothermal fluid flow and repeated fragmentation: fluidization, grain growth and deformation structures in the Pfahl shear zone (Germany) and the Rusey fault zone (UK)**
11:00	11:20	Stäb, C., Kruhl, J.H. **Deformation and microfabric development of UHP rocks: Quantification of brittle fabrics and indications for clinopyroxene-quartz phase boundary mobility**
11:20	11:40	Kilian, R. **Dynamic phase distribution in ultramylonites**
11:40	12:00	Keppler, R., Ullemeyer, K., Behrmann, J.H., Stipp, M., Kurzawski, R.M. **Crystallographic preferred orientations and elastic anisotropies of high pressure rocks from the Eclogite Zone of the Tauern Window, Austria**
12:00	12:20	Kenkmann, T., Poelchau, M., Deutsch, A., Thoma, K. **High-speed deformation processes during experimental impact cratering into geological materials – the MEMIN project**
12:20	13:40	**Mittagspause / Lunch break**
13:40	14:20	**Keynote presentation by J.H. Kruhl on** *Old and new work on grain and phase boundaries*
14:20	14:40	Buhl, E., Poelchau, M.H., Dresen, G., Kenkmann, T. **Impact induced deformation bands formed in sandstone**
14:40	15:00	**Kaffeepause / coffee break**
15:00	15:20	Hossain, Md. Sakawat, Kruhl, Jörn H. **Fracture patterns and fragment size distributions as indicators of shock-related brittle deformation**
15:20	15:40	Friedel, C-H. **Tectonic fragmentation in bimrocks – evidence for a tectonic origin of the formerly regarded olistostromes of the Harz Mountains (Germany)**
15:40	16:00	Bestmann, M., Pennacchioni, G. **Effects of recrystallization and strain on Ti re-equilibration in quartz in a cooling pluton**
16:00	18:00	**Poster-Session** mit Bier Wein, Saft, Snacks / **Poster session** with beer, wine, juice, snacks

Donnerstag, 3. April 2014		
09:00	09:40	**Keynote presentation by L. Baumgartner on** *Intrusion mechanisms in the upper crust*
09:40	10:00	Putlitz, B., Seitz, S., Ramirez, C., Baumgartner, L., Müntener, O. **The Chaltén Plutonic Complex (Fitz Roy, Argentina) – igneous evolution, contact-metamorphism and deformation**
10:00	10:20	Seitz, S., Putlitz, B., Baumgartner, L., Bouvier, A-S., Escrig, S., Vennemann, T., Leresche, S., Nescher, P. **Oxygen isotope and Ti diffusion in quartz: constraints from the contact-aureole of the Chaltén Plutonic Complex (Fitz Roy, Patagonia)**
10:20	10:40	**Kaffeepause / coffee break**
10:40	11:00	Ferrero, S., O´Brien, P., Hecht, L., Ziemann, M., Wunder, B. **Occurrence of silicate melt, carbonate-rich melt and fluid during medium pressure anatexis of metapelitic gneisses (Oberpfalz, Bavaria) revealed by melt and fluid inclusions study**
11:00	11:20	Dielforder, A., Herwegh, M., Berger, A. **Fluid flow and mineral vein formation during orogenic accretion of the Infrahelvetic flysch units, eastern Swiss Alps**
11:20	11:40	Halama, R., Konrad-Schmolke, M., Sudo, M., Schmidt, A., De Hoog, J.C.M., Wiedenbeck, M. **Unravelling timing of metamorphism and associated element transfer by combining in situ geochronological ($^{40}Ar/^{39}Ar$) with geochemical and isotopic information in phengitic white mica**
11:40	12:00	Schöbel, S., de Wall, H. **The Northern Deccan Traps - A magnetostraphic and ^{40}Ar-^{39}Ar radiometric correlation of the Malwa traps to the main Deccan LIP sequences**
12:00	12:20	Scheffler, F., Oberhänsli, R., Pourteau, A., Candan, O., Immenhauser, A. **Rosetta Marbles in Anatolia – Evidences for multiple polymorphism in a HP–LT metamorphic unit**
12:20	13:40	**Mittagspause / Lunch break**
13:40	14:20	**Keynote presentation** by **M. Konrad-Schmolcke** and **R. Halama** on *Combined thermodynamic and trace element modelling - using light elements to quantify fluid fluxes in subduction zones*
14:20	14:40	Wilke, F.D.H., O'Brien, P.J., Schmidt, A., Ziemann, M.A. **Petrography, petrology and REE-geochemistry of a coesite-bearing eclogite, Tso Morari, western Himalaya**
14:40	15:00	**Kaffeepause / coffee break** with **poster presentations**
15:00	15:20	Grande, A., Altenberger, U., Prosser, G., Günter, C. **Microstructure and ages of pseudotachylytes from the Serre Massif: gaining information on deep-seated tectonic processes**
15:20	15:40	Altenberger, U., Prosser, G.,Günter, C. **Pseudotachylytes - from upper to lower crust**
15:40	16:00	Duesterhoeft, E., Quinteros, J., Oberhänsli, R., Bousquet, R. **Early-stage subduction dynamics: a combined thermodynamic and geodynamic model**
16:00	18:00	**Sektions-Gründungssitzung (Tektonik – Strukturgeologie)**
19:00 – 22:00		**Abendessen** im Restaurant "Meierei" / **Conference dinner** in the restaurant "Meierei" (Im Neuen Garten 10, Potsdam)

Freitag, 4. April 2014		
09:00	09:40	**Keynote presentation** by **O. Oncken** on *Earthquakes, peninsulas, locking and fluids – what controls plate margins on the human time scale?*
09:40	10:00	Ballato, P., Landgraf, A., Stöckli, D., Ghassemi, M., Strecker, M., Kirby, E. **Variations in erosional efficiency modulate orogenic growth of the Alborz Mountains (N Iran)**
10:00	10:20	Sobel, E., Bande, A., Mikolaichuk, A. **Kinematic link between late Oligocene - Miocene deformation in the Northern Pamir and the Western Tien Shan**
10:20	10:40	**Kaffeepause / coffee break**
10:40	11:00	Stipp, M., Schumann, K., Leiss, B., Behrmann, J.H., Ullemeyer, K. **Tsunamigenic sea-floor breakage and slope destabilization controlled by weak sediment fabrics in the Nankai accretionary prism (SW-Japan)**
11:00	11:20	Zertani, S., Cionoiu, S., Deutsch, C., Evseev, S., Groß, P., Wannek, D., Handy, M., Ustaszewski, K., Giese, J., Le Breton, E. **Structure and kinematics of the Skutari-Pec-Fault in northern Albania**
11:20	11:40	Ruppel, A., Läufer, A., Lisker, F., Jacobs, J., Elburg, M., Damaske, D., Lucka, N. **The Main Shear Zone of Sør Rondane: Implications on the late pan-African structural evolution of Dronning Maud Land, East Antarctica**
11:40	12:00	Minor, A., Bestmann, M., de Wall, H. **Kinematic studies on the late Neoproterozoic Balda-Paladi Shear Zone and associated quartz mineralisation, Sirohi region, NW India**
12:00	12:20	Kurzawski, R.M., Stipp, M., Niemeijer, A., Spiers, C.J., Behrmann, J.H. **Frictional properties of subduction zone input material from the erosive continental margin offshore Costa Rica (IODP expeditions 334 and 344)**
12:20	13:40	**Mittagspause / Lunch break**
13:40	14:20	**Discussion – conclusions; Awards ceremony for best poster presentations; Next TSK meeting**

Teilnehmerliste

Name	Vorname	Institution und Ort
Altenberger	Uwe	Universität Potsdam
Appel	Peter	Universität Kiel
Artel	Julia	Universität Potsdam
Ballato	Paolo	Universität Potsdam
Balling	Philipp	Universität Potsdam
Baumgartner	Lukas	Université de Lausanne, Switzerland
Bestmann	Michel	Universität Erlangen-Nürnberg
Bousquet	Romain	Universität Kiel
Buhl	Elmar	Universität Freiburg / Deutsches GFZ, Potsdam
Bukovská	Zita	Charles University, Prague, Czech Republic
Centrella	Stephen	Universität Münster
Cionoiu	Sebastian	Freie Universität Berlin
Degen	Thomas Johannes	Universität Halle Wittenberg
Dielforder	Armin	Universität Bern, Switzerland
Döhmann	Maximilian	Universität Göttingen
Dresen	Georg	Deutsches GFZ, Potsdam
Düsterhöft	Erik	Universität Kiel
Ferrero	Sivio	Universität Potsdam
Friedel	Carl-Heinz	Leipzig
Friedrich	Andreas	TU Bergakademie Freiberg
Grafulha Morales	Luiz Fernando	Deutsches GFZ, Potsdam
Groß	Philip	Freie Universität Berlin
Günter	Christina	Universität Potsdam
Gürer	Derya	Universiteit Utrecht, The Netherlands
Halama	Ralf	Universität Potsdam
Hallas	Peter	TU Bergakademie Freiberg
Handy	Mark	Freie Universität Berlin
Hartmann	Holger	TU Bergakademie Freiberg
Heine	Timo	Universität Göttingen
Heinrich	Frances Christina	Universität Münster
Hossain	Md. Sakawat	Technische Universität München
Hoymann [Wawrzenitz]	Nicole	Universität Potsdam
Ismayilov	Ayaz	Baku State University, Azerbaijan
Junge	Robert	TU Bergakademie Freiberg
Kenkmann	Thomas	Universität Freiburg
Keppler	Ruth	Universität Kiel
Khan	Jahanzeb	TU Bergakademie Freiberg
Khatri	Sabina	TU Darmstadt
Kienitz	Marina	Universität Potsdam
Kilian	Rüdiger	Universität Basel, Switzerland
Kirsch	Josephine	Freie Universität Berlin
Konrad-Schmolke	Matthias	Universität Potsdam
Krietsch	Hannes	Universität Freiburg
Kruhl	Jörn H.	Technische Universität München
Kuehn	Rebecca	Universität Göttingen
Kurzawski	Robert Marek	GEOMAR Kiel
Le Breton	Eline	Freie Universität Berlin
Leiss	Bernd	Universität Göttingen
Linckens	Jolien	Universität Frankfurt
Löwe	Georg	TU Bergakademie Freiberg
Marti	Sina	Universität Basel, Switzerland
Mertineit	Michael	BGR, Hannover
Minor	Alexander	Universität Erlangen-Nürnberg
Nilius	Nils-Peter	Universität Bonn
Oberhänsli	Roland	Universität Potsdam / IUGS
Obermeyer	Hennes	Karlsruher Institut für Technologie (KIT)

Oncken	Onno	Deutsches GFZ, Potsdam
Ottermann	Thomas	Universität Göttingen
Pohl	Florian	Universität Bonn
Prosser	Giacomo	Università della Basilicata, Potenza, Italy
Putlitz	Benita	Université de Lausanne, Switzerland
Reinhardt	Tom	TU Bergakademie Freiberg
Rembè	Johannes	TU Bergakademie Freiberg
Richter	Bettina	Universität Basel, Switzerland
Roth	Daniel	TU Bergakademie Freiberg
Rudolf	Michael	Universität Freiburg
Ruppel	Antonia	BGR, Hannover / Universität Bremen
Rutte	Daniel	TU Bergakademie Freiberg
Sachwitz	Simon Johannes	Universität Halle Wittenberg
Scharf	Andreas	Freie Universität Berlin
Scharfenberg	Lars	Universität Erlangen-Nürnberg
Scheffler	Franziska	Universität Potsdam
Schmidt	Katharina	Freie Universität Berlin
Schmidt	Maike	Universität Göttingen
Schmidt	Volkmar	Universität Münster
Schnapperelle	Stephan	Universität Halle Wittenberg
Schöbel	Stefan	Universität Erlangen-Nürnberg
Schulze	Torben	Universität Göttingen
Seib	Nadine	RWTH Aachen
Seitz	Susanne	Université de Lausanne, Switzerland
Seybold	Lina Katharina	Universität München
Sobel	Edward	Universität Potsdam
Stäb	Christian	Technische Universität München
Stephan	Tobias	TU Bergakademie Freiberg
Stipp	Michael	GEOMAR Kiel
Stünitz	Holger	University of Tromsø, Norway
Sudo	Masafumi	Universität Potsdam
Swierczynska	Agnieszka	Universität Bochum
Tanner	David Colin	LIAG, Hannover
Teshebaeva	Kanayim	Deutsches GFZ, Potsdam
Thiede	Rasmus C.	Universität Potsdam
Timmerman	Martin Jan	Universität Potsdam
Walter	Jens M.	Universität Göttingen
Wellhäuser	Alexander	Universität Göttingen
Wemmer	Klaus	Universität Göttingen
Wilke	Franziska D.H.	Universität Potsdam / Deutsches GFZ, Potsdam
Witzke	Tim	TU Bergakademie Freiberg
Yilmaz	Tim Ibrahim	Technische Universität München
Zertani	Sascha Heinrich Pablo	Freie Universität Berlin
Ziemann	Martin	Universität Potsdam

Author(s)	Title	Page
Altenberger, U., Prosser, G.,Günter, C.	Pseudotachylytes - from upper to lower crust	12
Artel, J., Altenberger, U., Günter, C., Fernandez Lamus, J.	The formation of the rare earth element mineral parisite in emerald bearing carbonate veins of Muzo/Colombia	12
Ballato, P., Landgraf, A., Stöckli, D., Ghassemi, M., Strecker, M., Kirby, E.	Variations in erosional efficiency modulate orogenic growth of the Alborz Mountains (N Iran)	13
Balling, P., Ballato, P., Dunkl, I., Zeilinger, G., Heidarzadeh, G., Ghasemi, M., Strecker, M.	Deformation styles and exhumation patterns in the Northern Iranian Plateau: An integrated balanced cross sections and low-temperature thermochronology (AHe and ZHe) study	14
Baumgartner, L., Bodner, R., Floess, D., Leuthold, J., Müntener, O., Putlitz, B., Chiaradia, M., Schaltegger, U., Ovtcharova, M.	Comparing intrusion styles of a shallow (Torres del Paine Intrusion) and a mid-crustal intrusion (Western Adamello)	13
Bestmann, M., Pennacchioni, G.	Effects of recrystallization and strain on Ti re-equilibration in quartz in a cooling pluton	14
Braukmüller, N., Hannich, F., Hansen, B.T., Vollbrecht, A., Wemmer, K.	Exceptional younging of glauconite K/Ar and Rb/Sr ages from Ordovician platform carbonates of Öland (SE-Sweden) – evidence for far-field effects of the Caledonian orogeny	15
Buhl, E., Poelchau, M.H., Dresen, G., Kenkmann, T.	Impact induced deformation bands formed in sandstone	16
Bukovská, Z., Jeřábek, P.	Tectonometamorphic record in the cover sequences of the western Tauern Window, Eastern Alps	16
Cionoiu, S., Groß, P., Zertani, S., Handy, M.R., Onuzi, K., Ustaszewski, K.	Changes in style of deformation along the Dinaric-Hellenic chain in northern Albania and southern Montenegro	17
Degen, T.J.	Three high metamorphic events in the western part of the Idefjorden terrane, island Arndorsholmen (South-West Sweden)	18
Dielforder, A., Herwegh, M., Berger, A.	Fluid flow and mineral vein formation during orogenic accretion of the Infrahelvetic flysch units, eastern Swiss Alps	18
Duesterhoeft, E., Quinteros, J., Oberhänsli, R., Bousquet, R.	Early-stage subduction dynamics: a combined thermodynamic and geodynamic model	19
Ferrero, S., O´Brien, P., Hecht, L., Ziemann, M., Wunder, B.	Occurrence of silicate melt, carbonate-rich melt and fluid during medium pressure anatexis of metapelitic gneisses (Oberpfalz, Bavaria) revealed by melt and fluid inclusions study	20
Fiedrich, A., Kraus, K., Appel, P., Stipp, M., Friedel, C-H.	Age of metamorphism and structural development of the Eckergneiss, Harz Mountains	20
Friedel, C-H.	Tectonic fragmentation in bimrocks – evidence for a tectonic origin of the formerly regarded olistostromes of the Harz Mountains (Germany)	21

Grande, A., Altenberger, U., Prosser, G., Günter, C.	Microstructure and ages of pseudotachylytes from the Serre Massif: gaining information on deep-seated tectonic processes	22
Gürer, D., Van Hinsbergen, D., Matenco, L., Kaymakci, N., Corfu, F.	Late Cretaceous to recent tectonic evolution of the Ulukisla Basin (Southern Central Anatolia)	22
Halama, R., Konrad-Schmolke, M., Sudo, M., Schmidt, A., De Hoog, J.C.M., Wiedenbeck, M.	Unravelling timing of metamorphism and associated element transfer by combining in situ geochronological ($^{40}Ar/^{39}Ar$) with geochemical and isotopic information in phengitic white mica	23
Hallas, P., Kroner, U.	Variscan Tectonics in the Erzgebirge of the Saxo-Thuringian Zone: Lateral Extrusion into a Pre-Existing Nappe Pile	23
Heinrich, F.C., Schmidt, V., Hirt, A.M., Leiss, B.	Magnetic anisotropy of salt rocks: A possible tool for deformation analysis?	24
Hossain, Md. Sakawat, Kruhl, Jörn H.	Fracture patterns and fragment size distributions as indicators of shock-related brittle deformation	25
Kenkmann, T., Poelchau, M., Deutsch, A., Thoma, K.	High-speed deformation processes during experimental impact cratering into geological materials – the MEMIN project	25
Keppler, R., Behrmann, J.H., Stipp, M., Ullemeyer, K.	Timing of deformation in the Eclogite Zone of the Tauern Window, Austria: Insights from crystallographic preferred orientations of eclogites and metasediments	26
Keppler, R., Ullemeyer, K., Behrmann, J.H., Stipp, M., Kurzawski, R.M.	Crystallographic preferred orientations and elastic anisotropies of high pressure rocks from the Eclogite Zone of the Tauern Window, Austria	27
Kilian, R.	Dynamic phase distribution in ultramylonites	28
Konrad-Schmolke, M. Halama, R.	Combined thermodynamic and trace element modelling - using light elements to quantify fluid fluxes in subduction zones	28
Kött, A., Altenberger, U., Nesbor, D., Reischmann, T.	Deep drilling «Heubach» provides new insight on the metamorphic history of the Northern Böllstein Odenwald, Hesse	29
Krietsch, H., Rudolf, M., Kenkmann, T.	White light interferometer surface topography analysis of experimental and natural fractures	29
Kruhl, J.H.	Old and new work on grain and phase boundaries	30
Kuehn, R., Leiss, B., Lapp, M., Geissler, L., Friedel, C-H.	Texture development in marble lenses from the Erzgebirge crystalline complex (Germany) in respect to the regional deformation history	31
Kurzawski, R.M., Stipp, M., Niemeijer, A., Spiers, C.J., Behrmann, J.H.	Frictional properties of subduction zone input material from the erosive continental margin offshore Costa Rica (IODP expeditions 334 and 344)	32
Kurzawski, R.M., Stipp, M., Grimmer, J.C., Kontny, A., Behrmann, J.H.	Natural compaction and experimental deformation derived from magnetic fabrics of clayey sediments from the Nankai and Costa Rica trenches	32
Le Breton, E., Handy, M.R.	Kinematic reconstructions of the Western Mediterranean area - a key to understanding the independent motion of the Adriatic microplate	33
Linckens, J., Bruijn, R., Skemer, P.	Dynamic recrystallization and phase mixing in experimentally deformed harzburgite	34
Marti, S., Heilbronner, R., Stünitz, H.	The brittle-viscous transition in mafic fault rocks - an experimental study	34

Mertineit, M., Schramm, M., Hammer, J., Zulauf, G.	The influence of layer thickness on the deformation behavior of anhydrite rocks: Results of microstructural investigations of the Gorleben-Bank (z3OSM) in the Gorleben salt dome, Germany	35
Minor, A., Bestmann, M., de Wall, H.	Kinematic studies on the late Neoproterozoic Balda-Paladi Shear Zone and associated quartz mineralisation, Sirohi region, NW India	36
Morales, L.F.G., Lloyd, G.E., Mainprice, D.	Fabric transitions in quartz: VPSC modeling under constant strain and quantification of preferred orientations	37
Morales, L.F.G., Lloyd, G.E., Mainprice, D.	Fabric transitions in quartz: preferred orientation evolution under simple shear in high strains	37
Morales, L.F.G., Rybacki, E., Naumann, M., Dresen, G.	Shear zone initiation and strain localization due to the presence of heterogeneities in calcite rocks	38
Nilius, N-P., Froitzheim, N., Nagel, T., Tomaschek, F.	The Schwarzhorn Amphibolite (Eastern Rätikon, Austria): an Early Cambrian intrusion in the Lower Austroalpine basement	38
Pohl, F., Froitzheim, N., Tomaschek, F., Nagel, T., Schröder, O.	Permian detachment faulting, syntectonic magmatism and the relation to Alpine thrusting in the Orobic Anticline, southern Alps, Italy	39
Putlitz, B., Seitz, S., Ramirez, C., Baumgartner, L., Müntener, O.	The Chaltén Plutonic Complex (Fitz Roy, Argentina) – igneous evolution, contact-metamorphism and deformation	39
Richter, B., Kilian, R., Stünitz, H., Heilbronner, R.	Microstructural development of quartz gouge at the brittle-to-viscous-transition in shear experiments	40
Ruppel, A., Läufer, A., Lisker, F., Jacobs, J., Elburg, M., Damaske, D., Lucka, N.	The Main Shear Zone of Sør Rondane: Implications on the late pan-African structural evolution of Dronning Maud Land, East Antarctica	41
Rutte, D., Ratschbacher, L., Schneider, S., Stearns, M.A.	Extension controlled exhumation of the Cenozoic Muskol and Shatput Gneiss domes during orogen-wide contraction (Pamir, Tajikistan)	41
Sachwitz, S.J.	Modeling the basal plane of an andesitic magmatic body for prospection and characterization of the underlying Greywacke-Pelite-Series in the open pit Mammendorf (Germany)	42
Scharf, A., Handy, M., Crupi, P.	Configurations of the lithosphere and their expression on the surface – the tectonic evolution of the Namche Barwa Antiform, Tibet	42
Scharfenberg, L.	Use of Mobile devices (smartphones, tablets, GPS devices with data storage function) to facilitate mapping in the field	43
Scheffler, F., Oberhänsli, R., Pourteau, A., Candan, O., Immenhauser, A.	Rosetta Marbles in Anatolia – Evidences for multiple polymorphism in a HP–LT metamorphic unit	43
Schmidt, K., Handy, M.R., Scharf, A., Milke, R., John, T., Oberhänsli, R.	First evidence of subduction-related metamorphism in the most distal European continental margin unit of the Eastern Alps (Modereck Nappe, Tauern Window)	44
Schmidt, M., Friedel, C-H., Leiss, B.	Tektonische Brekzie versus Schlammstromsediment im Variszikum des Westharzes – Gefügeanalysen vom Sparenberg bei Lautenthal	45
Schöbel, S., de Wall, H.	The Northern Deccan Traps - A magnetostraphic and ^{40}Ar-^{39}Ar radiometric correlation of the Malwa traps to the main Deccan LIP sequences	46

Schöbel, S., Zwack, A., de Wall, H.	AMS and NRM – Watch out for interference!	46
Schulze, T., Leiss, B., Techmer, K.	Local texture analysis of 'High-Temperature-Texture-Type' mylonit marbles from the Alpi Apuane, Italy with EBSD – a first approach	47
Seib, N., Voigt, T., Reicherter, K.	Possible expression of seismic shaking in the Miocene-Quaternary sediments of the Ili basin (Kazakhstan)	48
Seitz, S., Putlitz, B., Baumgartner, L., Bouvier, A-S., Escrig, S., Vennemann, T., Leresche, S., Nescher, P.	Oxygen isotope and Ti diffusion in quartz : constraints from the contact-aureole of the Chaltén Plutonic Complex (Fitz Roy, Patagonia)	48
Seybold, L., Kruhl, J.H., Heuss, S., Ord, A.	Large-scale fluid flow and fault zone activity: repeated silicification and fragmentation along the Fountain Range Fault (Mt. Isa Inlier, Australia)	49
Sobel, E., Bande, A., Mikolaichuk, A.	Kinematic link between late Oligocene - Miocene deformation in the Northern Pamir and the Western Tien Shan	50
Stäb, C., Kruhl, J.H.	Deformation and microfabric development of UHP rocks: Quantification of brittle fabrics and indications for clinopyroxene-quartz phase boundary mobility	50
Stephan, T., Kroner, U., Hahn, T., Hallas, P., Heuse, T.	Fold/Cleavage Relationships as Indicator for Sinistral Transpression in the Rheno-Hercynian – Saxo-Thuringian Boundary Zone, Central European Variscides	51
Stipp, M., Schumann, K., Leiss, B., Behrmann, J.H., Ullemeyer, K.	Tsunamigenic sea-floor breakage and slope destabilization controlled by weak sediment fabrics in the Nankai accretionary prism (SW-Japan)	52
Stünitz, H., Thust, A., Kilian, R., Heilbronner, R.	H_2O weakening in experimentally deformed quartz single crystals	53
Sudo, M., Altenberger, U., Günter, C.	In-situ Ar isotope, $^{40}Ar/^{39}Ar$ analysis and mineral chemistry of nosean in the phonolite from Olbrück volcano, East Eifel volcanic field, Germany: Implication for status of excess ^{40}Ar in nosean	53
Tanner, D.C., Krumbholz, M., Hieroymus, C.F., Burchardt, S., Troll, V.R., Friese, N.	Weibull-distributed dyke thickness reflects probabilistic character of host-rock strength	54
Tanner, D.C., Ziesch, J., Beilecke, T., Krawczyk, C.M.	Kinematic analysis of normal faults in an extensional passive margin setting, the Otway Basin, Australia	54
Teshebaeva, K., Sudhaus, H., Echtler, H., Schurr, B., Roessner, S.	Strain-partitioning at the eastern Pamir-Alai revealed through SAR data analysis of the 2008 Nura earthquake	55
Thiede, R., Sobel, E., Ballato, P., Gadoev, M., Oimahmadov, I., Strecker, M.	Uplift and River Incision of the western Pamir Plateau - New insights from river-profile analysis and thermochronology	55
Timmerman, M.J., Sudo, M.	$^{40}Ar/^{39}Ar$ mica cooling ages for the Saxon Granulite Massif and Frankenberg Complex, Germany	56
Walter, J.M., Randau, C., Stipp, M., Leiss, B., Ullemeyer, K., Klein, H., Hansen, B.T., Kuhs, W.F.	Quantifying the Experimental Deformation and Recrystallisation Path at POWTEX Neutron Diffractometer, FRM II Garching, Germany	57

Wannek, D., Groß, P., Cionoiu, S., Deutsch, C., Evseev, S., Zertani, S., Giese, J., Le Breton, E., Handy, M.R., Onuzi, K., Pleuger, J., Ustaszewski, K.	A new 1:10,000 geological map of the Skutari-Pec Fault and surroundings, northern Albania – evidence of orogen-parallel extension	57
Wawrzenitz [Hoymann], N., Krohe, A., Kylander-Clark, A.R.C., Romer, R.L., Rhede, D., Grasemann, B.	Interplay of fluid-rock interaction, deformation mechanisms and the U-Th-Pb system in monazite: dating crustal deformation episodes	58
Wilke, F.D.H., O'Brien, P.J., Schmidt, A., Ziemann, M.A.	Petrography, petrology and REE-geochemistry of a coesite-bearing eclogite, Tso Morari, western Himalaya	58
Yilmaz, T.I., Prosser, G., Liotta, D., Kruhl, J.H., Gilg, H.A., Ord, A.	Quartz formation during hydrothermal fluid flow and repeated fragmentation: fluidization, grain growth and deformation structures in the Pfahl shear zone (Germany) and the Rusey fault zone (UK)	59
Zertani, S., Cionoiu, S., Deutsch, C., Evseev, S., Groß, P., Wannek, D., Handy, M., Ustaszewski, K., Giese, J., Le Breton, E.	Structure and kinematics of the Skutari-Pec-Fault in northern Albania	60

Abstracts

Pseudotachylytes - from upper to lower crust

ALTENBERGER, U.[1], PROSSER, G.[2], GÜNTER, C.[1]

[1] Institut für Erd- und Umweltwissenschaften, Universität Potsdam, Karl-Liebknecht-Str. 24-25, 14476 Potsdam-Golm, uwe@geo.uni-potsdam.de
[2] Dipartimento di Scienze, Università della Basilicata, Via dell'Ateneo Lucano, 10, 85100 Potenza

Pseudotachylytes are the evidence of fossil frictional melts formed by seismic slip, meteoric impacts or large landslides. The present work will show the main distinguishing features of tectonically induced pseudotachylytes in relation to its formation depth. Our results are based on numerous examples of pseudotachylytes produced at different crustal depths, e.g. the Mather Peninsula/Antarctica, Serrre Massif/Calabria, Idefjord Terra/N Sweden, the Ivrea Zone/Italy, Alpine Fault/New Zealand, and the Guajira Complex/Colombia.

One of the best criterions to obtain data on the depth of formation is the stability of minerals, preserved as unmelted clasts and the formation of new minerals. Garnet, biotite and pyroxene play a major role in estimating the depth of frictional melts and therefore the depth of the approximately paleo-hypocenters. Furthermore, the occurrence of amygdules, reactivation fabrics and different types of injection veins as well as the composition of the newly formed melts are typical signatures of the paleo-depth. Compositional layering reveals the sequence of melted minerals and fluid contents. In addition, opaque minerals are indications of the physical and chemical parameters of melt formation and are in some cases diagnostic for the formation depth. Frictional melts from normal crust and subducted crust, show in most parts a similar behavior in respect to fabric evolution. However, melt generated-high-pressure minerals are diagnostic for seismic events in subduction zones.
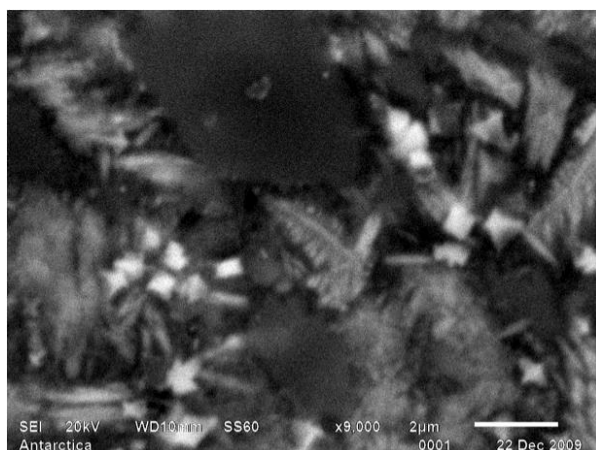
Fig. 1: Typical image of an upper crustal pseudotachylyte formed in a lower crustal rock. Garnet clasts (white) and dentritic growth of biotite. Antarctica. Back-scattered electron image.

The formation of the rare earth element mineral parisite in emerald bearing carbonate veins of Muzo/Colombia

ARTEL, J.[1], ALTENBERGER, U.[1], GÜNTER, C.[1]
FERNANDEZ LAMUS, J.[2]

[1] Institute of Geosciences, University Potsdam, D 14476 Potsdam, Germany, uwe@geo.uni-potsdam.de
[2] Departamento de Geociencias,Universidad Nacional de Colombia, Bogota, Colombia

The emeralds of the eastern Cordillera of Colombia sometimes coexist with the rare earth (REE) mineral pariste $(Ca(Ce,La)_2(CO_3)_3F_2)$. Emerald, parisite, pyrite, albite and other minerals are formed in carbonate-dominated veins from non-magmatic fluids or brines of saline sodium-rich sources. The veins are formed in a strong tectonically controlled environment and are often reactivated by crack and seal vein. The country rocks are low grade metamorphic black shales (chloritoide- and andalusite- bearing) of Cretaceous age. The veins are probably of Tertiary age.

Electron microscopy, electron microprobe as well as REE (rare earth elements) analyses by ICP indicate a complex formation of "single" parisite crystals. The growth started after calcite is formed. Parisites nucleate around calcite until several grains meet at equilibrium angles. This initial growth pattern is followed by a lamellar growth in direction to the c-axes. In BSE images the lamellae show weak but significant differences in brightness. This is probably due to small differences in the REE concentration and in parts due to twinning. However, locally lamellae of bastnaesite, the Ca-free REE fluor-carbonate, occur. The epitaxial growth of baestnesite reveals changing composition of the fluid influx as well as changing physical and chemical parameters. In the lamellar part of parisite stretched or needle shaped calcite inclusions as well as wholes occur (Fig. 1). These may reflect remnants of the calcite fibers formed by "crack and seal" processes.

Whereas sodium, calcium and fluorine mainly originated from evaporite sources, the REE, as well as chromium and vanadium, originate mainly from the
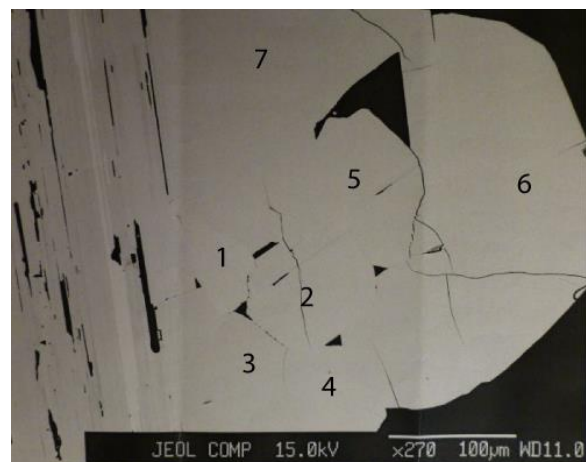

Fig.1: Parisite „single" crystal, c-axes horizontal. Several grains (1-6) with equilibrium angles on the right and lamellar growth to the left. Note the wholes (black) parallel to the lamellae.

neighbouring black shales. Geochemical profiles over the parisite-bearing veins indicate leaching of REE in the black shales near to the veins.

In conclusion, the parisites are formed after the first vein-calcites are formed. Growth started by nucleation of several grains until equilibrium fabrics are reached. The further evolution of parisite is controlled by lamellar growth, syn-to posttectonic to the calcite fibers formed during crack- and seal "dominated widening of the vein(s).

Variations in erosional efficiency modulate orogenic growth of the Alborz Mountains (N Iran)

PAOLO BALLATO[1], ANGELA LANDGRAF[1], DANIEL STOCKLI[2], MOHAMMAD GHASSEMI[3], MANFRED STRECKER[1], ERIC KIRBY[4]

[1] Institut für Erd- und Umweltwissenschaften, Universität Potsdam, 14476 Potsdam, Germany; ballato@geo.uni-potsdam.de
[2] Department of Geological Sciences, Jackson School of Geosciences, Austin, TX 78712, USA;
[3] Research Institute for Earth Sciences, Geological Survey of Iran, Tehran 13185-1494, Iran;
[4] College of Earth, Ocean, and Atmospheric Sciences Oregon State University, Corvallis OR 97331-5503, USA

The recognition that redistribution of mass by erosion governs orogenic evolution has radically changed our perspective on the coupling between climate and mountain building processes. Climate modulates the efficiency of surface processes, which modifies crustal stresses and this is expected to produce the cessation of shortening at the orogenic front, onset of out-of-sequence thrusting, and increased rates of rock -uplift and sediment supply. Unambiguous characterization of these multiple responses through field-based studies, however, has remained challenging.

Here, we show that coordinated changes in the rates and patterns of exhumation and deformation during the development of the Alborz Mountains (N Iran) were driven by abrupt, large magnitude (0.6 to 1.5 km) fluctuations in base level in the adjacent Caspian Sea. We argue that sustained regression of the paleoshoreline from ~6 to 3.2 Ma enhanced erosional efficiency of fluvial systems and increased exhumation within the axial orogenic zone and along the northern range flank which, in turn, drove coordinated retreat of the deformation fronts. When base level rose again at 3.2 Ma, exhumation in the orogen interior slowed and range-bounding faults were reactivated. This led to the progressive establishment of a feedback loop between precipitation and rock uplift rates. These coordinated changes offer compelling evidence that enhanced erosion can indeed trigger a structural reorganization within an actively deforming orogen.

Comparing intrusion styles of a shallow (Torres del Paine Intrusion) and a mid-crustal intrusion (Western Adamello)

LUKAS BAUMGARTNER[1], ROBERT BODNER[1], DAVID FLOESS[1,2], JULIEN LEUTHOLD[3], OTHMAR MÜNTENER[1], BENITA PUTLITZ[1], MASSIMO CHIARADIA[2], URS SCHALTEGGER[2], MARIA OVTCHAROVA[2]

[1] Institute of Earth Sciences, University of Lausanne, Switzerland, lukas.baumgartner@unil.ch
[2] Department of Earth Sciences, University of Geneva, Switzerland
[3] School of Earth Sciences, University of Bristol, England

The Torres del Paine Intrusive Complex belongs to a series of sub-volcanic and plutonic igneous bodies of Miocene age in Patagonia. It is a composite laccolith (1.5-2 km thick, ca. 90k km^3), which intruded in 150 ky into a Cretaceous turbidite sequence with pre-existing kilometer-sized folds. Intrusion depth is ca. 3 km. Three major granite batches accreted from top downwards in 90 ky. The intrusive sequence was established based on crosscutting relationships and TIMS dating of zircons. The magma created space by ballooning the roof, documented by rotated fold axis in the host rocks. Extension in the roof is documented by a myriad of dykes arranged as cone-sheets surrounding the side and the front of the intrusion. The subsequent mafic intrusions underlay the granite laccoliths. It was built from bottom up. Individual mafic pulses intruded into granite mush overlaying the precursor pulse. Granite magma trapped below a pulse attempted to escape upwards in small diapirs and dykes.

The Western Adamello Tonalite in the Italian Alps is an example of a homogeneous tonalite pluton (stock) with at least 200 km^3. The narrow compositional range of these rocks makes it difficult to draw clear boundaries be¬tween units. Nevertheless, some vertical zones of rich in xenoliths, mafic enclaves hornblende-rich cumulates occur. Based on trace element, radiogenic, and stable isotope compositions, along with TIMS ages, we were able to identify 4 major tonalite batches, partly delineated by xenoliths and enclave zones. The pluton was built over 1.2 Ma, roughly 38 Ma ago. The oldest unit is located at the contact with the host rock. It shows a vertical oblate magnetic fabric. Thermal models reveal that a prolonged, pulsed activity is needed in the oldest tonalite to match the observed temperatures in the contact aureole. Hence the first intrusion acted as a feeder zone to either a volcano or a shallow magma chamber. Ductile deformation in the partially molten carbonate host rocks indicate that a (small) part of the space was accommodated was by ballooning. How much space was created by lifting the roof or pushing down the bottom is unknown, since the outcrops are missing.

Emplacement of laccoliths and stocks are in pulses and batches, separated by quiescent times large enough to partially cool the pulses. This prolongs the intrusion time. It allows the rocks to react mechanically to the emplaced magma over a longer time interval. In either case, but definitively in the Paine, pulsing is not governed by the tectonic regime on the emplacement level. In the case of the Paine, magma pressures were high enough to induce deformation of the host rocks of up to several kilometers.

Deformation styles and exhumation patterns in the Northern Iranian Plateau: An integrated balanced cross sections and low-temperature thermochronology (AHe and ZHe) study

PHILIPP BALLING[1], PAOLO BALLATO[1], ISTVÁN DUNKL[2], GEROLD ZEILINGER[1], GHASEM HEIDARZADEH[3], MOHAMMAD GHASEMI[3], MANFRED STRECKER[1]

[1] University of Potsdam, Institute of Earth- and Environmental Science; Balling@uni-potsdam.de
[2] University of Göttingen, Sedimentology & Environmental Geology
[3] Geological Survey of Iran (GSI), Tehran

Located within the Arabia-Eurasia collision zone, the Iranian Plateau forms a NW-SE-striking, elevated, low-relief, arid to semiarid, 40 to 55-km-thick crustal block bounded to the south by the High Zagros Mountains and to the north by the Urumieh Dokhtar Volcanic Zone. GPS data across the plateau suggest low present-day deformation rates in agreement with a very limited seismic activity. The typical basin and range morphology, the high mean elevation of about 2 km, the occurrence of a thickened crust, the exposure of folded and faulted Pre-Cambrian basement rocks and the presence of Oligo-Miocene shallow-water marine deposits within the plateau interior, suggests that a significant fraction of plate convergence must have been accommodated across the plateau during the past 20 million years in association with surface uplift. Unclear remains the exact timing and style of this Late Cenozoic contractional deformation phase and the resulting amount of crustal shortening and thickening occurred in the northern Iranian Plateau during continental collision processes.

To answer these questions we collected structural data across four different mountain ranges at the northern margin of the Iranian Plateau (NW Iran). The northernmost mountain rage (Bozgosh) is E-W oriented, whereas the three other profiles (Tarom, Sultanie, and Mahneshan) are NW-SE striking. Based on surface structural data several forward and backward models were generated with Move (Midland Valley, structural model software) in order to understand the driving mechanism and exhumation patterns of the most recent collisional deformation phase. This structural modeling analysis was combined with a low-temperature thermochronological study (apatite and zircon (U-Th)/He, AHe and ZHe, respectively).

In the northern part of the plateau clastic sediments younger than Cretaceous/Palaeocene(?) were deposited in an angular unconformity onto older deformed rocks, suggesting that contractional deformation predated the Arabia-Eurasia continental collision. This phase of active mountain building was associated with the deposition of red continental conglomerates (Fajan Formation) and occurred before the deposition of a locally up to 4 km thick Eocene volcanic to volcanoclastic sequence (Karaj Formation). Our structural results suggest that this older deformation phase was dominated by thick-skinned tectonics and locally by duplexing through the involvement of basement units. During collision deformation these inherited structures were reactivated, while thin-skinned tectonics occurred through the development of multiple detachment horizons as observed in the Early Miocene evaporites of the continental Upper Red Formation (URF). Fully reset AHe ages at the base of the URF suggest a minimum thickness of this unit of about 3 km. The oldest AHe cooling ages (25-20 Ma) were obtained in the more internal part of the Plateau. This was followed by an outward propagation (to the north and northeast) of the deformation fronts from ca. 12 to 8 Ma. These processes led to the development of a basin and range contractional morphology most likely in association with an outward growth of the Iranian Plateau.

Effects of recrystallization and strain on Ti re-equilibration in quartz in a cooling pluton

MICHEL BESTMANN [1], GIORGIO PENNACCHIONI [2]

[1] GeoZentrum Nordbayern, Friedrich-Alexander-Universität Erlangen-Nürnberg (FAU), Germany; michel.bestmann@fau.de
[2] Dipartimento di Geoscienze, Università di Padova, Padova, Italy

Since a couple of years the trace amount of Ti in quartz (Ti-in-quartz or TitaniQ) has been used to constrain the deformation temperature in quartzitic rocks. Independently of how precise the estimate of deformation temperature could be, a basic question still remains controversial of how effective is dynamic recrystallization to reset the Ti in quartz in mylonites. The study of a heterogeneous ductile shear zone developed during post-magmatic cooling of a titanite-bearing granodiorite allows the effect of strain and recrystallization on Ti re-equilibration in quartz to be
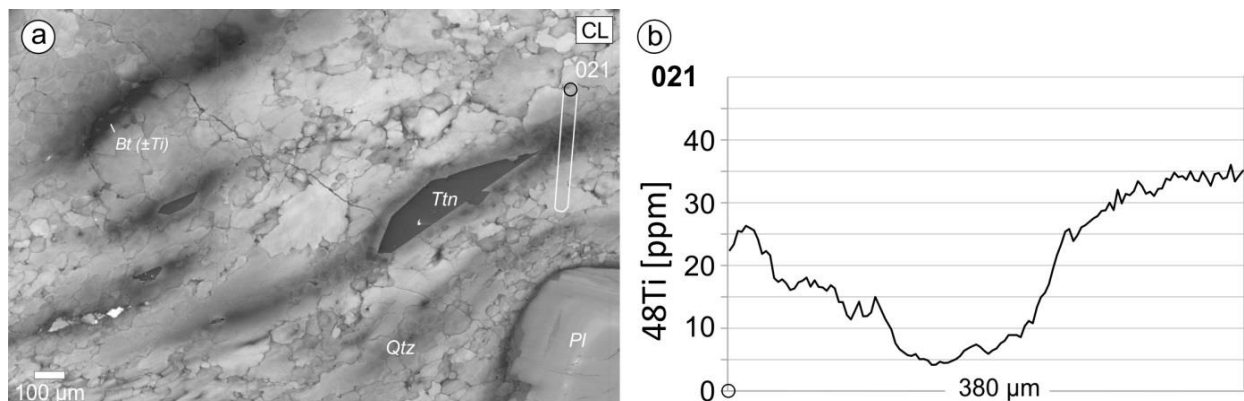
(a) CL image of protomylonite with SIMS profile line. (b) SIMS measurements of Ti in quartz along profile line.

assessed.

The different strain facies show a heterogeneous distribution of Ti content (measured by SIMS) which correlates well with cathodoluminescence (CL) intensity. In the granodiorite protolith CL-bright Ti-rich (20-38 ppm) quartz shows CL-dark Ti-poor haloes (Ti as low as 6-8 ppm) surrounding euhedral titanite. Grain-scale heterogeneities include Ti depleted (CL-darker) grain boundaries (Ti 4-6 ppm). In the protomylonite quartz shows a variable degree of recrystallization associated with strain gradients along S-C foliations anastomosing around feldspar porphyroclasts. Original CL-dark haloes surrounding titanite were passively stretched into the foliation; away from these haloes recrystallized quartz appears mainly bright in CL and retained high Ti contents as in the protolith. Quartz-filled pressure shadows, appended to disrupted feldspar porphyroclasts, show dark CL indicative of very low Ti content (1-3 ppm). In the mylonites and ultramylonites quartz forms totally recrystallized layers that are dominantly dark in CL but show internally a "subtle" CL layering subparallel to foliation reflecting variations of Ti in the range of 3 to 12 ppm. EBSD analysis of quartz indicates that prism <a> was the dominant crystallographic slip system, associated with subgrain formation and subgrain rotation recrystallization, at all stages of deformation. This indicates together with dynamic recrystallization of K-feldspar and plagioclase (Oligoclase: An 16-20%) deformation conditions at ~500 °C.

We conclude that under, the dominant conditions of deformation at ~500°C: (i) Ti content is strongly dependent on microstructure; (ii) high strain and complete recrystallization produced only incomplete homogenization of Ti, (iii) water-assisted synkinematic precipitation of new quartz in pressure shadows dramatically changed the Ti content of quartz to very low values. These observations pose serious limitations to the use of the Ti-in-quartz thermo-barometer to constrain ambient conditions of ductile deformation.

Exceptional younging of glauconite K/Ar and Rb/Sr ages from Ordovician platform carbonates of Öland (SE-Sweden) – evidence for far-field effects of the Caledonian orogeny

Ninja Braukmüller, Felix Hannich, Bent T. Hansen, Axel Vollbrecht, Klaus Wemmer

Geoscience Centre of the Georg-August University of Göttingen, Goldschmidtstr. 3. 37077 Göttingen
ninja.braukmueller@stud.uni-goettingen.de

Glauconite embedded in Lower Ordovician platform carbonates on the island of Öland (Köpingsklint Formation; ca. 480 Ma) were dated with the K/Ar and Rb/Sr method. Glauconites were selected because their radiometric ages usually reflect the time of sedimentation, as they form directly at the sediment-seawater contact. The results for samples from three localities consistently yield Silurian ages between 440 and 420 Ma. It is concluded that this exceptional reset of the original sedimentation/stratigraphic age results from far field effects related to the climax of the Caledonian orogeny. A thermal reset leading to the loss of radiogenic daughter nuclides can be excluded, at least for the Rb/Sr system. Thus, a metasomatic K and Rb influx is considered (Fig. 1). This is indicated by a K-content of the glauconites close to the saturation limit (8.3 wt.%).

A channelized circulation of the related fluid along local fracture zones can be excluded for the largely undisturbed platform sediments on Öland. Presumably, fluid migration occurred through the rock matrix, which is indicated by alteration of primary sparitic calcite cement, as visible from cloudy diffuse cathodoluminescence patterns.
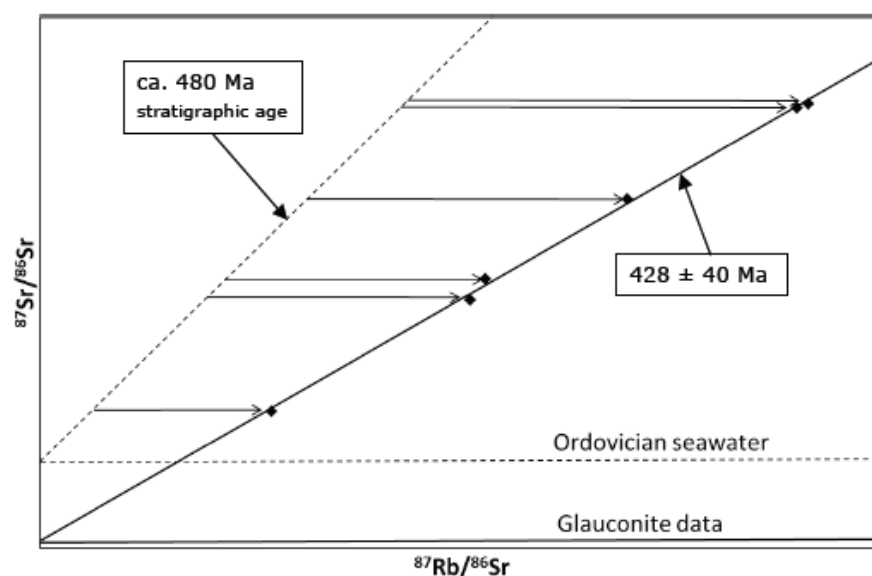
Fig. 1: Schematic shift of data points due to Silurian K-, Rb-metasomatism

Impact induced deformation bands formed in sandstone

ELMAR BUHL[1,2], MICHAEL H. POELCHAU[1], GEORG DRESEN[2], AND THOMAS KENKMANN[1]

[1] Albert-Ludwigs-Universität Freiburg, Germany;
   elmar.buhl@googlemail.com
[2] German Research Center for Geosciences, GFZ, Potsdam, Germany.

Introduction – Deformation bands are common features in tectonically deformed sandstone. In the framework of the MEMIN research network experimental hypervelocity impact experiments into sandstone targets have shown that deformation bands can also be formed under highly dynamic loading conditions.

Methods - Three hypervelocity impact experiments (table) into Seeberger Sandstein have been performed at the Fraunhofer Ernst-Mach-Institute, Freiburg, Germany. They were investigated regarding the influence of water saturation of the target and different projectile sizes on the sub-surface deformation beneath the impact craters. Thin section analysis by means of optical and SEM microscopy was used for mapping of the deformation. The shapes of the localized deformation bands were analyzed by means of digital image analysis (JMicrovision). Aspect ratios and long axes orientations of the deformation bands were analyzed to infer the mechanism of deformation band formation.

Exp.	Water saturation [%]	Impact velocity [km/s]	Projectile size [mm]	Impact energy [J]
A6-5126	0	4.8	2.5	773
A11-5181	~90	5.3	2.5	941
D3-3298	0	4.6	10	42627

Results – Deformation bands have been found in all three experiments. The deformation bands found in experiment A11-5181 (water saturated) are larger but show the same length to width ratio as in experiment A6-5126 (dry). No preferred orientation was found for deformation bands in the wet target experiment. The deformation bands

in the dry target experiments show preferred orientations of their long axes (figure). Comparison of the orientations between experiment A6-5126 and experiment D3-3298 showed that in both cases the deformation bands are developed under shear deformation with an orientation of their long axis at ~ 30° from the maximum principal stress.

Conclusion & Outlook – Deformation bands seem to be a common phenomenon in impact deformed sandstone. Experimental results may help to better understand the development of deformation bands found at natural impact sites (e.g. Upheaval Dome, Utah). Field investigations of deformation band orientations at natural impact sites would be a next step for understanding this phenomenon.

Tectonometamorphic record in the cover sequences of the western Tauern Window, Eastern Alps

ZITA BUKOVSKÁ, PETR JEŘÁBEK

Charles University in Prague, Faculty of Science, Albertov 6, 128 43 Prague 2, Czech Republic; zita.bukovska@natur.cuni.cz

The Tauern Window in the Eastern Alps represent a tectonic window within Austroalpine crystalline nappes. The window is formed by the Venediger (Zentralgneiss) nappe system forming large scale antiformal dome structure with preserved Mesozoic cover sequences. This system is overlain by the Subpenninic nappes (namely Modereck and Wolfendorn nappe and Eclogite zone) distinguished from the rest of the nappes by discrete deformation record. The Subpenninic nappes are overlain by the Penninic nappes represented by the Glockner nappe, Reckner Ophiolitic Complex and Matrei zone. In the studied area, the Venediger duplex is composed of nappes of late Variscan/Permian Tux Gneiss and Zillertal Gneiss with its post-Variscan (Permo-Carboniferous and Mesozoic) cover sequences (Veselá et al., 2011). The Subpenninic nappes in the hanging wall are represented by the Modereck and Wolfendorn nappes which are overlain by the Glockner nappe being part of the Penninic units (Schmid et al., 2013). The nappes alltogether were previously named as Lower Schieferhülle, Upper Schieferhülle and their P-T conditions of up to blueschist facies were described by Selverstone (1988, 1993).

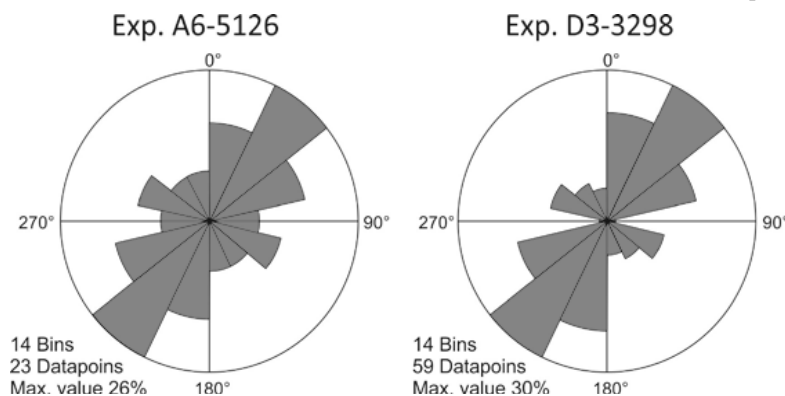Our detailed structural and petrological study focused

Figure: Orientation of the deformation bands mapped for the experiments A6-5126 and D3-3298. 0° is the orientation of the maximum principal stress in the plastic deformation wave.

mainly on the cover sequences represented by the post-Variscan cover and Subpenninic nappes and their tectono-metamorphic evolution with respect to the Central gneiss complexes. The cover sequences consist mainly of schists, amphibolites, marbles and quartzites and they show dominant W to NW-dipping fabric in the western and central parts of studied area and S to SW-dipping fabric in the western part. The observed stretching lineation plunge generally to W. This dominant fabric is subsequently folded by open to tight folds with steep E-W trending axial planes and axes gently plunging to the W. The rocks were later affected by cleavage showing dip-slip kinematics with lineations perpendicular to fold axes. The overlying Glockner nappe (former Upper Schieferhülle) is composed of deformed greenschists, calcschists, micaschists and marbles, which are together folded by large-scale open folds with NW trending fold axes and lineations and steep NW dipping cleavage in fold planes. The metamorphic overprint observed in the cover sequences is characterized by occurence of syn- to post-kinematic garnet with respect to the main foliation. These garnets show decrease in spessartine and sometimes also grossular component, while almandine and pyrope increase towards the rim. The core to rim increase in XMg documents the overall prograde growth of these garnets. The metamorphic PT conditions of garnet growth were estimated using Perple_X computational programs (J.Connolly, ETH Zürich). Garnets show prograde evolution, where core conditions are 470-515°C and 3.6-5.7 kbar and rim conditions 535-570°C and 6.1-7.4 kbar.

The PT conditions are in agreement with structural observation where the E-W stretching in the studied area is presumably associated with burial related to overthrusting of nappes similarly as presented by Jeřábek et al. (2012) from West Carpathians, contrary to previous studies (Selverstone, 1988). The exhumation is than associated with formation of cleavage and dip slip kinematics towards W.

Changes in style of deformation along the Dinaric-Hellenic chain in northern Albania and southern Montenegro

Sebastian Cionoiu[1], Philip Groß[1], Sascha Zertani[1], Mark R. Handy[1], Kujtim Onuzi[2], Kamil Ustaszewski[3]

[1] Freie Universität Berlin, Institut für Geologische Wissenschaften, Malteserstr. 74-100, 12249 Berlin, Germany; .cionoiu@fu-berlin.de
[2] Polytechnic University of Tirana, Institute of GeoSciences, Energy, Water and Environment, Rr. Don Bosko, 60, Tiranë, Albania
[3] Friedrich-Schiller-Universität Jena, Institut für Geowissenschaften, Burgweg 11, 07749 Jena, Germany

Cenozoic Adria-Europe convergence was accommodated by markedly different styles of thrusting and folding along the Dinaric-Hellenic chain as revealed in three cross sections (A, B and C in Fig. 1) located on either side of the Skutari-Pec Fault (SPF). In section A, the Permian to Jurassic layers of the Pre-Karst and High-Karst Units are each about 3 km thick and form laminar thrust sheets overthrusting the Budva-Krasta-Cukali Unit. Section B, in the footwall of the SPF, contains a major top-SW thrust that emplaced the stacked High-Karst and Pre-Karst Units onto tightly folded Cenozoic flysch and Mesozoic pelagic carbonates of the Budva-Krasta-Cukali Unit. We interpret this thrust to be the basal thrust of the High-Karst Unit, which developed a large ramp anticline. We further propose that this High-Karst basal thrust is itself cut by an overlying thrust that emplaced the West Vardar ophiolites of the Shkoder Klippe (Fig. 1) onto the Budva-Krasta-Cukali Unit. The High-Karst basal thrust arches upward and dips ~15° to the N around the Cukali half-window (Fig. 1). The thrust-related folds in this half-window verge to the SW. In section C, south of the SPF, the Pre-Karst and High-Karst Units are missing entirely between the West Vardar Ophiolite above and the Budva-Krasta-Cukali Unit below. This omission extends eastwards into the Peshkopia half-window (Fig. 1).
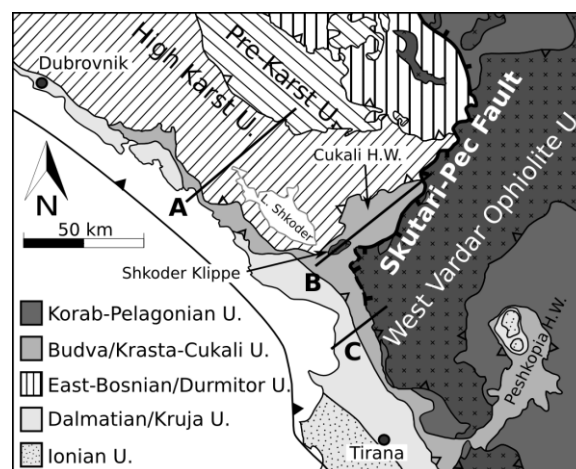

Fig. 1: Map showing positions of transects and main tectonic units, including the proposed continuation of the SPF along the base of the West Vardar Ophiolite. H.W.= half-window; L. = lake (map modified from Schmid et al. 2011).

This prominent along-strike omission probably reflects a combination of Mesozoic paleogeography and Cenozoic tectonics (Zertani et al., this volume). We propose that the occurrence of the West Vardar Ophiolite on the Budva-Krasta-Cukali Unit south of the SPF represents the eroded front of the same thrust system exposed to the north. However, S of the SPF, this thrust system was probably modified by extensional faulting to explain the missing High-Karst and Pre-Karst Units in the Peshkopia half-window. The nature of this extension remains enigmatic; orogen-parallel extension along the SPF and/or orogen-normal extension may have caused this omission (Zertani et al., this volume).

In section A shortening along each of the three main thrusts is about 5 – 15 km, corresponding to a total of about 32 km (50%) shortening for the entire cross section. In section B across the Cukali half-window, the fold-related shortening within the Budva-Krasta-Cukali Unit is about 30 km (50%) and shortening on the High-Karst basal thrust is at least 60 km (100%). In section C, south of the SPF, shortening estimates are complicated by the possibility of extensional reactivation of the basal thrust, as discussed above.

An important conclusion reached here is that the ophiolites of the Shkoder Klippe occur in the footwall of

the SPF and correspond to the West Vardar Ophiolite Unit exposed to the NE..

References:

Schmid, S.M., Bernoulli, D., Fügenschuh, B., Kounov, A., Matenco, L., Oberhänsli, R., Schefer, S., van Hinsbergen, D. & Ustaszewski, K. 2011: Similarities and differences between Alps-Carpathians, Dinarides-Hellenides and Anatolides-Taurides. AGU Fall Meeting 2011, T43E-2425, San Francisco, California, USA

Three high metamorphic events in the western part of the Idefjorden terrane, island Arndorsholmen (South-West Sweden)

THOMAS JOHANNES DEGEN

Martin-Luther-Universität, Germany; thomas.degen@geo.uni-halle.de

Introduction

The small island Arndorsholmen is situated in the northwest of Kungälv, south of Ödsmålsmosse (SW Sweden). It is geological situated in the Stora Le-Marstrand Formation that is a part of the Östfold-Marstrand Belt in the Idefjorden terrane (Ahäll & Connelly 2008). The Stora Le-Marstrand Formation mainly consists of marine clastic sediments, which have been intruded by several suites of magmatic rocks, giving ages of about 1.7 Ga. This succession of rocks was accreted on the Baltic Shield at ca. 1.1 Ga (Ahäll & Connelly 2008). During the collision event different sheets of rocks were stacked up whereas some of them can consist of a "conglomerate" of different formations.

The island Arndorsholmen can be recognized as one of these sheets and it shows an internal tectonic structure that cannot be identified anywhere in the surrounding areas.

Metamorphism and structural evidences

The island is characterized by a vertical shear zone with highly ductile characteristics. It separates the island in a western and an eastern part. Thereby in the western part strongly migmatised meta-sediments can identified, whereas in the eastern part a mixture of coarse crystallized amphibolites, meta-sediment layers as well as layers of amphibolites and pegmatites can be observed. These layers show an isoclinal folding.

Associated with the shear zone is an about 1 m thick mafic intrusion which was strongly sheared at its western margin whereas the eastern boundary seems nearly undeformed. Within the intrusion xenoliths can be identified which consist of isoclinal folded rocks of the eastern side of the shear zone. They show only minor shearing. The mafic intrusion itself is overprinted by amphibolite facies conditions and contains up to 2 cm idiomorphic garnets.

East of the shear zone an isoclinal folded layer of meta-sediment shows an amphibolite layer in its core. Within this structure boudins of neosome layers are included, which formed at the margins of the amphibolites and which have been isoclinal folded before. Furthermore the movement of material can be observed at the fold hinge.

Results and interpretation

The island Arndorsholmen consists of "Granodiorite, gneissic" on the geological map 1:50 000 (SGU 1985). Detailed investigation of the island shows a more complicated structure with at least three tectono-metamorphic events.

Thereby the first event can be identified by the boudinage of neosome layers in the isoclinal fold which indicates a highly ductile overprint (migmatisation/granulite facies, event I). The formation of the isoclinal fold itself as well as the transport of material into the hinge of the fold documents a second highly metamorphic stage at amphibolite facies conditions (event II). The intrusion of the mafic rock, now situated at the shear zone, might have taken place at lower metamorphic conditions. Shearing occurred again at high metamorphic and ductile conditions along the intrusion. The garnets within the mafic rock can be referred to this event (event III).

References:

Ahäll, K.-I. & Connelly, J. N. (2008). Precambrian Research 163, 402–421.
SGU (1985). Ser. Af nr 146, Bergundskartan, 7A Marstrand NO/7B Göteborg NV, Uppsala.

Fluid flow and mineral vein formation during orogenic accretion of the Infrahelvetic flysch units, eastern Swiss Alps

ARMIN DIELFORDER, MARCO HERWEGH, ALFONS BERGER

University of Bern, Switzerland; armin.dielforder@geo.unibe.ch

The Infrahelvetic flysch units represent an accretion-collision assemblage comprising a <5 km thick sequence of carbonaceous shelf sediments and syn-orogenic turbidites, similar to trench-fill sediments formed at ocean-continent subduction zones. The sequence has been interpreted to consist of three thrust slices with different paleogeographic origin (Ultrahelvetic, South Helvetic and North Helvetic) that were originally accreted and thrusted on top of each other during northward propagation of the Alpine orogenic wedge up from middle Eocene time. After accretion, the Infrahelvetic flysch units were intensively deformed during the Oligocene-Miocene Alpine orogeny. The most pronounced feature associated with this deformation phase is the Glarus thrust, a large-scale out-of-sequence thrust that cuts through the Infrahelvetic flysch complex, which places Helvetic nappes on top of the flysch units.

In the past, a number of studies have envisaged fluid flow along the Glarus thrust under peak metamorphic conditions (~300 °C, 2–3 kbar), whereas fluid migration and vein emplacement within the footwall remained mostly unexplored. Based on structural and geochemical data, we propose for the first time a chronology of vein emplacement in the Infrahelvetic flysch units relative to the main Alpine deformation (i.e. folds, cleavage). We suggest that the oldest vein generations evolved already during early orogenic accretion of the thrust slices, i.e. prior to the development of the Glarus thrust. Early fluid flow within weakly consolidated sediments is indicated by (a) soft sediment deformation structures like fluidized sandstone injections, and (b) mineral veins that are generally restricted to clay-rich lithologies. They occur in all three

flysch thrust slices and represent pure calcite veins. Interestingly they comprise veins of different orientations and fracture mechanics: (a) stripped bedding veins that lie subparallel to bedding and were formed by bedding-parallel slip, (b) hybrid extensional shear veins formed at an acute angle to bedding, and (c) extensional veins formed almost perpendicular to the stripped bedding veins. Cross-cutting relationships indicate that all types of veins formed coevally in an incremental manner. In contrast, syntectonic veins related to the main Alpine deformation evolved during extensional fracturing of the host rock and consist of quartz, calcite and minor amounts of ore minerals. The changing mineralogy indicates a change in fluid chemistry during prograde metamorphism compared to the syn-accretionary vein population. Stable isotope data of vein and matrix calcite of all vein generations suggest that the fluid was derived locally from the host rock without or with only little contribution of fluids derived from deeper levels of the subduction channel further downdip. In addition, absolute isotope values vary between different sampling sites indicating that there was no equilibration of the fluid within the thrust slices by pervasive fluid flow. These evidences clearly indicate that fluid liberation and flow was spatially rather restricted.

Early-stage subduction dynamics: a combined thermodynamic and geodynamic model

ERIK DUESTERHOEFT[1,2], JAVIER QUINTEROS[3], ROLAND OBERHÄNSLI[1], ROMAIN BOUSQUET[1,2]

[1]*Institute of Earth and Environmental Science, University of Potsdam, Potsdam, Germany;* eduester@geo.uni-potsdam.de
[2]*Institute of Geosciences, Christian-Albrechts-Universität zu Kiel, Kiel, Germany*
[3]*GFZ - German Research Centre for Geosciences, Potsdam, Germany*

Subduction is primarily driven by the densification of the downgoing oceanic slab, due to dynamic P-T-fields in subduction zones. It is crucial to unravel slab densification induced by metamorphic reactions to understand the influence on plate dynamics. By analyzing the density and metamorphic structure of subduction zones, we may gain knowledge about the driving, metamorphic processes in a subduction zone like the eclogitization, the breakdown of hydrous minerals and the release of fluid or the generation of partial melts.

We have therefore developed the tool THERIAK_D (www.min.uni-kiel.de/~ed/theriakd), which combines thermodynamic equilibrium computations and geodynamic models. Here, we present a 2D subduction zone model that computes the "metamorphic density" of rocks at different time stages. We have used this model to investigate how the hydration, dehydration, partial melting and fractionation processes of rocks all influence the metamorphic density and greatly depend on the temperature field within subduction systems.

The process of eclogitization is assumed as being important to subduction dynamics, based on the very high density (3.6 g/cm3) of eclogitic rocks. The eclogitization in a MORB-type crust is possible only if the rock reaches the garnet phase stability field. This process is primarily temperature driven. Our model demonstrates that the initiation of eclogitization of the slab is not the only significant process that makes the descending slab denser and is responsible for the slab pull force. Indeed, our results show that the densification of the downgoing lithospheric mantle (due to an increase of pressure) starts in the early subduction stage and makes a significant contribution to the slab pull, where eclogitization does not occur. Thus, the lithospheric mantle acts as additional ballast below the sinking slab shortly after the initiation of subduction. Our calculation shows that the dogma of eclogitized basaltic, oceanic crust as the driving force of slab pull is overestimated during the early stage of subduction. These results improve our understanding of the force budget for slab pull during the intial and early stage of subduction. Therefore, the complex metamorphic structure of a slab and mantle wedge has an important impact on the development and dynamics of subduction zones
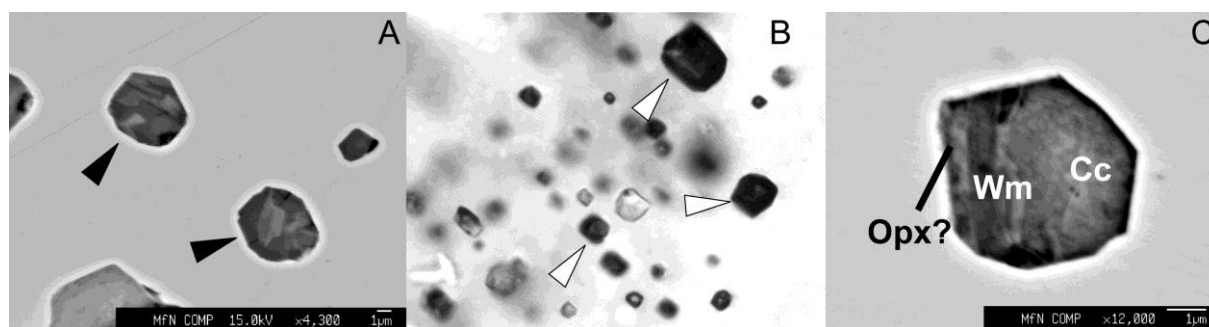
Fig.1 (A) Nanogranites (black arrows); (B) Fluid inclusions (white arrows); (C) Cc-bearing inclusion

Occurrence of silicate melt, carbonate-rich melt and fluid during medium pressure anatexis of metapelitic gneisses (Oberpfalz, Bavaria) revealed by melt and fluid inclusions study

SILVIO FERRERO[1], PATRICK O´BRIEN[1], LUTZ HECHT[2], MARTIN ZIEMANN[1], BERND WUNDER[3]

1 Universität Potsdam, Germany; sferrero@geo.uni-potsdam.de
2 Museum für Naturkunde, Leibniz-Institut für Evolutions- und Biodiversitätsforschung, 10115 Berlin, Deutschland;
3 Helmholtz-Zentrum Potsdam, GFZ, D-14473 Potsdam, Deutschland

In the last decades our understanding of partial melting processes in the lower crust profited from the investigation of fluid inclusions (Touret et al., 2009) and more recently of anatectic melt inclusions (Cesare et al., 2011; Ferrero et al., 2012) within enclaves and high-grade terranes. The latter finding allowed us to directly analyse the original anatectic melt preserved within peritectic phases. The occurrence of primary fluid inclusions (FI) and anatectic melt inclusions (MI) within enclaves allowed the characterization of the COH fluid present during anatexis under fluid+melt immiscibility conditions (Ferrero et al., 2014).

Primary crystallized MI, or "nanogranites", and FI occur as clusters in garnet from stromatic migmatites (Zeilengneise) from Oberpfalz, Eastern Bavaria (Moldanubian Zone). During the late Carboniferous, these Grt+Bt+Sill+Crd+Spl metapelitic gneisses underwent HT/MP metamorphism, followed by a HT/LP event (Tanner & Behrmann, 1995). Nanogranites, ≤ 20 μm in size, consist of Qtz+Bt+Wm+Ab±Ap, and show abundant nanoporosity, localized in the quartz. Fluid inclusions are smaller, generally ≤ 10 μm, and contain $CO_2+N_2+CH_4$ plus siderite, pyrophillite and cristobalite, mineral phases not observed in the surrounding rock or as mineral inclusion in garnet. Polycrystalline inclusions containing Cc+Wm+Opx±Qz, commonly ≤ 10 μm in diameter, occur in the same cluster with MI and FI. Microstructural features, negative-crystal shape and the well-developed crystalline faces of calcite within inclusions suggest that they may result from the crystallization of a carbonate-rich melt. The lack of arrays of carbonate-bearing MI, verified by cathodoluminiscence investigation, supports their primary nature, i.e. they formed during garnet growth. This would suggest the occurrence of a silicate melt, a COHN fluid and a carbonate-rich melt during anatexis at relatively shallow crustal levels. This hypothesis needs to be further

tested through re-homogenization experiments by piston cylinder means.

References:
Cesare, B., Ferrero, S., Salvioli–Mariani, E., Pedron, D. and Cavallo, A. (2009). Geology 37, 627-630.
Ferrero, S., Bartoli, O., Cesare, B., Salvioli Mariani, E., Acosta-Vigil, A., Cavallo, A., Groppo, C. and Battiston, S. (2012). J. Met. Geol. 30, 303-322.
Ferrero, S., Braga, R., Berkesi, M., Cesare, B. and Laridhi Ouazaa, N., 2014. J. Met. Geol. 32, 209-225.
Tanner, D.C. and Behrmann, J.H. (1995). Neues Jahrb. Geol. Palaeontol., Abh. 197, 331-355.
Touret, J.L.R. (2009). Russ. Geol. Geophys. 50, 1052-1062.

Age of metamorphism and structural development of the Eckergneiss, Harz Mountains

ALINA FIEDRICH[1], KATRIN KRAUS[1], PETER APPEL[1], MICHAEL STIPP[2], CARL-HEINZ FRIEDEL[3]

1 Institut für Geowissenschaften, Chrisitian-Albrechts-Universität, 24098 Kiel; pa@min.uni-kiel.de
2 GEOMAR, Helmholtz-Zentrum für Ozeanforschung Kiel, Wischhofstr. 1-3, 24148 Kiel
3 D-04158 Leipzig, Karl-Marx-Str. 56

The Eckergneiss is the only known unit within the Rhenohercynian Zone which is composed of high-grade metamorphic rocks. However, its formation and its tectonic exhumation and emplacement adjacent to the Brocken granite and within the low-grade metamorphic Hercynian country rocks are still under debate. We here present the results of recent studies from the northern part of the Eckergneiss.

The analysis of field structural data show a multiphase deformation history. The main foliation, stretching lineation and isoclinal folding are assigned to the early D_1 deformation phase which probably occurred during an amphibolite facies metamorphism. Grain boundary migration recrystallization microstructures of quartz with large irregular grains and lobate grain boundaries are probably related to D_1. However, these microstructures are largely obliterated by a successive static annealing indicated by fairly isometric grains, straight grain boundaries and 120° triple junctions. Also plagioclase shows similar static recrystallization microstructures and the occurrence of anatectic melts point to granulite facies metamorphic conditions. PT-estimations on garnet gneiss and kinzigite samples indicate metamorphic temperatures and confining pressures above 700°C and 0.4-0.5 GPa. This granulite facies metamorphism must have been reached before the second D_2 deformation phase lead to the development of tight folds and locally a second foliation in

some fold hinges, overprinting the earlier isoclinal folds. These fabrics are omnipresent in the northern part of the Eckergneiss unit. Afterwards, a D_3 deformation phase developed gentle and open folds. The tectonometamorphic record, in combination with the conventional thermobarometry data and reaction textures in pelitic and semipelitic metasediments can tentatively be explained by a clockwise P-T-t path.

Monazite from two samples of the northern part of the Eckergneiss were dated in-situ with the U-Th-total Pb method by using an electron microprobe. The data yield a late Variscan age of 309 ± 5 Ma for a high-grade kinzigitic metapelite and an age of 322 ± 7 Ma for a semipelitic garnet-bearing gneiss. We interpret these ages as the time of granulite facies metamorphism during which monazite crystallized. To our knowledge, these are the first dates that provide direct evidence for a Variscan metamorphism of the Eckergneiss. Although there is a difference of about 13 Ma between the two ages, they are significantly older than the intrusion age of the adjacent Brocken granite, which has an early Permian post-Variscan intrusion history. Hence, it appears to be unlikely that the magmatic intrusion is related to the granulite facies metamorphism of the Eckergneiss unit.

Tectonic fragmentation in bimrocks – evidence for a tectonic origin of the formerly regarded olistostromes of the Harz Mountains (Germany)

CARL-HEINZ FRIEDEL

D-04158 Leipzig, Karl-Marx-Str. 56; chfriedel@gmx.de

About 50 years ago, Reichstein (1965) introduced submarine mass flows (Rutschmassen, olistostromes) into the geology of the Harz Mountains (eastern Rhenohercynian). His idea rapidly found increasing acceptance because it could well explain the occurrence of blocks of different lithology and age in a pelitic matrix. It was further assumed that submarine sliding nappes developed during mass flows. Such slices of intact (coherent) rock bodies were considered as large olistolites.

The typical rock fabrics, commonly described as block-in-matrix fabrics or as bimrocks, occur in more or less strongly foliated rocks of anchizonal metamorphic grade. Therefore the bimrocks of the Harz Mountains were considered as being of sedimentary origin, but overprinted by Variscan deformation (deformed olistostromes).

Structural investigations of several drill cores and outcrops show, that the rock fabric is stronger affected by the Variscan deformation than previously thought. To distinguish tectonic fragmentation from a possible sedimentary, mass-flow related stratal disruption, relationships between block fragmentation and tectonic foliation fabric were established. In order to clarify what causes fragmentation, also coherent units with only incipient bimrock fabrics have been involved in the fabric studies. Timing and cause of fragmentation are considered to be crucial for the interpretation of the origin of bimrocks as a whole.

The most prominent tectonic features associated with fold and trust tectonics are bedding parallel foliation, crenulation cleavage (Schubklüftung), mylonitic fabrics, intrafolial folds and strong mineralization commonly associated with boudinage. This brittle-ductile deformation developed in a depth of more than 15 km (Theye & Friedel 2012). At first glance, some of these features may resemble soft-rock deformation fabrics. Especially, strongly sheared or transposed intrafolial folds could be misinterpreted as slump folds.

The relationship of the block-in-matrix fabrics with the foliation allows distinguishing soft rock deformation from solid state tectonic fabrics. Helpful criteria for a tectonic origin at microscale are:

- rotated tectonic foliation in rotated single blocks
- constant dip of bedding traces from blocks to blocks over larger distance (commonly some of the blocks may be reoriented parallely to the main foliation)
- brecciation and mylonitic fabrics crosscutting the rocks along shear planes
- the strong veining of blocks down to blocks of small grain size, indicating a multiple tectonic boudinage and fragmentation
- mineralized shear planes, folded or stretched veins and veining in intrafolial folds

Some further characteristic features observed are an intensively sheared pelitic matrix, the commonly occurrence of native instead of "exotic" blocks (broken formations), the prefered fragmentation along the margins of hard layers or larger blocks, the occurrence of bimrocks in rocks for which a mass-flow origin can be excluded (sequences of diabase, tuffs and slates, e.g. Stiege beds). All these characteristics indicate a tectonic origin of probably most of the formerly assumed olistostromes in the Harz Mountains (see also Friedel & Zweig 2013). The consequences arising from the structural analysis of the bimrocks concern fundamental geological concepts and the geodynamic modelling of the Harz Mountains.

References:

Reichstein, M. (1965). Geologie, 14, 1039-1076.

Theye, Th. and Friedel, C.-H. (2012). Hall. Jb. Geow., Beiheft, 28, 51-56.

Friedel, C.-H. and Zweig, M. (2013). Hall. Jb. Geow., Beiheft, 31, 1-34.

Microstructure and ages of pseudotachylytes from the Serre Massif: gaining information on deep-seated tectonic processes

ANTONELLA GRANDE[1], UWE ALTENBERGER[2], GIACOMO PROSSER[3], GÜNTER CHRISTINA[2]

[1] CNR-IGG, Area della ricerca di Pisa, Via Giuseppe Moruzzi 1, 56124 Pisa, Italy
[2] Institut für Erd- und Umweltwissenschaften, Universität Potsdam, Karl-Liebknecht-Str. 24-25, 14476 Potsdam-Golm, Germany
[3] Dipartimento di Scienze, Università della Basilicata, via dell'Ateneo Lucano 10, 85100 Potenza, Italy; giacomo.prosser@unibas.it

The Calabria terrane, mostly consisting of Paleozoic basement, represents the upper plate of the NW-dipping subduction of the Tethyan oceanic crust, now preserved within the narrow corridor represented by the Ionian Sea. Within the Paleozoic basement of Calabria, mylonites and pseudotachylytes occur at the base of a 20-25 km thick section of the Hercynian continental crust. The crustal section was emplaced above other minor tectonic units, consisting of medium to low grade metamorphic rocks. The main basal tectonic contact (the Curinga-Girifalco Line), exposed in the Northern sector of the Serre Massif, is interpreted as a thrust, later offset by extensional faulting.

Mylonites and pseudotachylytes form localized and thin (some mm to few cm thick) shear zones within felsic and mafic granulites. In felsic granulites, mylonites show stable biotite and sillimanite on foliation planes and are frequently associated to ultramylonites. Microstructural relationships indicate that pseudotachylyte-bearing faults and injection veins developed along pre-existing weakness zones represented by the mylonitic bands. This is documented by the occurrence of pseudotachylytes within narrow zones characterized by localized dynamic recrystallization of quartz, plagioclase or clinopyroxene or injection veins within pre-existing S-C mylonites. At the μm scale, the presence of disrupted sigma-clasts or S-C microstructures, which appear healed and pervaded by later pseudotachylyte melt, is a further indication of co-seismic slip occurring after a period of steady-state creep.

Several lines of evidence suggest that co-seismic faulting took place in the deeper crust at pressures in excess of 0.85 GPa (about 30 km). The minimum formation depth is constrained by the crystallization of almandine garnet and orthopyroxene in pseodotachylyte melts from felsic and mafic host rocks, respectively. These data appear consistent with thermobarometric estimates of 0.75-0.9 GPa obtained from the main mylonite belt of the Curinga-Girifalco Line.

In situ laser-probe ^{40}Ar–^{39}Ar dating of synkinematic biotite within S-C mylonitic bands yielded ages from 48.06 ± 1.14 to 50.10 ± 1.63 Ma, which indicate an Eocene age for the mylonitic event. On the other hand, ^{40}Ar–^{39}Ar laser step-heating analysis on fault-vein pseudotachylyte matrices gave strongly discordant age spectra with anomalous old ages, which exceed the age of the Hercynian Orogeny; however the distribution of step data in a isochron diagram suggest an early Oligocene age

(30.78 ± 3.45 Ma). These results are consistent with Alpine ages obtained in other sectors of the Calabria terrane.

Summing up, mylonites and pseudotachylytes within granulites of the northern Serre Massif (Calabria) record tectonic processes in the upper plate at the onset of the Tethyan oceanic subduction. Deformation in deep crustal rocks produced strongly localized mylonitic bands, which drove the nucleation of later seismically active faults.

Late Cretaceous to recent tectonic evolution of the Ulukisla Basin (Southern Central Anatolia)

DERYA GÜRER[1], DOUWE VAN HINSBERGEN[1], LIVIU MATENCO[1], NURETDIN KAYMAKCI[2], FERNANDO CORFU[3]

[1] Department of Earth Sciences, Utrecht University, The Netherlands; M.D.Gurer@uu.nl
[2] Department of Geological Engineering, Middle Eastern Technical University, Turkey
[3] Department of Geosciences & Centre for Earth Evolution and Dynamics (CEED), University of Oslo, Norway

Anatolia is located in a complex zone resulting from the collision and subduction of several continental fragments previously separated by strands of the Neotethys Ocean. Around 90 Ma ago the geology of Turkey exhibited (arguably at least) two subduction zones: one dipping below the Pontides in the North, and one dipping below oceanic lithosphere, now found as ophiolites, to the south of the Pontides. Subsequent subduction led to the accretion of (parts of) the following terranes (from N-S and old to young): the Central Anatolian Crystalline complex (85 Ma); the HP-LT Tavsanli (80-75 Ma) and Afyon (70-65 Ma) belts; and the essentially non-metamorphic Tauride fold and thrust belt (Paleocene Eocene). In Central Turkey, continental rocks arrived earliest in the subduction zone below the ophiolites and now form the Central Anatolian Crystalline Complex (CACC). To the east, however, the continental passive margin was farther to the south and there is no evidence that continental rocks arrived in the southern subduction zone before the Late Cretaceous (70-65 Ma). Overlying these accretionary wedges and ophiolites are sedimentary basins, which potentially form a geological archive of the subduction and collision history of the region.

The Late Cretaceous to early Tertiary Ulukisla basin is straddling and sandwiched between the CACC in the north and the Taurides in the south. Our results show that the lower part of the infill was deposited in an E-W extensional basin expressed by large-displacement, listric normal faults. This extension direction was widespread during the late Cretaceous to Paleocene of the CACC, as shown by extensional detachments and sedimentary basins. Subsequently, the infill was folded by N-S compression, thrusted northwards by a back-thrust that cuts the south-vergent Tauride fold-thrust belt, and transported northwards. Compression likely occurred during the deposition of a sequence of continental redbeds and lacustrine sediments found in the southwestern part of the modern basin. We will show results of a preliminary paleomagnetic study that constrains the amount of rotation in the Ulukisla basin. Time constraints for different deformational phases and rotations will be provided based

on field relations and absolute age dating, whereas the amount of deformation is quantified by restored regional cross sections. Integrating structural and sedimentological mapping results with a paleomagnetic and geochronological dataset will allow us to build a kinematic restoration of Central Anatolia back to the Late Cretaceous.

Unravelling timing of metamorphism and associated element transfer by combining in situ geochronological (^{40}Ar/^{39}Ar) with geochemical and isotopic information in phengitic white mica

RALF HALAMA[1], MATTHIAS KONRAD-SCHMOLKE[1], MASAFUMI SUDO[1], ALEXANDER SCHMIDT[1], JAN C.M. DE HOOG[2], MICHAEL WIEDENBECK[3]

[1] *University of Potsdam, Germany; rhalama@geo.uni-potsdam.de*
[2] *University of Edinburgh, UK*
[3] *GFZ German Research Centre for Geosciences, Potsdam, Germany*

Potassic white mica is ideally suited to exploit the recent advances in high spatial resolution analytical techniques because it is amenable to ^{40}Ar/^{39}Ar age dating, provides constraints on P-T conditions, and is an important carrier of fluid-mobile trace elements (Bebout et al., 2007). The combination of in situ ^{40}Ar/^{39}Ar analyses with textural and geochemical data is often critical to understand the geological relevance of ^{40}Ar/^{39}Ar dates (Halama et al., 2014), which might be hampered due to incomplete re-crystallization and loss of daughter and/or parent isotopes by volume diffusion (Bröcker et al., 2013). Here, we attempt to link effects of fluid-rock interaction to ^{40}Ar/^{39}Ar dates by using concentrations and isotopic compositions of boron (B) and lithium (Li) in phengites from partially overprinted rocks from the Western Alpine Sesia-Lanzo zone (SLZ).

Weakly deformed, eclogite-facies samples from the Eclogitic Micaschists (EMS) and greenschist-facies samples from the Gneiss Minuti (GM) contain phengites with compositional differences between cores and overprinted rims (Konrad-Schmolke et al., 2011). Samples from the blueschist-facies Tallorno Shear Zone (TSZ), which separates the EMS from the GM, contain fine-grained, mylonitic phengite. In the weakly deformed EMS samples, inverse isochrons define two core crystallization periods of 88–82 and 77–74 Ma. The younger cores have lower B contents than the older ones, suggesting that loss of B and resetting of the Ar isotopic system were related. Compared to the phengite cores (δ^{11}B = -18 to -10‰), overprinted rims have younger apparent ^{40}Ar/^{39}Ar ages, lower B and Li abundances, and similar δ^{11}B values (-15 to -9‰). These features reflect internal redistribution of B and Li and internal buffering of the B isotopic composition during metasomatism. Mylonitic phengite from the TSZ yields an inverse isochron age of 65.0±3.0 Ma. Almost complete B and Li removal is due to leaching into a fluid. The B isotopic composition is heavier than in phengites from the weakly deformed EMS samples, indicating an external control by a high-δ^{11}B fluid (δ^{11}B = +7 ± 4). Recrystallization of mylonitic phengite is linked to deformation and fluid flow in the TSZ. In the GM unit, phengite cores yield apparent ^{40}Ar/^{39}Ar ages of 58-67 Ma

and δ^{11}B values overlapping with mylonitic phengite from the TSZ, suggesting a close relation to fluid flux in the TSZ. Overprinted rims in the GM unit yield a continuous distribution of younger ^{40}Ar/^{39}Ar ages (58-33 Ma) and lack isotopic and trace elemental changes compared to the cores, reflecting either continuous re-crystallization or the variable influence of a discrete greenschist-facies event that caused incomplete rejuvenation.

In summary, fluid-induced resetting of Ar isotopes in phengitic mica is controlled by deformation and associated fluid flux during exhumation and juxtaposition of two tectonometamorphic segments in the SLZ. Our study underlines the importance of metasomatic processes for interpretation of ^{40}Ar/^{39}Ar data in partially metasomatised rocks.

References:
Bebout, G. et al., 2007, Chem. Geol. 239:284-304.
Bröcker, M. et al., 2013, J. metamorph. Geol. 31:629-646.
Halama, R. et al., 2014, GCA 126:475-494.
Konrad-Schmolke, M. et al., 2011, EPSL 311:287-298.

Variscan Tectonics in the Erzgebirge of the Saxo-Thuringian Zone: Lateral Extrusion into a Pre-Existing Nappe Pile

PETER HALLAS, UWE KRONER

TU Bergakademie Freiberg, Germany; hallas@student.tu-freiberg.de

Prolonged subduction-exhumation processes represent one of the most important tectono-metamorphic features of the Variscan Orogeny in the Late Paleozoic. For these processes the Allochthonous domain of the Saxo-Thuringian zone constitutes one of the key areas of the orogen. Especially in the Erzgebirge, the particular (ultra) high pressure units are sandwiched with medium to low grade metamorphics, and point to different metamorphic peak ages. Although, the generally flat lying main foliation feigns a relatively simple architecture, the complexity of the Allochthonous domain is revealed by the scattering of the mineral stretching lineation with main azimuths in northeast-southwest, east-west, and northwest-southeast directions.

Because of the predominance of a W-E oriented stretching lineation, our structural investigations followed roughly a W-E profile from the Catherine-Reitzenhain gneiss dome of the Central Erzgebirge to the overlying allochthonous units of the Western Erzgebirge / Vogtland. This profile constitutes an almost complete section from the orogenic middle crust to upper crustal levels and is separated by the late Variscan Eibenstock granite.

Here we present field investigations in combination with microstructural analyses of orientated thin sections classifying the particular strain increments. SW-NE oriented stretching axis as the earliest strain increment (D_1) can be observed in all units in the hanging wall as well as in the footwall of the particular occurrences of the UHP gneisses and eclogites. In contrast, the pervasive fabric of the UHP gneisses is characterized by an uniform W-E to (W)NW-(E)SE oriented stretching lineation (regional D_2). Especially in the lowermost part of the profile, i.e. the

medium grade Catharine-Reitzenhain dome structure, both increments can be observed. Here, the orthogneisses exhibit a fabric indicative for an initial tectonic transport top to the SW during D_1 eventually overprinted by WNW directed D_2 shearing. It is important to note that in the westernmost part of the profile, i.e. west of the Eibenstock granite, typical D_2 fabrics are absent. Here, late orogenic NNW-SSE shortening led to the formation of a crenulation cleavage obliterating pervasive D_1 structures.

The observations of this study corroborate a tectonic scenario for the Allochthonous domain of the Saxo-Thuringian zone, comprising three deformation stages. Pervasive SW directed nappe stacking during D_1 is seen as the primary response to the plate convergence during the Variscan orogeny. D_2 tectonics is causally related with the isothermal exhumation of deeply subducted continental crust and the subsequent emplacement into the preexisting nappe stack. Lateral channel flow extrusion is proposed as the underlying cause for the observed architecture in the Erzgebirge reactivating preexisting décollements of the initial nappe pile.

Late Variscan D3 compression is most pronounced in the upper crustal units west of the Eibenstock batholith. Hence the Eibenstock batholiths probably followed a steeply dipping, crustal scale fault zone separating tectonic subdomains west and east of it.

Magnetic anisotropy of salt rocks: A possible tool for deformation analysis?

FRANCES C. HEINRICH[1], VOLKMAR SCHMIDT[1], ANN M. HIRT[2], BERND LEISS[3]

[1] Institut für Geophysik, Westfälische Wilhelms-Universität Münster, D-48149 Münster; volkmar.schmidt@uni-muenster.de
[2] Institut für Geophysik, ETH Zürich, CH-8092 Zürich.
[3] Geowissenschaftliches Zentrum der Georg-August-Universität Göttingen, D-37077 Göttingen.

The anisotropy of magnetic susceptibility (AMS) of rocks is the effect of crystallographic and/or shape preferred orientations of minerals and can give information on the rock fabric development processes (e.g. sedimentation, deformation). As an advantage, the AMS can be measured fast and without laborious sample preparation. The AMS method is not yet established in salt rocks, because pure salt is very weakly magnetic and therefore thought to be ill-suited for AMS studies. The aim of this project is to study the AMS of salt rocks by taking advantage of the refined measurement and analysis methods, which were developed in the last years (Hirt and Almqvist, 2012).

Plastic deformation processes of salt deposits are leading to the crystallographic and/or shape preferred orientations of rock salt and accessories. Especially the rock salt fabric can be modified by thermally controlled recrystallizations (Friedel et al. 2013, Urai and Boland, 1985). Due to the coarse-grained crystalline salt rocks, it is necessary to analyse a large volume as it is possible by AMS-measurements. In some salt rocks there are ferromagnetic and paramagnetic accessory minerals with strong magnetic anisotropies like hematite and clay-minerals, which could produce an AMS when they are aligned. Therefore, AMS measurements could give additional information on the deformation history.

In a first approach, we analyzed 16 samples of the Stassfurt-series and the Leine-series from the salt mine in Sondershausen (Thuringia) and from the Gorleben salt dome (Lower Saxony). The values of the low-field magnetic susceptibility generally increase from white rock salt to red sylvinite. For rock salt, the susceptibility varies from -14E-6 [SI] to -7E-6 [SI] and some samples show a weak anisotropy. The carnallitite samples have susceptibilities from 8E-6 to 98E-6, and some of them are anisotropic. The sylvinite sample has the highest susceptibility of about 200E-6 and is anisotropic. The relatively high values for the susceptibility suggest a significant content of ferromagnetic and paramagnetic minerals. A measurable magnetic anisotropy exists in numerous samples. However, in all samples, even in those samples from presumably strongly deformed regions, the difference between maximum and minimum susceptibility is less than 2E-6, which is very weak compared to other rocks and at the resolution limit of low-field instruments. Therefore, more sensitive high-field torque measurements are carried out. To evaluate the relative influence of these two hematite or clay minerals, XRD measurements of the insoluble residuum have been made. Magnetization experiments showed that high-coercive minerals such as hematite or goethite are the most important ferromagnetic minerals in the samples. In order to interpret the measured susceptibilities and anisotropies correctly, it is important to know the mineralogical composition of the samples and the intrinsic magnetic properties of pure salt minerals. To this end, further microprobe, X-ray diffraction, optical microscopy and chemical analyses will be applied.

References:
Hirt, A.M., and Almqvist, B.S.G. (2012) International Journal of Earth Sciences 101, 613-624.
Friedel, C.-H., Leiss, B., Blanke, H. und Stottmeister, L. (2013) Jb. Mitt. Oberrhein. Geol. Ver., 95, 91-106.
Urai, J.L. und Boland, J.N. (1985) N.Jb. Min.-Monatshefte, 58-72.

Fracture patterns and fragment size distributions as indicators of shock-related brittle deformation

MD. SAKAWAT HOSSAIN[1, 2], JÖRN H. KRUHL[1]

[1] Tectonics and Material Fabrics Section, Faculty of Civil, Geo and Environmental Engineering, Technical University Munich, 80333 Munich, Germany, sakawat.hossain@tum.de
[2] Department of Geological Sciences, Jahangirnagar University, 1342 Dhaka, Bangladesh

Fracture patterns and fragment size distributions (FSD) are parameters frequently used to describe and quantify brittle fabrics of rocks. The Ries meteorite crater represents an excellent example for studying impact fragmentation of thin sedimentary cover and basement rocks. Shock-related brittle deformation is characterized. It includes analyses of large-scale fracture orientations from Malm limestone exposures and quantification of fracture patterns and FSD from boulders and the drill core of the 1973 Ries Research Bore Hole. Fracture orientation analysis leads to two main sets of fractures. Both sets are approximately vertical. One is tangential and the other one radial to the crater centre. Based on the radial fracture set in different outcrops around the crater, the impact centre can be located (Fig.1). Impact-related brittle deformation is observed as far as ca. 71.8 km away from crater centre.

Fractal-geometry-based quantification of fracture patterns in Malm limestone from a vertical N-S section of the Eireiner quarry (Fig. 1) suggests impact-related brittle deformation together with pre-impact, possibly compaction-induced fracturing. These two fragmentation processes are indicated by two different fractal dimensions on two different scales. Map Counting and Mapping of Rock Fabric Anisotropy (Peternell et al., 2011) reveal inhomogeneity and anisotropy of the fracture patterns respectively. Fracture patterns and FSD from boulders, again, follow power laws. This is interpreted as resulting

from nappe formation during crater growth (Chao et al., 1978). Fracture patterns and FSD from core samples show two different fractal dimensions, interpreted as resulting from, first, fragmentation during impact and, second, from shearing and comminution during elastic rebound of the transient crater basement.

References:
Peternell, M., Bitencourt, M.F. and Kruhl, J.H. (2011). J. Struct. Geol. 33, 609-623.
Chao, E.C.T., Schmidt-Kaler, H. and Hüttner, R. (1978). Bayer. Geol. Landes. 84. München..

High-speed deformation processes during experimental impact cratering into geological materials – the MEMIN project

THOMAS KENKMANN[1], MICHAEL POELCHAU[1], ALEX DEUTSCH[2], KLAUS THOMA[3]

[1] Institut für Geo- und Umweltnaturwissenschaften, Univ. Freiburg Germany; thomas.kenkmann@geologie.uni-freiburg.de
[2] Institut für Planetologie, WWU Münster, Germany
[3] Fraunhofer Institut für Kurzzeitdynamik, EMI, Freiburg, Germany

The MEMIN research unit (Multidisciplinary Experimental and Modeling Impact research Network) is focused on performing hyper-velocity impact experiments, analyzing experimental impact craters, and modeling cratering processes in geological materials. The main goal of MEMIN is to comprehensively quantify impact processes. We use two-stage light gas accelerators capable of producing impact craters in the decimeter size-range in solid rocks that allow detailed spatial analysis of petrophysical and structural changes in target rocks.

A total of 24 experiments have been performed at the facilities of the Fraunhofer EMI, Freiburg, so far. Steel, aluminum, and iron meteorite projectiles ranging in
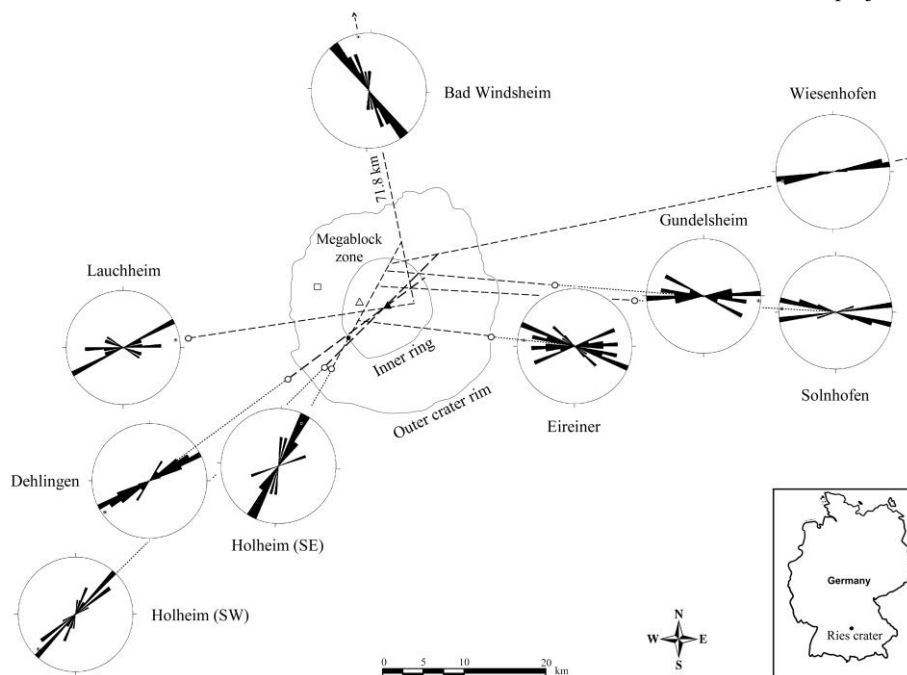

Figure 1: Positions (open circles) and names of the quarries around the Ries impact. Open rectangle and triangle: boulders and drill core locations respectively. Rose diagrams represent the strike directions of prominent radial fractures in each quarry. Broken lines: mean strike of radial fractures in each quarry.

diameter from 2.5 to 12 mm were accelerated to velocities of 2.5 to 7.8 km/s. The solid rock targets chosen to cover a range of porosities included sandstone, quartzite, and tuff that were either dry or saturated with water. In the experimental setup, high speed framing cameras monitored the impact process, ultrasound sensors attached to the target recorded the passage of the shock wave, and special particle catchers positioned opposite of the target surface captured the ejected target and projectile material.

Crater volumes are depended (amongst other parameters like velocity, density and size of the projectile) by the target's strength and porosity. An increase in either value reduces crater size. Saturating pore space with water leads to an increase in crater volume in both tuff and sandstone by reducing the dampening effects of porosity on the shock wave, while keeping the target's strength roughly constant. Depth-diameter ratios are much higher for craters in dry tuff than for those in sandstones or quartzites. The increase in depth-diameter ratios is correlated with decreasing target density and the corresponding increase in target porosity.

A structural analysis of the crater subsurface of dry and water-saturated sandstone targets was carried out on thin-sections. Near the crater surface, areas of pervasive grain crushing and compaction are located that contain tensile fractures sub-parallel to the target surface. The zone of grain crushing is highly subdued in experiments with saturated targets. In the area below, localized bands of intense deformation occur within otherwise intact sandstone. Using image analysis software, the change in porosity with depth was measured. Near the surface, dilatancy is strongly reduced in dry targets and slowly increases with depth. This phenomenon is not visible in water saturated targets, where subsurface pore space remains intact. The damaging of the subsurface of impacted sandstone and quartzite targets was also imaged via ultrasound measurements. Interestingly, reduction of p-wave velocities indicates a much larger volume of damaging than determined by optical and scanning-electron microanalysis of the sandstone targets. Furthermore, the zone of velocity reduction is much less pervasive in quartzite targets than in sandstone targets, possibly due to the quartzite's higher strength.

Based on our data, MEMIN plans to refine numerical models of impact cratering. These models help to quantify and evaluate the processes, ranging from contact to ejection, while experimental data serve as benchmarks to validate the improved numerical models, thus helping to "bridge the gap" between experiments and nature.

Timing of deformation in the Eclogite Zone of the Tauern Window, Austria: Insights from crystallographic preferred orientations of eclogites and metasediments

Ruth Keppler[1], Jan H. Behrmann[2], Michael Stipp[2], Klaus Ullemeyer[1]

[1] Universität Kiel, Christian-Abrechtsplatz 4, D-24118 Kiel
[2] GEOMAR Helmholtz Centre for Ocean Research, Wischhofstr. 1-3, D-24148 Kiel; rkeppler@geomar.de.de

The Eclogite Zone (EZ) of the Tauern Window (Austria) is an exhumed high-pressure unit of the Alpine orogen and offers the possibility to study deformation processes in a paleo-subduction channel. The unit comprises boudins of eclogites within a matrix of paragneisses, micaschists, and metaconglomerates. The EZ was part of the distal European continent to the north of the Penninic ocean. After the Penninic ocean was subducted beneath the Adriatic continent, the EZ entered the subduction channel driven by the negative buoyancy of the downgoing slab, reaching peak conditions of 600°C and 2.0-2.5 GPa in the Oligocene. Despite fast subsequent exhumation within a few million years, only part of the rocks escaped retrogression.

In previous crystallographic preferred orientation (CPO) studies of rocks from the EZ, contrasting conclusions on the deformation processes and their timing were drawn, having either focused on omphacite CPOs in eclogites or on quartz CPOs in metasediments. Furthermore, no regards were paid to retrogressed eclogites, clearly documenting the exhumation. In this study, we analyzed metasedimentary rocks as well as eclogites with different degrees of retrograde deformation using time-of-flight neutron diffraction, which offers the possibility to evaluate the CPOs of all mineral phases simultaneously.

The eclogites exhibit a pronounced omphacite CPO, displaying either S-type, SL-type, or L-type fabrics,
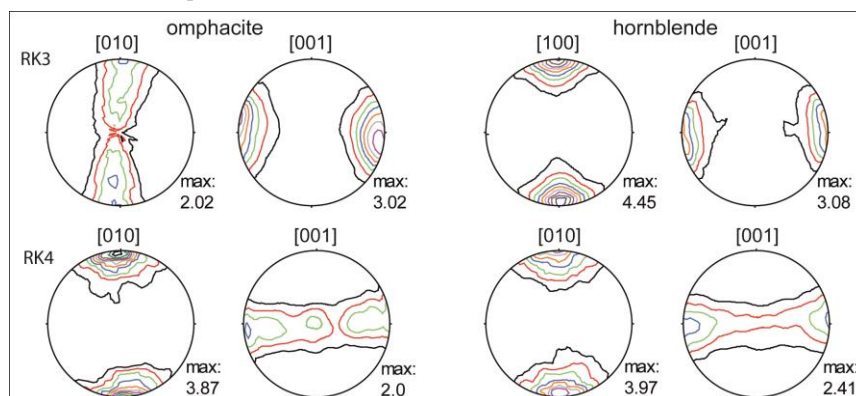

Figure 1: Omphacite and hornblende CPOs of two eclogite samples. Contour lines are multiples of a random distribution. Similar positions of the maxima point to formation of both CPOs during exhumation of the EZ.

whereas transitional SL-type fabrics predominate. In retrogressed samples (8-37 vol.-% hornblende) the hornblende CPO is likewise pronounced and similar to the omphacite CPO regarding location of the (001) maxima (Fig. 1). If quartz approaches a considerable volume fraction in the eclogites (8-15 %), its CPO is weak, but distinct and symmetric with respect to foliation and lineation. On the other hand, the quartz CPO in the metasediments is well-pronounced and asymmetric.

The corresponding maxima of omphacite and retrograde hornblende indicate that both CPOs were generated by deformation during exhumation of the rocks. The strong and asymmetric quartz CPO in the metasediments, which is missing in the eclogites, suggests that deformation of the metasediments was probably stronger and outlasted the deformation in the eclogites. Our results indicate that the CPO-forming deformation processes in the EZ persisted over a long time during exhumation, starting at high-pressure conditions. They completely obliterated the CPOs of earlier prograde deformation.

Crystallographic preferred orientations and elastic anisotropies of high pressure rocks from the Eclogite Zone of the Tauern Window, Austria

Ruth Keppler[1], Klaus Ullemeyer[1], Jan H. Behrmann[2], Michael Stipp[2], Robert M. Kurzawski[2]

[1] Universität Kiel, Christian-Abrechtsplatz 4, D-24118 Kiel
[2] GEOMAR Helmholtz Centre for Ocean Research, Wischhofstr. 1-3, D-24148 Kiel; rkeppler@geomar.de.de

Despite elaborate field investigations of paleo-subduction channels and numerous models on the exhumation of oceanic crust from depths in excess of 70 km, the exact deformation processes within subduction channels are not completely understood. High resolution seismic imaging of their interior is not possible so far, and the lack of crystallographic preferred orientation (CPO) and elastic anisotropy data of subduction channel rocks hampers evaluation of the deformation processes. CPOs of polymineralic rocks, however, are difficult to obtain. In this study, we measured CPOs of a set of subduction channel rocks by means of time-of-flight neutron diffraction, which allows the investigation of large polymineralic samples and the application of full pattern fit methods for the texture evaluation. From the CPOs, P-wave velocity distributions and particular anisotropies were calculated.

The samples were collected in the Eclogite Zone of the Tauern Window, Austria. The Eclogite Zone originally formed during subduction of the Penninic ocean beneath the Adriatic continent in the Tertiary. It comprises metasediments (paragneisses, micaschists, quartzites) enclosing lenses of eclogites, which were exposed to peak PT-conditions of 2.0-2.5 GPa and 600 +/- 30°C, in the Oligocene, and subsequently exhumed within a few million years. Despite fast exhumation, only small rock volumes escaped retrogression and conserved the HP fabric.

In eclogites preserving the high-pressure assemblage Grt + Omph ± Phe ± Qtz ± accessories, the omphacite CPO is pronounced and determines the P-wave velocity anisotropy, leading to small anisotropies of up to 1.5% (Fig. 1). In retrogressed samples, the hornblende CPO usually corresponds to the omphacite CPO and elastic anisotropies are small. However, if the hornblende (001) maximum deviates from the omphacite (001) maximum, higher anisotropies of about 3% are achieved. In the metasediments, the mica always exhibit a strong preferred orientation with the basal plane aligned in the foliation. In some samples, quartz exhibits a strong CPO, but weaker CPOs are also observed. In quartz-rich samples (50-90%) displaying strong preferred orientation of quartz, P-wave velocity anisotropy is determined by quartz. In metasediments, which exhibit a weak quartz CPO, highest velocities are within the foliation plane due to mica. Generally, anisotropies in the metasediments range from 5.2 to 7.4%.

Our results show that retrogression during exhumation frequently modifies elastic anisotropy of eclogites. However, the generally low anisotropy of the eclogites causes only a weak contrast to the surrounding mantle rocks, i.e., they are hard to detect in a seismic experiment. Surrounding metasediments, however, exhibit higher anisotropies and are, therefore, of importance for high resolution imaging of the interior of subduction channels.
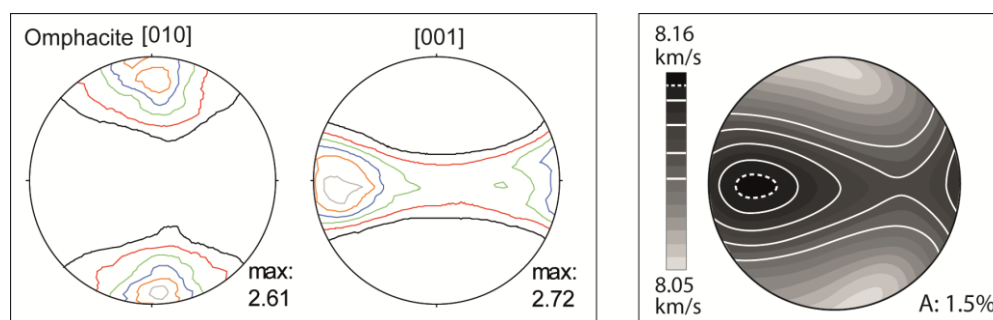

Figure 1: Left: Omphacite CPO of an eclogite. Contour lines are multiples of a random distribution. Right: P-wave velocity anisotropy of the same sample, predicted from the CPOs of all constituent mineral phases.

Dynamic phase distribution in ultramylonites

RÜDIGER KILIAN

University Basel, Switzerland; ruediger.kilian@unibas.ch

High strain zones in the middle and lower crust are often defined by polymineralic ultramylonites. These rocks are characterized by a small grain size, a weak or no crystallographic preferred orientation and an anti-correlated phase distribution of which the latter gives the most revealing insight into the active deformation mechanism, commonly referred to as diffusion creep (s.l.). The distribution of phases can be related to many different processes, including reaction, grain boundary sliding and diffusive or fluid assisted mass transfer. The present study focuses on the phase distribution in an amphibolite facies ultramylonite from a several meters wide shear zone within the Nordmannvik Nappe of the Norwegian Caledonides.

In the shear zone, a granulite facies protolith is transformed to a fine grained matrix of quartz (50%), biotite (20%), white mica (20%), oligoclase (7%) and ilmenite/titanite with grain sizes below 10 µm (eq. diameter). Large grains of garnet, white mica and plagioclase form porphyroclasts. At high matrix proportions white mica and plagioclase porphyroclasts are less abundant.

The matrix shows a strong anti-correlation of phases and a very homogeneous fabric across the whole shear zone. Quartz forms single grains or clusters with a long axis inclined at 30 - 60° to the foliation, antithetically against to the sense of shear. Quartz clusters have a regular spacing of ~30 µm, separated by biotite-stacks and oligoclase. White mica replaces longer biotite stacks and defines the foliation, which is subsequently thinned between foliation-parallel quartz contacts. Concurrently new biotite grows at those quartz grain boundaries, which are oriented at a high angle to the foliation. Only adjacent to porphyroclasts, the matrix homogeneity is disturbed. Biotite and plagioclase are depleted in the compressional sector and grow in the extensional sector. Correspondingly, garnet porphyroclasts have newly grown Ca-rich rims in compressional sectors and signs of dissolution in extensional ones.

Thermodynamic modeling suggests that the modal composition of the matrix and the Ca-rich garnet rims form the stable assemblage. The microstructural positions of the phases can be related to the kinematics of granular flow. The alignment of quartz grains into clusters subparallel to the inferred shortening direction can be compared to the dynamic formation of force chains permitting high and low pressure sites in the matrix. Biotite + oligoclase occupy sites of locally lower pressure and garnet rims + white mica those of higher pressure. It is suggested that a cyclic reaction of garnet + white mica = plagioclase + biotite, driven by dynamically changing, local gradients, causes the distribution of phases by nucleation, growth and mutual replacement during granular flow. Additionally, straining of biotite might contribute to its replacement by white mica.

Combined thermodynamic and trace element modelling - using light elements to quantify fluid fluxes in subduction zones

MATTHIAS KONRAD-SCHMOLKE & RALF HALAMA

Institute of Earth- and Environmental Sciences, University of Potsdam, Karl-Liebknecht Str. 24-25, 14476 Potsdam-Golm, Germany; mkonrad@geo.uni-potsdam.de; rhalama@geo.uni-potsdam.de

Quantitative geochemical modeling is today applied in a variety of geological environments from the petrogenesis of igneous rocks to the oceanic realm. In addition, the development of thermodynamic databases and computer programs to calculate equilibrium phase diagrams have greatly advanced our ability to model geodynamic processes from subduction to orogenesis. Combined with experimental data on elemental partitioning and isotopic fractionation, thermodynamic forward modeling unfolds enormous capacities that are far from exhausted.

The combination of thermodynamic and trace element forward modeling can be used to study and to quantify processes in metamorphic petrology at spatial scales from µm to km. The thermodynamic forward models utilize Gibbs energy minimization to quantify mineralogical changes along a reaction path of a chemically open fluid/rock system. These results are combined with mass balanced trace element calculations to determine the trace element distribution between rock and melt/fluid during the metamorphic evolution. Thus, effects of mineral reactions, fluid-rock interaction and element transport in metamorphic rocks on the trace element and isotopic composition of minerals, rocks and percolating fluids or melts can be predicted.

Here we illustrate the capacities of combined thermodynamic-geochemical modeling based on two examples relevant to mass transfer in subduction zones. The first example focuses on fluid-rock interaction in and around a blueschist-facies shear zone in felsic gneisses, where fluid-induced mineral reactions and their effects on boron (B) concentrations and isotopic compositions in white mica are modeled. In the second example, fluid release from a subducted slab and associated transport of B and variations in B concentrations and isotopic compositions in liberated fluids and residual rocks are modeled. We compare the modeled results of both examples to geochemical data of natural minerals and rocks and demonstrate that the combination of thermodynamic and geochemical models enables quantification of metamorphic processes and insights into element cycling that would have been unattainable if only one model approach was chosen.

Deep drilling «Heubach» provides new insight on the metamorphic history of the Northern Böllstein Odenwald, Hesse

ANNE KÖTT[1], UWE ALTENBERGER[2], DIETER NESBOR[1] & THOMAS REISCHMANN[1]

[1] Hessisches Landesamt für Umwelt und Geologie, Rheingaustr. 186, 65203 Wiesbaden, Germany, anne.koett@hlug.hessen.de

[2] Institute of Earth- and Environmental Sciences, University of Potsdam, Karl-Liebknecht Str. 24-25, 14476 Potsdam-Golm, Germany; altenber@uni-potsdam.de

In a pilot study for testing the feasibility of the crystalline basement of the Odenwald region for deep geothermal energy a borehole was deepened to 775 m depth. This drilling provided new information on the structure and composition of the basement, and gave access to unique rock material for detailed investigation of the metamorphic history of this part of the basement.

The drilling site at Heubach/Groß-Umstadt is located in the northeastern part of the Böllstein Odenwald, which is a part of the Mid-German Crystalline Rise. The Otzberg fault zone separates the Böllstein from the Bergsträßer Odenwald to the west, whose structural, chemical, magmatic and metamorphic history is different (summary in STEIN 2001). The Böllstein Odenwald, however, is a metamorphic complex forming a large NNE-SSW striking anticline. The central part of this anticline is built up by granitoid gneisses. These are surrounded by a metamorphosed volcano-sedimentary unit, which is a relic of a pre-Variscan accretionary prism.

The samples from the borehole comprise mainly biotite gneisses of tonalitic and granodioritic composition and hornblende gneisses, some of which are garnet-bearing. Minor rock types are amphibolites, mica-schists, metacarbonates, and quartzites. The geochemical composition of the igneous rocks, especially the Nb and Y concentrations, reveals similarities to volcanic arc granites and subordinate collision granites indicating an active margin environment. The core samples are characterized by metamorphic layering, a pervasive schistosity and augengneiss textures in places. Locally, the rocks show evidence of partial melting. Strain is heterogenously distributed and concentrated in mylonitic zones. Hornblende, plagioclase and K-feldspar recrystallized dynamically. In places, quartz with chessboard subgrain texture occurs, indicating temperatures higher than 700°C at pressure about 0.7 GPa. Hence, the mineral assemblages and fabrics demonstrate that the metamorphic event took place under medium pressure – high temperature conditions of higher amphibolite to lower granulite facies.

Analyses of garnet-bearing samples by classic thermometry obtained temperatures of 600°C-705°C and retrograde and post-kinematic re-equilibration at 550-670°C. Thermobarometric studies on hornblende-bearing samples report similar conditions (680-740 °C, 0.55-0.75 GPa). Thermodynamic modelling of garnet-sillimanite bearing gneisses from the nearby Wiebelsbach indicates even higher temperatures (760-800°C and retrograde 700-740 °C). The uplift through greenschist facies conditions is documented by the formation of chlorite, actinolite, and albite.

These results confirm investigations of WILLNER et al. (1991) who reported granulite facies metamorphism for a kyanite-garnet-bearing assemblage in the Böllstein Odenwald (763-805°C, 0.78-0.86 GPa). The established clockwise PT-path indicates that the gneisses of the Heubach region reached lower crustal depth, probably during an early Variscan stage and rose to mid crustal level during the main Variscan phase at the end of the lower Carboniferous. The most likely scenario is an evolution in a syn- to postcollisional setting probably in a convergent geodynamic system.

References:
STEIN, E. (2001): Mineral. Petrol., 72, 7-28.
WILLNER, A.P., et al. (1991): Geol. Rundsch., 80, 369-389.

White light interferometer surface topography analysis of experimental and natural fractures

HANNES KRIETSCH, MICHAEL RUDOLF AND THOMAS KENKMANN

Institute of Earth and Environmental Sciences, Geology, Albert-Ludwigs-Universität Freiburg, Albertstraße 23-B, D-79104 Freiburg

The surface characteristics of fractures reveal insights into the structural and geomechanical development of artificially and naturally generated fracture zones. With the application of white light interferometry (WLI) we started to quantify fracture topographies at the sub-micrometer scale, and relate the obtained digital surface models to experimental parameters during deformation. This study is aimed at proving possible interrelations between fracture topographies and mechanical parameters such as the applied stress, the confining pressure, strain and total displacement.

The lithologies used for the experiments are Malsburg granite, Buntsandstein and Muschelkalk. All originate from
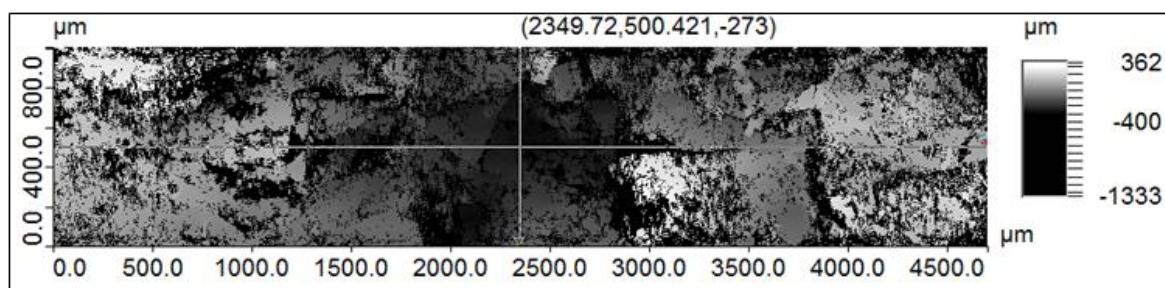

Figure 1: Scan of a granite fracture surface with an area of approx. 4.6 x 1 mm, threshold of 2, overlap of 40%, grains with sharp escarpments (indicated by black linear areas) and different heights due to material contrasts are visible.

the Upper Rhine Rift Valley. The samples are deformed in the triaxial loading frame FORM+TEST Alpha 2-3000 S. Experiments with sample dimensions of 42 x 84 mm reach maximum conditions of $\sigma_1 = 900$ MPa and $\sigma_3 = 150$ MPa at a temperature of up to 200°C. We systematically load the cylindrical samples at various confining pressures (0-150 MPa) until failure occurs to obtain a Mohr-Coulomb failure envelope. The fractures are characterized macroscopically by means of the length, width, displacement and orientation to the sample axis. In addition to the experimental generation of fault zones we determine the elastic parameters of the lithologies.

The deformed samples are then disassembled and the fracture surface topography is determined with the white light-interferometer BRUKER Contour GT-KO. White light interferometers are typically used for the characterization of very smooth to moderately structured technical surfaces like laser engraved surfaces or microchips. The interferometer uses a white light beam which is split into a reference and an analysis beam. The analysis beam is directed onto the sample. The reference beam is superimposed by the reflected light from the sample. The resulting interference allows determining the surface heights of the sample in a certain area with a precision in the order of a nanometer. Additionally a statistical surface analysis is done including parameters like surface height distribution and surface roughness. The minimum scanning area consists of rectangular approx. 1.2 x 1 mm in size. Stitching measurements are performed with an overlap of up to 50 % and allows to cover fracture areas of >1 cm^2. The surface is analyzed with respect to its roughness which will be correlated to the deformation conditions.

The scan of a granite sample is shown in figure 1. The black dots in the scan are errors due to regions with less reflective properties or a too steep inclination. We are currently improving our methodology to better resolve local asperities on fracture surfaces.
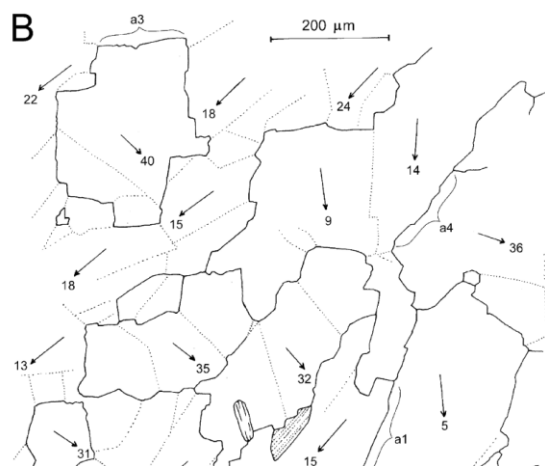
Old and new work on grain and phase boundaries

JÖRN H. KRUHL

Tectonics and Material Fabrics Section, Technical University Munich, D-80333 Munich, Germany; kruhl@tum.de

Classical polarized light and universal-stage microscropy and the recently developed FIB technique, combined with TEM studies, provide useful information about the nature of grain and phase boundaries, their importance for deformation and metamorphism, and their effect on physical properties of rocks. In metamorphic and syntectonic magmatic rocks sutured grain boundaries are common, as a result of strain-induced grain-boundary migration and stabilisation of facets in preferred crystallographic orientations (Fig.1). Although these orientations and the geometry of the sutured boundaries are affected by various parameters, such as deformation intensity, they mainly reflect temperature at the end of deformation and, under certain conditions, allow relating deformation events to temperature development. In addition, the crystallographic control on grain-boundary facets governs grain coarsening after deformation, which may also serve as a fabric-related geothermometer.

Transmission electron microscopy shows that grain and phase boundaries of various rock-forming minerals (calcite, quartz, plagioclase, K-feldspar, amphibole, pyroxene) from magmatic and metamorphic rocks (basalt, syenite, quartzite, marble, metagabbro, eclogite) are partially open up to several hundred nanometres and form a connected network that serves as pathway for fluids. The data are in agreement with cooling-related anisotropic volume reduction below the diffusion thresholds of the different minerals, which is not totally compensated by decompression-induced anisotropic volume expansion. The voids are partially filled with newly grown quartz, biotite, chlorite or amphibole (Fig.2), indicating the presence of open grain and phase boundaries already at deeper crustal levels, with consequences for porosity, fluid flow, reactivity and elasticity of the rocks. In addition, open grain and phase boundaries most probably play an important part for weathering and alteration of building/ornamental stones

Fig. 1: Recrystallized quartz grains with c-axis orientations (arrows) and facetted boundaries. Circle segment: crystallo-graphic orientations of facets. After Kruhl & Peternell (2002) and Kuntcheva et al. (2006).
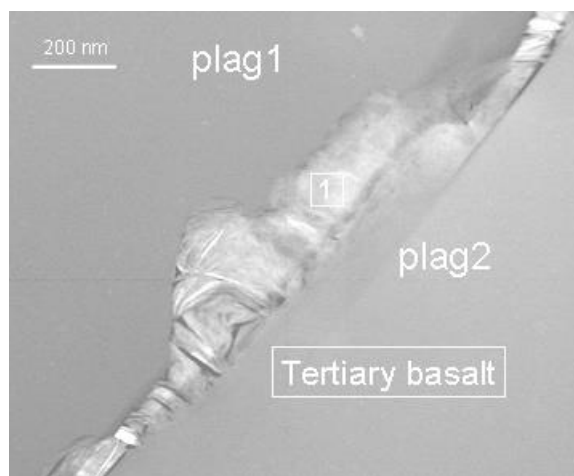

Fig. 2: TEM image of an open plagioclase grain boundary and cavity, filled with chlorite. Kruhl et al. (2013) and unpublished data).

and concrete and should be also considered in technical applications

References:

Kruhl, J.H., Peternell, M., 2002. Journal of Structural Geology 24, 1125-1137.

Kuntcheva, B.T., Kruhl, J.H., Kunze, K., 2006. Tectonophysics 421, 331-346.

Kruhl, J.H., Wirth, R., Morales, L.F.G., 2013. Journal of Geophysical Research Solid Earth 118, 1-11.

Texture development in marble lenses from the Erzgebirge crystalline complex (Germany) in respect to the regional deformation history

Rebecca Kuehn[1], Bernd Leiss[1], Manuel Lapp[2], Lutz Geissler[3], Carl-Heinz Friedel[4]

[1] *Geowissenschaftliches Zentrum, Georg-August-Universität Göttingen, D-37077 Göttingen; rebeccakuehn@gmx.de*
[2] *Sächsisches Landesamt für Umwelt, Landwirtschaft und Geologie, D-09599 Freiberg*
[3] *GEOMIN – Erzgebirgische Kalkwerke GmbH, D-09514 Lengefeld*
[4] *Karl-Marx-Str. 56, D-04158 Leipzig*

Texture (crystallographic preferred orientation) analyses of samples from deformed marble lenses at 100 m scale from the Erzgebirge crystalline complex in Germany shall reveal new constraints on the texture development of calcite rocks and the deformation history of the Erzgebirge. The Erzgebirge crystalline complex is a Variscan nappe stack of a discontinuous series of high to low grade metamorphic rocks. The intercalated marble lenses are suitable material for methodical texture studies due to their monomineralic composition and the geometrically well-defined - and in underground mining galleries well exposed - fold structures. Especially for the investigation of fold-related texture development, the marble lenses represent relatively simple systems, which is important in view of open questions on the parameters for the development of the different texture types in naturally deformed calcite rocks (e.g. Leiss & Molli 2003) compared to experimentally, deformed carbonatic rocks (e.g. Pieri et al. 2001).

For 16 marble samples originating from Hermsdorf (E-Erzgebirge) and Hammerunterwiesenthal (W-Erzgebirge), X-ray and neutron texture analysis as well as microstructural analyses by hot cathodoluminescence microscopy and grain parameter analyses have been performed.

While samples from Hammerunterwiesenthal, a folded complex of calcite and dolomite marbles, do all show the same texture type of a single c-axes maximum, samples from Hermsdorf, a complex of five horizontally arranged layers of calcite and dolomite marble intercalated with phyllitic rocks, show different texture types in the two sampled horizons. The lower one of the two horizons shows the single c-axes maximum as well, while the upper horizon shows an intermediate type between single c-axes maximum and a girdle distribution. In contrast to the differences of the texture types, the results from both localities are consistent regarding the fact that textures in folded parts of the marble lenses were passively rotated during folding (Kuehn 2013). The microstructure in the Hammerunterwiesenthal samples varies between coarse grained (~1mm) equigranular domains, core-mantle structures, coarse (~1 mm) and fine grained (0,1–0,3 mm) layers as well as fine grained (0,1–0,3 mm) equigranular domains. In opposition to this, the microstructure of the Hermsdorf samples is fine grained (0,1–0,4 mm) and equigranular. Samples from both sites can contain mica, chlorite and quartz as accessories. Multiple carbonate generations are visualized by cathodoluminescence microscopy indicating high fluid-controlled grain boundary mobility.

Passive rotation of textures at both localities suggests a two-phase kinematic development of texture and microstructure, with texture development in a shear zone, possibly during nappe stacking and uplift and later a folding process which did not influence the texture. This conclusion fits well to the actual model (Kroner et al. 2007) of the Erzgebirge evolution history. Texture preservation during folding was possible because fluid-controlled grain boundary mobility was the dominant deformation mechanism and not intracrystalline slip.

Different texture types in the sampled layers of the Hermsdorf marbles indicate different kinematic conditions during nappe stacking and uplift.

References:

Kroner, U. et al (2007) in Linnemann, U. et al (Eds.) Geol.Soc.Am.Spec.Pap. 423, 153-172.

Kuehn, R. (2013) Master thesis, Universität Göttingen.

Leiss, B. and Molli, G. (2003) J.Struct.Geol. 25, 649-658.

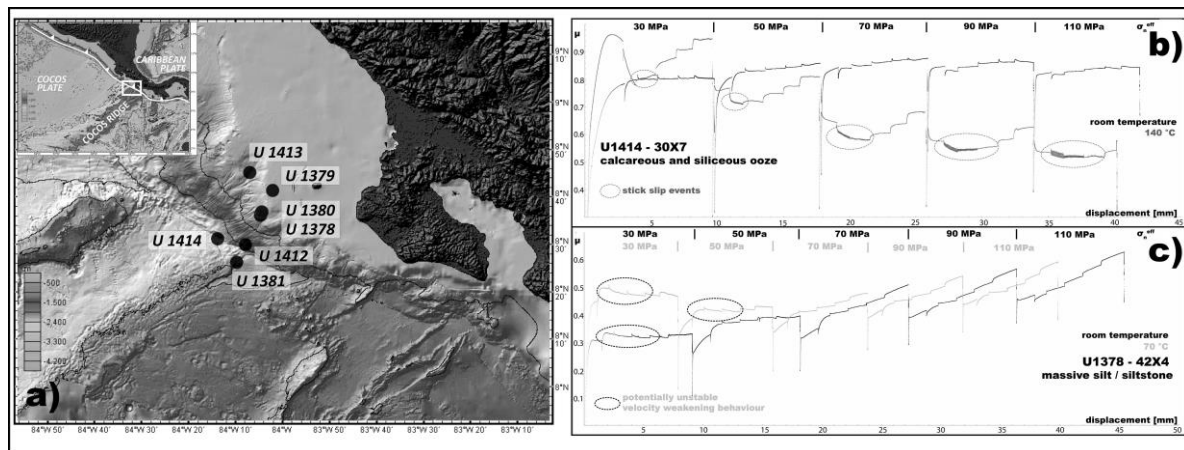Pieri, M.et al (2001) Tectonophysics 330, 119-140.

Fig. 1: (a) Bathymetric map of the CRISP area offshore Osa Peninsula with indicated drilling sites and tectonic overview inset map. (b,c) Evolution of friction with shear displacement during velocity-stepping experiments at different temperatures on (b) calcareous ooze from the incoming plate (IODP site U1414) and (c) clayey silt from the upper plate (U1378). At each applied effective normal stress velocity is stepped in the following order: 10-1-3-10-30-100 µm/s.

Frictional properties of subduction zone input material from the erosive continental margin offshore Costa Rica (IODP expeditions 334 and 344)

Robert M. Kurzawski[1], Michael Stipp[1], André Niemeijer[2], Christopher J. Spiers[2], Jan H. Behrmann[1]

[1] Department of Marine Geodynamics, GEOMAR Helmholtz Centre for Ocean Research, Wischhofstr. 1-3, D-24148 Kiel; rkurzawski@geomar.de

[2] HPT Laboratory, Faculty of Geosciences, Utrecht University, Budapestlaan 4, NL-3584 Utrecht

The **C**osta **R**ica **S**eismogenesis **P**roject (CRISP) investigates processes involved into the genesis of megathrust earthquakes and tsunamis at erosive active continental margins. Subduction erosion, i.e. the basal tectonic removal of overriding plate material occurs along the entire Middle America Trench (MAT), where the oceanic Cocos plate is subducted beneath the continental Caribbean plate. The incoming plate's topography exhibits considerable lateral variations affecting the overall geometry, thermal structure and seismicity pattern of the plate boundary interface. The Costa Rica segment of the MAT is the locus of increased tectonic erosion due to the subduction of the Cocos Ridge (Fig. 1a). This extensive topographic high originates from Galapagos hotspot volcanism and is oriented approximately perpendicular to the trench. Cocos Ridge subduction causes a steepening of the geothermal gradient and results in a shift in seismicity towards shallower levels equivalent to lower normal stresses.

Here we report on velocity stepping experiments performed on simulated fault gouges prepared from natural samples. Seven samples from 4 different CRISP drilling sites (U1378, U1379, U1412, U1414; Fig 1a) were experimentally deformed in the hydrothermal rotary shear apparatus described in detail by Niemeijer et al. (2008). Experimental conditions were defined to suitably cover the expected conditions at the CRISP updip limit of seismogenesis in approximately 5-6 km depth. Several temperature and effective normal stress combinations were explored to simulate the increasing geothermal gradient

towards the Cocos Ridge. First results indicate important differences in the frictional behaviour of different sediments. Calcareous ooze from the incoming plate is frictionally strong at room temperature and exhibits a "normal stress weakening" and unstable slip (i.e. "stick-slip" events) at 140 °C (Fig. 1b). Clayey silt from the forearc of the overriding plate shows potentially unstable (i.e. velocity weakening) behaviour at low effective normal stress independent of investigated temperatures (Fig. 1c). As the active margin off Costa Rica changed repeatedly from accretion to tectonic erosion, it can be assumed that both incoming plate and forearc sediments are incorporated into the subduction channel and essentially affect seismogenesis and rupture propagation. Based on our experiments the shift in seismicity in the vicinity of the Cocos Ridge might be explained by a temperature-controlled change in frictional behaviour without mineral transformations, e.g. the smectite – illite transition.

References:
Niemeijer, A.R., Spiers, C.J. and Peach, C.J. (2008). Tectonophysics, 460, 288-303.

Natural compaction and experimental deformation derived from magnetic fabrics of clayey sediments from the Nankai and Costa Rica trenches

Robert M. Kurzawski[1], Michael Stipp[1], Jens C. Grimmer[2], Agnes Kontny[2], Jan H. Behrmann[1]

[1] Department of Marine Geodynamics, GEOMAR Helmholtz Centre for Ocean Research Kiel, Germany; rkurzawski@geomar.de

[2] Institute of Applied Geosciences, Karlsruhe Institute of Technology (KIT), Germany

Two major endeavors of the International Ocean Discovery Program (IODP), the Nankai Trough Seismogenic Zone Experiment (NanTroSEIZE) and the Costa Rica Seismogenesis Project (CRISP), investigate the processes and controlling factors of deformation and seismogenesis at accretionary and erosive continental margins including the incidence of megathrust earthquakes and tsunamis. A key for the formation of faults in the soft

sediments of forearc wedges of subduction zones is the capability for strain localization within these sediments. Natural compaction modifies the deformability of the sediments. This compaction as well as the effects of natural and experimental deformation can be investigated conducting shape- and crystallographic preferred orientation measurements including the analysis of the anisotropy of the magnetic susceptibility (AMS). Such measurements allow to quantify compaction and deformation and to unravel if the investigated sediments tend to deform more locally by strain concentration or, alternatively, by distributed deformation over the entire sample volume. Here, we studied the deformability of soft sediments from the Nankai accretionary margin (NanTroSEIZE Expeditions 315, 316, 333, 338) and the Costa Rica erosive margin (CRISP Expeditions 334 and 344).

Thirty-one IODP samples were selected to investigate the AMS in a low magnetic field of 300 A/m. The AMS reveals the crystallographic preferred orientation (CPO) of paramagnetic minerals so that magnetic fabrics correlate to bulk CPO analysis. We have measured the AMS of 14 original CRISP samples from a depth down to 365 mbsf, 8 original NanTroSEIZE samples from a depth range of 28 to 522 m and 9 NanTroSEIZE samples experimentally deformed to variable strain conditions (Stipp et al., 2013). 15 of the 17 NanTroSEIZE samples used here were previously analyzed by synchrotron texture (=CPO) analysis (Schumann et al., subm). A comparison of the naturally compacted and experimentally deformed samples is used here to evaluate the effect of compaction and triaxial deformation on magnetic fabrics of weakly consolidated sediments.

K_{mean}-values show a large variation ranging from 70 to 3700 x 10^{-6} SI units due to a heterogenous distribution of magnetite. CRISP samples show lower Kmean-values than samples from the Nankai Trough. Experimentally deformed samples show the highest susceptibilies. In the absence of magnetite, magnetic fabrics of the clay-rich samples are controlled by the orientation of paramagnetic sheet silicates. The orientations of the principal susceptibility axes of the ferrimagnetic samples are coaxial with the paramagnetic samples. Naturally compacted Nankai samples predominantly show oblate fabrics. Experimentally deformed samples consistently show oblate magnetic fabrics with T-values > 0.2 and P'-values of up to 1.15. A comparison of the orientations of principal susceptibility axes of natural and experimentally deformed samples nicely document the reorientation of platy sheet silicates into an orientation perpendicular to the axis of shortening and can be interpreted as the formation of a new subhorizontal planar fabric (foliation). In contrast to the Nankai material, samples from the CRISP area show both, oblate and prolate magnetic fabrics. The prolate fabrics occur predominantly at the lower trench slope (U1412) possibly indicating the superposition of two sub-fabrics.

References:
Stipp, M., Rolfs, M., Kitamura, Y., Behrmann, J.H., Schumann, K., Schulte-Kortnack, D. and Feeser, V. (2013). Geochemistry, Geophysics, Geosystems, 14, 4791-4810.

Kinematic reconstructions of the Western Mediterranean area - a key to understanding the independent motion of the Adriatic microplate

ELINE LE BRETON AND MARK R. HANDY

Institut für Geologische Wissenschaften, Freie Universität Berlin, 12249 Berlin; eline.lebreton@fu-berlin.de

The Western Mediterranean area is a very mobile tectonic system with highly arcuate plate boundaries. Its geodynamic evolution is enigmatic due to intermittently independent motion of two microplates, Adria and Iberia, at rates of up to 1-3 cm/a; these microplates are caught between two major plates, Africa and Europe that have been converging at much slower rates of 1 mm - 1 cm/a since Late Cretaceous time. The plates and their boundaries are highly deformable, making the use of classical Euler poles to describe the relative motion of such plates problematic. In order to circumvent this problem and evaluate plate reconstructions of the Western Mediterranean area, we selected models that combine one or more of the following datasets: (1) oceanic magnetic anomalies; (2) surface geology data (e.g., estimates of shortening/extension, timing of tectonic events obtained from syn-tectonic sediments and high-pressure metamorphic rocks); (3) sub-surface data from geophysics (e.g., depth of Moho and Lithosphere-Asthenosphere boundary) and seismic tomography (e.g., slab length).

We evaluated plate motions of Africa, Iberia, Adria and the Corsica-Sardinia block relative to a stationary European plate. Our comparison revealed discrepancies of several hundreds of kilometres in the locations of Adria, Iberia, the Corsica-Sardinia block and Africa through time. The object of comparing the motion of these plates was to pinpoint any overlaps in their location through time, because such overlaps reflect incompatibilities in kinematic datasets. The most important criterion for judging the viability of a model or combination of models is the degree of consistency between geological and geophysical data; for example, plates that are predicted to converge or diverge should be consistent with evidence for the age and amount of shortening or extension along the margins of the plates involved.

We present a model that combines rotation poles for Iberia from Vissers and Meijer (2012a, b) and for Africa and Corsica-Sardinia from Seton et al. (2013). We calculate new rotation poles for Adria from the kinematic reconstructions of Handy et al. (2010; in revision). This allows us to show that Adria moved faster and independently of Africa after the onset of Alpine subduction (c. 84 Ma) and raises the question of what drives the motion of Adria. A push from Africa seems unlikely given that Adria moved faster than Africa. Likewise, slab pull is questionable given the limited length of Neogene Adriatic continental slab beneath Eastern Alps (c. 200 km) and the absence of a slab beneath the Dinarides in seismic tomography. We therefore speculate that viscous drag of upper mantle flow drove motion of the Adriatic plate.

References:
Handy, M.R., Schmid, S.M., Bousquet, R., Kissling E., Bernoulli, D. (2010). Earth Science Reviews 102, 121–158.

Handy, M.R., Ustaszewski, K., Kissling E, in revision, Int. J. Earth Sciences.

Seton, M., Müller, R.D., Zahirovic, S., Gaina, C., Torsvik, T.H., Shephard, G., Talsma, A., Gurnis, M., Turner, M., Maus, S., Chandler, M. (2012). Earth Science Reviews, 113 (3-4), 212-270.

Vissers, R.L.M., Meijer, P.Th. (2012a). Earth-Science Reviews, 110, 93–110.

Vissers, R.L.M., Meijer, P.Th. (2012b). Earth Science Reviews, 114, 61-83.

Dynamic recrystallization and phase mixing in experimentally deformed harzburgite

JOLIEN LINCKENS[1], ROLF BRUIJN[2], PHIL SKEMER[2]

[1] Institut für Geowissenschaften, Goethe-Universität, Frankfurt; linckens@em.uni-frankfurt.de

[2] Department of Earth and Planetary Sciences, Washington University in St. Louis, United States

The strength of the upper mantle is controlled by zones of localized deformation (i.e. shear zones). In order for shear zones to form, weakening needs to occur. One possible weakening process in the upper mantle is a switch from grain size insensitive to grain size sensitive deformation by dynamic recrystallization due to an olivine grain size reduction. For the resulting weakening to be long-lived, grain growth needs to be inhibited and the small olivine grain size needs to be preserved. Pinning of olivine grain boundaries by secondary phases (e.g. pyroxenes, spinel) has been widely observed to inhibit olivine grain growth in experimentally and naturally deformed mantle rocks. A well-mixed microstructure is a prerequisite for effective pinning. Therefore, for dynamic recrystallization to lead to long-lived weakening, coarse-grained undeformed mantle rocks need to evolve to a fine-grained polyphase mixture. To improve our understanding of under which conditions phase mixing occurs in the absence of melt-rock or metamorphic reactions, we conducted deformation experiments on mm-sized olivine and orthopyroxene clasts, embedded in a fine-grained (< 10 μm) olivine matrix. Triaxial deformation experiments were conducted in a Griggs apparatus at a confining pressure of ~1 GPa, temperature of 1400 to 1550 K and strain rate of 10^{-5} - 10^{-6} s^{-1} under nominally dry conditions. The samples reached a macroscopic natural strain ranging from 0.31 to 0.74. The orthopyroxene and olivine clasts deformed by dislocation creep and are dynamically recrystallized by subgrain rotation. The neoblasts range in grain size from 2-20 μm. Strain of individual recrystallized olivine and orthopyroxene clasts varies from 0.12 to 1.05, and 0.06 to 2.36, respectively. To study phase mixing, we focused on the interfaces between orthopyroxene and olivine clasts that were both dynamically recrystallized. At the majority (~2/3) of these interfaces no mixing is observed. Instead these interfaces show serrations that are correlated with grain boundary triple junctions. We propose that these serrations developed by phase boundary migration to form energetically more favorable triple junctions (i.e. 120° angles between grain boundaries instead of 90°). The resulting serrations could act as nucleation sites for phase mixing. At some of the interfaces a small amount of incipient mixing is observed. This result indicates that the serial processes of dynamic recrystallization, phase boundary migration and grain boundary sliding are a plausible mechanism for the mixing of olivine and orthopyroxene. However, more extensive deformation may be needed to reproduce the near steady-state microstructure observed in highly deformed mantle shear zones. We conclude that the processes of dynamic recrystallization, phase boundary migration and grain boundary sliding may play a critical role in the preservation of weak shear zones over geologic timescales, but do not provide an adequate mechanism for initiating localized deformation in the mantle lithosphere.

The brittle-viscous transition in mafic fault rocks - an experimental study

SINA MARTI[1], RENÉE HEILBRONNER[1], HOLGER STÜNITZ[2]

[1] Institute for Geology, University of Basel, Switzerland; sina.marti@unibas.ch

[2] Department of Geology, University of Tromsø, Norway

Shear-experiments have been performed in a Griggs-type deformation apparatus with solid confining medium, at confining pressures (P_c) of 0.5 GPa, 1 GPa, and 1.5 GPa, temperatures (T) between 300 °C and 700 °C and at constant displacement rates of 10^{-8} m s^{-1} and 10^{-7} m s^{-1}. We used a natural diabase, crushed and sieved to a grain size of < 125 μm, to simulate the fault gouge. The starting composition of the material is ~ 57% plagioclase, 41% pyroxene and 2% accessories. 0.2 μl H_2O is added.

The mechanical data indicates that fault rocks at depth can be strong (differential stresses of 0.6 to 2.2 GPa at P_c = 0.5 GPa, and 1.4 to 2.4 GPa at P_c = 1 GPa) and are able to deform at high displacement rates without abrupt failure (bulk shear strain up to γ = 4). There is a positive P_c dependence, as well as a pronounced negative T dependence of strength.

We observe that all samples develop a foliation due to pervasive fracturing, shearing and rotation of fragments. The foliation itself is either cross-cut by discrete shear fractures or deflected by broader slip zones (SLZs), both in an R1 Riedel shear orientation. In contrast to shear fractures where displacement takes place on a surface, SLZs are characterized as highly strained thin volumes (thickness between 5 and 40 μm) with compositional banding, flow structures and a strong decrease in grain size (down to < 1 μm). In grains adjacent to SLZs fragments are still visible, but inside the SLZs, material appears amorphous when observed with a FE-SEM. Increasing the confining pressure to P_c = 1 GPa, we find that SLZs are thinner and occur only at 300 °C and 700 °C. At 500 °C and 600 °C shear fractures dominate. At T = 700 °C, SLZs change their characteristics. They are shorter, more distributed and inclined at a lower angle with respect to the shear zone boundaries. Also, the usually observed continuous decrease in grain size towards SLZs is not observed anymore for plagioclase. No difference between plagioclase inside and outside the SLZs can be identified.

In experiments at T > 500 °C we find evidence for mass transfer processes such as the growth of fibres and abundant pore trails. So far, no evidence for crystal plasticity is found neither in plagioclase nor pyroxene.

Microstructures indicate that the bulk of the material of the simulated fault rock deforms by cataclastic flow, which we interpret to cause the positive P_c dependence of

strength. The high strain, however, is accumulated by the small volume of material within SLZs. The active deformation mechanism, however, is not yet identified. Flow structures within SLZs and the negative T-dependence of strength indicate a viscous deformation mechanism, such as diffusion creep, operating at high strain rates in the very small grain sizes.

The influence of layer thickness on the deformation behavior of anhydrite rocks: Results of microstructural investigations of the Gorleben-Bank (z3OSM) in the Gorleben salt dome, Germany

MICHAEL MERTINEIT[1], MICHAEL SCHRAMM[1], JÖRG HAMMER[1], GERNOLD ZULAUF[2]

[1] Bundesanstalt für Geowissenschaften und Rohstoffe, Germany; *michael.mertineit@bgr.de*
[2] Institut für Geowissenschaften, Goethe-Universität Frankfurt

In Germany, upper Permian rock salt is investigated intensively for the suitability to construct a repository for high level heat generating radioactive waste. The composition of different Zechstein units is characterized by stratigraphically and locally changing amount and number of anhydrite layers. For long-term safety considerations, the mechanical behavior of these anhydrite layers should receive attention.

The studied anhydrite samples were collected at the two opposite walls of Bohrort 1.8 at the 820 m floor level in the Gorleben exploration mine (Mertineit et al. 2014), and are part of the so-called Gorleben-Bank (z3OSM). Bohrort 1.8 is situated close to the transition z2-z3, which is affected by boudinage and shearing related to salt emplacement (Bornemann et al. 2008). The habitus of the Gorleben-Bank is significantly different at the two opposite walls of the outcrop.

On the western wall, the thickness of the Gorleben-Bank averages several cm. The layer is fractured with single fragments sized between mm and a few cm. A clearly pronounced foliation developed, caused by a preferred grain shape orientation and colour change. SEM and fluorescence microscopic analyses show that seams of opaque material consist of organic material, magnesite, pyrite, talc, and clay minerals. Hydrous minerals such as polyhalite and carnallite argue for brine-controlled mineral reactions. The Gorleben-Bank in place seems to be almost completely recrystallized. High amounts of opaque phases enriched along seams, suggest solution-precipitation creep to be an important deformation mechanism.

On the eastern wall, the layer thickness reaches 35 cm. The layer is boudinaged, single boudins were rotated by ca. 90°. Boudin necks and fractures in the anhydrite layer are filled with halite and carnallite. Old anhydrite generations consist of large fan-shaped and blocky crystals, which show intracrystalline deformation microstructures like undulose extinction and subgrains. These crystals are interpreted to result from postsedimentary processes. They are partly replaced by fine-grained, granular to subhedral and acicular grains. The content of old anhydrite generations is much higher than in the thin layered Gorleben-Bank. Grain boundaries are often decorated by an opaque seam, where a pressure-solution foliation developed. But locally, serrated grain boundaries suggest strain-induced grain boundary migration was also active to accommodate strain. Single crystals show intensive deformation twins.

The observed structures suggest, that the Gorleben-Bank was deformed multiple. At first, brittle-ductile deformation of anhydrite occurred, at which solution-precipitation creep is an important deformation mechanism. The rupture of the Gorleben-Bank can be explained by a subsequent deformation under different P-T and chemical conditions as well as reorientation of the principal stresses.

References:

Bornemann, O., Behlau, J., Fischbeck, R., Hammer, J., Jaritz, W., Keller, S., Mingerzahn, G. & Schramm, M. (2008). Description of the Gorleben Site Part 3: Results of the geological surface and underground exploration of the salt formation. 223 pp., Bundesanstalt für Geowissenschaften und Rohstoffe, Hannover

Mertineit, M., Hammer, J., Schramm, M. & Zulauf, G. (2014). Deformation behavior of anhydrite rocks in a high-strain domain: Results from field and microfabric studies of the Gorleben-Bank (z3OSM) at drilling site 1.8, Gorleben salt dome, Germany. Z. Dt. Ges. Geowiss. 165 (1), DOI: 10.1127/1860-1804/2013/0048.

Kinematic studies on the late Neoproterozoic Balda-Paladi Shear Zone and associated quartz mineralisation, Sirohi region, NW India

ALEXANDER MINOR, MICHEL BESTMANN, HELGA DE WALL

Friedrich-Alexander-Universität Erlangen-Nürnberg, Germany;
Alexander-Minor@gmx.de

NW India has been regarded as a tectonically stable block after the ~1 Ga Delhi Orogeny but there are now indications for a Cryogenian tectonically active corridor W of the Delhi-Fold Belt (Just et al., 2011; de Wall et al., 2012). Within this corridor, the Sirohi region has been identified as one of the key areas as the structural imprint (770 to 765 Ma) is coeval with the initial closure of the Mozambique Ocean, as constrained for central and northern Madagascar. Hence, a continuation of Cryogenian mobile belts into NW India is likely. The Balda-Paladi Shear Zone (BPSZ) is a prominent N-S trending high strain zone with a length of more than 10 km and a width of few meters which cuts across thrusts and fold structures of late-Neoproterozoic rock units (Sirohi metasediments, Erinpura granite-gneisses). Fluids infiltrated the BPSZ and several meters of quartz have been mineralised. Petrographical and structural observations in the field combined with microstructural analysis using optical microscopy and a scanning electron microscope (cathodoluminescence (CL), electron backscatter diffraction (EBSD) and energy-dispersive X-ray spectroscopy (EDS)) have been carried out to identify temperature conditions and kinematics and describe the relationship of mineralisation and deformation in sections along strike and across the BPSZ.

Quartz shows features of crystalplastic deformation all over, while brittle behaviour is evident for feldspar (k-feldspar, plagioclase). Quartz veins in the central part show dynamic recrystallisation by subgrain rotation (SRG) while bulging recrystallization is prominent at the northern and the southern edge suggesting along-strike variations of deformation temperatures. Deformation mechanism and kinematics have been studied in detail in a section across the central part of the BPSZ (see figure). EBSD analysis shows cluster of misorientation axes around the crystallographic c-axis (0001), indicating prism <a> slip in all cases. Therefore, medium-grade conditions ~400-450°C should be valid for the central part of the shear zone. Kinematic analysis of deformation structures reveals a sinistral sense of shear where the western block is translated to the south. Pole figure patterns with a transition from well-defined cross-girdles, over simple girdles to a maximum around the vorticity axis (y-axis) indicates that the amount of simple shear is highest at the contact between Erinpura-Granite and the quartz vein and decreases gradually towards west, where pure shear imprint dominates. Increasing shear deformation and probably increasing strain rate are considered to be related to variable stresses as recorded in decreasing grain size distribution from west to east. The findings indicate a transition of regional ductile deformation to localized shear during predominantly NE-SW directed compression.

References:

Just, J., Schulz, B., de Wall, H., Jourdan F., Pandit, M.K. 2011. Monazite CHIME/EPMA dating of granitoid deformation: implications for Neoproterozoic tectono-thermal evolution of NW India, Gondwana Research, 19, 402-412.

de Wall, H., Pandit, M.K., Dotzler, R., Just, J. 2012. Cryogenian transpression and granite intrusion along the western margin of Rodinia (Mt. Abu region): Magnetic fabric and geochemical inferences on Neoproterozoic geodynamics of the NW Indian block. Tectonophysics 554-557, 143-158.
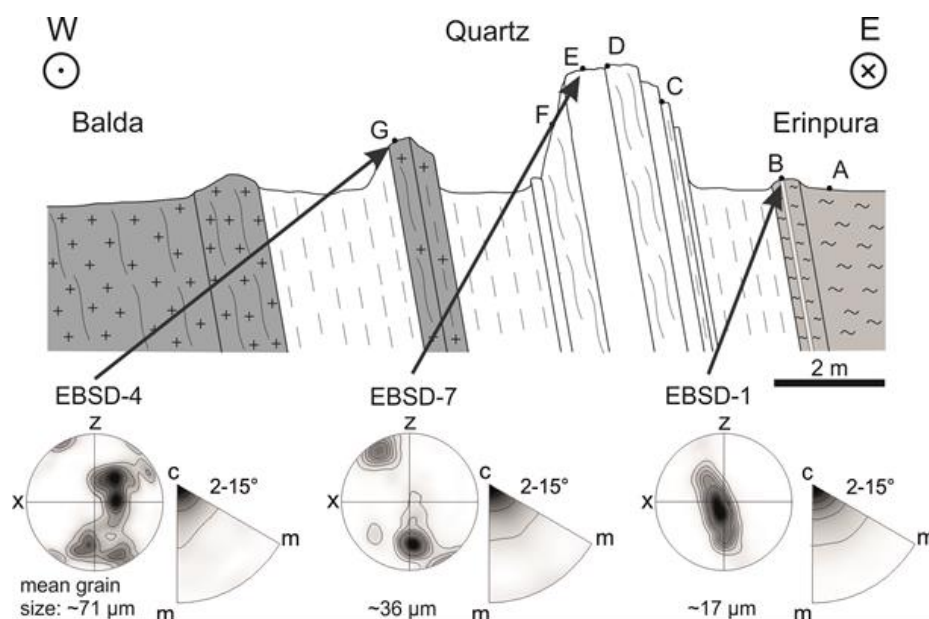

Figure: Section across the BPSZ. A to G: sample location and associated EBSD results.

Fabric transitions in quartz: VPSC modeling under constant strain and quantification of preferred orientations

LUIZ F. G. MORALES[1], GEOFFREY E. LLOYD[2], DAVID MAINPRICE[3]

[1] GFZ Potsdam, Germany; morales@gfz-potsdam.de
[2] University of Leeds, UK;
[3] Géosciences Montpellier & Université Montpellier 2, France

Quartz is a common crustal mineral that deforms plastically in a wide range of temperatures and pressures, leading to the development of different types of crystallographic preferred orientation (CPO) patterns. In this contribution we present the results of an extensive modeling on the fabric transitions of quartz via viscoplastic self- consistent (VPSC) approach. For that, we have used systematic variation on the relative CRSS of the main slip systems of this mineral (temperature-dependent), in axial compression and simple shear regimes. The main slip systems used in our models were <a>(c), <a>{r}, <a>{m} and [c]{m}, assuming an initial aggregate if 1000 spherical grains of random orientation. Some of the predicted CPOs patterns are similar to those observed in naturally and experimentally deformed quartz. Nevertheless, some classical CPO patterns usually interpreted as result from dislocation glide (e.g. Y-maxima due to {m}<a>) are clearly not developed in the simulated conditions. We have demonstrated that CPOs generated under axial compression are usually stronger that those predicted under simple shear, due to the continuous rotation observed in the later simulations. The fabric strength depends essentially on the dominant active slip system, and normally the stronger CPOs result from dominant basal slip in <a>, followed by rhomb <a>, prism [c] and prism <a> slips. While some of the predicted CPO patterns may be repeated over a large range of different sets of relative CRSS, other patterns are developed in very specific conditions. Considering that all the simulations carried out here were under constant strain, we suggest that while some combinations or different CRSS do not affect the general aspect of the CPO, other combinations may produce significantly different patterns. In our simulations, the effect of [c]{m} slip system seems to be the most pronounced in producing different CPO patterns at specific combinations of the other studied slip systems in quartz. The opening angle of quartz [0001] fabric used as a proxy of temperature seems to be reliable for deformation temperatures of ~400°C, when the main slip system have similar behaviors. We also show the results of fabric strength quantification and 2D statistical analyses from eigenvalues.

Fabric transitions in quartz: preferred orientation evolution under simple shear in high strains

LUIZ F. G. MORALES[1], GEOFFREY E. LLOYD[2], DAVID MAINPRICE[3]

[1] GFZ Potsdam, Germany; morales@gfz-potsdam.de
[2] University of Leeds, UK;
[3] Géosciences Montpellier & Université Montpellier 2, France

In the second part of this contribution about fabric evolution in quartz, we present the results of crystallographic preferred orientation (CPO) transitions under evolving simple shear. We have used the systematic variation of the relative critical resolved shear stresses of quartz (<a>(c), <a>{r/z}, <a>{m} and [c]{m}), considering aggregates of 1000 spherical grains of random orientation. These aggregates were deformed in increments of 2.0 % up to a maximum of 210 steps, resulting in a Von Mises equivalent strain of 420% ($\gamma = 6.25$). An initial crystallographic preferred orientation is already observed with low γ depending on the slip systems that are dominant. In the basal-rhomb <a> transition, CPOs are stronger when both slip system has the same relative CRSS, rather than the "single-slip" cases. Classical CPO patterns for quartz, such as the [0001] Y-maxima, which were not observed in the simulations under relative constant low strain, are develop in high-strain conditions, when $\gamma > 3.5$. Differently of what happens in axial compression simulations, where the grains rotate to the position of "easy slip system" and become stable, the grains in simple shear continuously rotate, leading to an almost continuous process of "development-obliteration-development" of preferred orientations. Apparently for this reason, and depending on the slip systems that have been activated, the CPOs might present an apparent reversal of shear sense at the high strains, and it is not clear yet if this is representative or result of an artifact of the models. The activities of different slip systems vary considerably with evolving strain, and it is not uncommon that the activity of an assumed relatively hard slip system overcomes the activity of a weak slip system, in order to accommodate the imposed strain. In our simulations, the fabric strength (J-index) increases almost linearly with increasing strain. This behavior contrasts the results from high strain torsion experiments in calcite (e.g. Barhoorn et al., 2004), where the CPO continues to strengthen with increasing strain, but more slowly after the microstructure becomes steady-state. This probably reflects the effect of recrystallization on the experiments, which is not taken into account here. For the same reason, the CPO patterns for a given strain condition simulated by VPSC are much stronger then the CPOs in naturally and experimentally deformed quartz-rich rocks.

Shear zone initiation and strain localization due to the presence of heterogeneities in calcite rocks

Luiz F. G. Morales, Erik Rybacki, Michael Naumann, Georg Dresen

GFZ Potsdam, Germany; morales@gfz-potsdam.de

The deformation of rocks in the Earth's middle to lower crust is often localized in shear zones variable scale that are normally responsible for the strain accommodation related to tectonic processes. Although there are a number of studies that focus on the evolution of brittle fault zones that occur in the upper crust, little is known about the initiation and localization of strain under high temperature conditions, such as those in the lower crust. Strain localization in rocks deforming at high temperature and pressure may be induced by material inhomogeneities, geometric boundary conditions, or may be related to a number of physical and chemical that might occur in depth. To better understand the initiation and propagation of high-temperature shear zones induced by the presence of heterogeneities, we developed a novel experimental approach in which inclusions of different shapes and contrasting rheological behavior were inserted in Carrara marble specimens for torsion and axial compression experiments. This allows studying in detail effects of stress concentration at inclusions and how the microstructure of the material evolves with the imposed strain. Initial results from shear experiments carried out at T=900°C, P=400 MPa and strain rates of $8x10^{-5}$ s^{-1} (axial compression) and of $2x10^{-4}$ s^{-1} (torsion) show that strain initially localizes at the inclusions when they are weaker than the host rock. For example, inclusions produced from relatively weaker Solnhofen limestone localize strain, forming a process zone that evolves to narrow but long bands that extends several mm into the host Carrara marble. The degree of localization decays exponentially with increasing distance from the tip of the inclusion. The strain localization in this process zone induces substantial microstructural modification of the host Carrara marble. This includes intense twinning of the calcite grains, the development of strong undulose extinction and subgrain boundaries, that evolve to newly recrystallized grains, resulting in grain size reduction driven by dynamic recrystallization processes. The development of crystallographic preferred orientations of calcite in the process zone is evident and starts at much lower bulk strains than without the presence of inclusions. The microstructural modifications observed at the tip of the inclusions are possibly caused by the stress concentration in this region. Under higher strains, deformation is no longer localized in front of the inclusions but starts to affect the material surrounding of the heterogeneities. Our results demonstrate the importance of structural and stress heterogeneities for the nucleation and formation of localized shear bands at elevated temperatures.

The Schwarzhorn Amphibolite (Eastern Rätikon, Austria): an Early Cambrian intrusion in the Lower Austroalpine basement

Nils-Peter Nilius, Nikolaus Froitzheim, Thorsten Nagel, and Frank Tomaschek

Steinmann-Institut, Universität Bonn, Poppelsdorfer Schloss, 53115 Bonn, Germany; s6ninili@uni-bonn.de

The geology of the Penninic-Austroalpine boundary in the eastern Rätikon is characterized by a north-dipping imbricate stack stack of very diverse rock units. The lowermost unit in the south is the Middle Penninic Sulzfluh Nappe, mostly Late Jurassic platform limestone. It is followed by flysch and mélange of the Upper Penninic Arosa-Zone, including ophiolites. The uppermost part of the Arosa Zone, a serpentinite mélange, is overlain by a ca. 3 km long and ca. 1 km thick sliver of meta-diorite, known as the Schwarzhorn Amphibolite. Previous authors interpreted it either as a Penninic or an Austroalpine tectonic unit. Typical Austroalpine units with gneissic basement and Mesozoic sediment cover follow further to the North. The meta-diorite has an amphibolite-facies foliation and is in the east unconformably overlain by unmetamorphic Lower Triassic sandstone, which is again unconformably covered by Jurassic and Cretaceous post-rift sediments (Nagel, 2006). To the north, the metadiorite is locally transformed into a tectonic breccias along a fault zone. Brecciation can be shown to be younger than Early Triassic but older than Late Jurassic. It is hence interpreted as Early to Middle Jurassic in age, and the whole Schwarzhorn Unit represents an eastward-tilted fault block from the Jurassic rifted margin of the Austroalpine. A similar rift-related architecture is observed in the Lower Austroalpine Err and Bernina nappes further south. Also from lateral correlation of nappes, the Schwarzhorn Unit is most likely an extension of the Err Nappe. Few geochronological data are available for the basement protoliths of these units. Permian intrusives have been dated by von Quadt et al. (1994) and Spillman and Büchi (1993) in the basement of the Bernina Nappe..

The Schwarzhorn meta-diorite yielded a homogeneous population of zircons with clear magmatic growth zoning. U-Pb dating of these using LA-ICP-MS at the Steinmann Institute of Bonn University yielded concordant ages of ca. 520 to 530 Ma, Lower Cambrian, interpreted as the crystallization age of the magmatic protolith. This is the first finding of a larger intrusive body of Cambrian age in the Lower Austroalpine units of Graubünden and Vorarlberg. However, meta-plagiogranites of similar age are found in the Upper Austroalpine Silvretta Nappe east of the Rätikon area. The Schwarzhorn meta-diorite and its southward extension, the "Gabbrozug Klosters-Davos-Arosa" (Streckeisen, 1948) probably represents Cambrian volcanic arc rocks, as are typical for the Variscan basement of Austroalpine and Penninic units in the Alps.

References:

Nagel, T., 2006, Structure of Austroalpine and Penninic units in the Tilisuna area (Eastern Rätikon, Austria): implications for the paleogeographic position of the Allgäu and Lechtal nappes. Eclogae Geologicae Helvetiae, 99, 223-235.

Spillmann, P., Büchi, H.J., 1993, The Pre-Alpine Basement of the Lower Austro-Alpine Nappes in the Bernina Massif (Grisons, Switzerland;

Valtellina, Italy). In: von Raumer, J. F. & Neubauer, F. (eds): Pre-Mesozoic Geology in the Alps, Springer, 457-467.

Streckeisen, A., 1948, Der Gabbrozug Klosters-Davos-Arosa. Schweizerische Mineralogische und Petrographische Mitteilungen, 28, 195–214.

Von Quadt, A., Grünenfelder, M., Büchi, H., 1994, U-Pb zircon ages from igneous rocks of the Bernina nappe system (Grisons, Switzerland). Schweizerische Mineralogische und Petrographische Mitteilungen, 74, 373-382.

Permian detachment faulting, syntectonic magmatism and the relation to Alpine thrusting in the Orobic Anticline, southern Alps, Italy

FLORIAN POHL, NIKO FROITZHEIM, FRANK TOMASCHEK, THORSTEN NAGEL, OLIVER SCHRÖDER

Universität Bonn, Germany; florian.pohl@uni-bonn.de

The Grassi Detachment Fault is located in the Orobic Alps east of Lake Como. It was first described by Froitzheim et al. (2008) as an Early Permian extensional structure which separates the Variscan Basement (Morbegno Gneiss) in its footwall from the volcanic and sedimentary rocks of the Early Permian Collio Formation within its hanging wall. This contact is marked by a mylonitic and cataclastic layer whose textures indicate a top-to-the-southeast displacement. The exact timing of faulting and the extension from the well-exposed part of the detachment towards west is still not clear. The Variscan Morbegno Gneiss in the footwall is intruded by two granitic intrusions, the Val Biandino Quarz Diorite (VBQD) and the Valle Biagio Granite (VBG). The VBQD is syntectonic with respect to the detachment, whereas for the VBG, the relation to the detachment is unknown. The VBG has not been dated while the age of the VBQD is poorly defined as 312 Ma ± 48 Ma (Thöni et al. 1992). Volcanic rocks of the Collio Formation in the hanging wall may represent the extrusive part of the magmatic system.

In our study area in the southern part of the Orobic anticline, several faults and shear zones are exposed: (1) The Grassi Detachment Fault between the basement rocks and the Collio Volcanics, represented by mylonites and cataclasites with top-SE shear sense. The detachment is truncated by the unconformably overlying Late Permian Verrucano Lombardo towards the NW which may reflect the eroded culmination of a Permian metamorphic core complex. (2) Further west in the footwall a steeply NW-dipping, brittle normal fault is found between VBQD and VBG. Like the Grassi Detachment, it is also sealed by the basal unconformity of the Verrucano Lombardo and therefore should also be of Early Permian age (Sciunnach, 2001). It may represent an antithetic fault with respect to the detachment, accommodating the uplift of the magmatically inflated core complex. (3) Further North a steeply SE-dipping reverse fault is found, affecting also the Late Permian Verrucano Lombardo. It is therefore an Alpine structure called the Biandino Fault. (4) Several south-directed Alpine thrusts duplicate the lithostratigraphy, including the detachment, and are related to the Orobic thrust further north. They also offset the Biandino Fault.

In order to clarify the temporal relations between the intrusions, volcanics, and the shear zones, U-Pb zircon dating with LA-ICP-MSin in progress.

References:

Froitzheim, N., Derks, J.F., Walter, J.M. & Sciunnach, D. 2008. Evolution of an Early Permian extensional detachment fault from synintrusive, mylonitic flow to brittle faulting (Grassi Detachment Fault, Orobic Anticline, southern Alps, Italy) Geological Society, London, Special Publications, 298; 69-82. doi:10.1144/SP298.4

Thöni, M., Mottana, A., Delitala, M. C., De Capitani, L. & Liborio, G. 1992. The Val Biandino composite pluton: A late Hercynian intrusion into the South-Alpine metamorphic basement of the Alps (Italy). Neues Jahrbuch für Mineralogie–Monatshefte, 12, 545–554.

Sciunnach, D. 2001. Early Permian palaeofaults at the western boundary of the Collio Basin (Valsassina, Lombardy). Natura Bresciana. Annuario del Museo Civico di Scienze Naturali, Brescia, Monografia, 25, 37–43.

The Chaltén Plutonic Complex (Fitz Roy, Argentina) – igneous evolution, contact-metamorphism and deformation

BENITA PUTLITZ[1], SUSANNE SEITZ[1], CRISTOBAL RAMIREZ[2], LUKAS BAUMGARTNER[1], OTHMAR MÜNTENER[1]

[1] *Institute of Earh Sciences, University of Lausanne, Switzerland; benita.putlitz@unil.ch*
[2] *Escuela de Ciencias de la Tierra, Universidad Andrés Bello, Chile*

The Fitz Roy or Chaltén Plutonic Complex (CHPC) is located in Southern Patagonia near the village of Chaltén in Argentina. The CHPC intruded during early Miocene in a context of major tectonic changes, and this small intrusion provides important insights on the role of arc migration and timing of deformation in southern Patagonia.

The CHCP consists of a suite of calc-alkaline mafic and granitic rocks, which were emplaced between 16.90 Ma and 16.37 Ma (Ramirez et al. 2012). The host-rocks include a Paleozoic clastic sequence (Bahia de la Lancia Formation), Jurassic rhyolites and volcanoclastic rocks (El Quemado Complex), and a Cretaceous pelitic sequence (Rio Mayer Formation).

The CHPC with its host rocks is located in the Patagonian fold and thrust belt, which has been intensively, deformed during early Miocene, yet the timing and duration of this deformation phase is a matter of debate. Hence the chronology and deformation history of the CHCP - and other Miocene back-arc intrusions (like e.g. the Torres del Paine) - plays an important role for the interpretation of ages assigned to the Miocene tectonic events, especially in the view of contrasting interpretations (Coutand et al. 1999; Kraemer at al. 1998). We will argue, that the emplacement of the CHCP post-dates regional deformation.

The CHPC was emplaced at upper crustal levels (3.5 to 2 kbar), and we distinguish a coherent sequence from early ultramafic cumulates and diverse mafics (gabbros, diorites, and tonalites) to late granodiorites and granites. The oldest rocks belong to gabbroic and tonalitic units (16.9 Ma – 16.70.Ma). The Fitz Roy granodiorite (16.58 ± 0.03) and the Cerro Torre granite (16.37 ± 0.02) occupy the by far largest volumes on today's outcrop level and form the main central granodioritic-granitic body of the CHPC. These pulses post-date all tonalitic-mafic magmatic batches.

Accordingly the contacts with the mafic bodies are sharp (i.e. cold), steep and clearly intrusive.

One of our key observations is that the younger granodioritic and granitic units are undeformed. In contrast, ductile deformation at macro and microscopic scale is widespread in the older mafic rocks. Locally, a penetrative sub-solidus foliation is present, often marked by metamorphic amphibole, biotite, feldspar and quartz. Regional metamorphism – in contrast - is sub-greenschist facies. Hence, the deformation took place during cooling of the CHPC.

Since deformation is absent in the granites, it either pre-dates the intrusion of the granitic bodies, or the emplacement of the granite and granodiorites themselves causes it. The results illite-crystallinity studies clearly indicate that regional metamorphism during thrusting and folding of the foreland belt never exceeded anchizone conditions. In addition, we can observe the static growth of contact-metamorphic assemblages (i.e. andalusite and cordierite porphyroblasts).

Based on these observations we suggest that the emplacement of the main igneous body (i.e. the granites s. l.) post-dates the regional deformation. We think that the deformation (and alteration) of the older mafic rocks is most likely related to the emplacement of the main granitic suite, but we do need more structural and metamorphic data to better quantify this suggestion.

Microstructural development of quartz gouge at the brittle-to-viscous-transition in shear experiments

BETTINA RICHTER[1], RÜDIGER KILIAN[1], HOLGER STÜNITZ[2], RENÉE HEILBRONNER[1]

[1] Department of Environmental Science, Basel University, CH-4056 Basel; bettina.richter@unibas.ch
[2] Department of Geology, Tromsø University, N-9037 Tromsø

We conducted a series of shear experiments on quartz gouge in a Griggs-type solid medium deformation apparatus to investigate the brittle-to-viscous transition. The starting material is obtained by crushing quartz single crystals (sieved grain size <100 μm) with 0.2 wt% water added. The powder is introduced in a 45° pre-cut in Al forcing blocks forming a ~1 mm thick zone. Samples were deformed at confining pressures of 0.5 GPa, 1.0 GPa or 1.5 GPa, at temperatures between 500°C and 1000°C, and at constant shear strain rates of ~2.5 x 10^{-5} s^{-1}.

At high confining pressures, the strength of the samples decreases with increasing temperature while at high temperatures, it decreases with increasing confining pressure. At high pressure and temperature, continued deformation occurs at a constant flow stress whereas at lower temperature, experiments show strain hardening. The stress-strain curves of two experiments performed at lower confining pressures and high temperature display a peak strength followed by minor weakening.

At intermediate shear strain the c-axis pole figures show a random distribution at low temperatures and/or low confining pressures, an incomplete girdle at intermediate temperatures and a single y-maximum at high temperatures.

At low temperatures or low confining pressures, cataclastic flow is the dominant deformation mechanism. Deformation can be localised in R1-riedel shear orientated slip zones independent of the shear strain. An S-C' fabric is developed at 700°C/1.5 GPa and intermediate shear strain. At high shear strain most of the sample is recrystallised but several large clasts still exist. With increasing temperature the number of remaining clasts is reduced and recrystallisation is nearly complete.

A sample (500°C/1.5 GPa) was loaded to ~2.6 GPa differential stress, i.e., peak strength was not reached, the sample was still hardening, no significant shear deformation had occurred. Several 5-10 μm wide slip zones with small displacement cut the sample. They are filled with cataclastic material. At one interface between these fragments and the un-fragmented region next to these zones a highly localised band with bubble-like structures can be observed. This band is marked by slightly lower backscatter contrast and some of the bubbles are elongated in the shear direction. Similar structures have been identified in experimental studies on granitoid gouge as (partly) amorphous material (Pec et al. 2012a, 2012b). In some places the band is reworked by the ongoing comminution in the slip zones.

The transition from brittle to viscous dominated deformation processes is illustrated by the inverse pressure dependence at higher temperature. At higher confining pressures crystal plastic deformation processes become more important with increasing temperature. Furthermore, a presumably amorphous material develops at high differential stresses without large amounts of displacement in the brittle field. This material has to be analysed in more detail to reveal its development.

References:
Pec, M., Stünitz, H., Heilbronner, R., 2012a. Semi-brittle deformation of granitoid gouges in shear experiments at elevated pressures and temperatures. JSG, 13, 200-221.
Pec, M., Stünitz, H., Heilbronner, R., 2012b. Origin of pseudotachylites in slow creep experiments. EPSL, 355-356, 299-310.

The Main Shear Zone of Sør Rondane: Implications on the late pan-African structural evolution of Dronning Maud Land, East Antarctica

ANTONIA RUPPEL[1], ANDREAS LÄUFER[1], FRANK LISKER[2], JOACHIM JACOBS[3], MARLINA ELBURG[4], DETLEF DAMASKE[1], NICOLE LUCKA[2]

[1] Federal Institute for Geosciences and Natural Resources (BGR) ; antonia.ruppel@bgr.de

[2] Department of Geosciences, University of Bremen, Bremen, Germany;

[3] Department of Earth Science, University of Bergen, Bergen, Norway;

[4] University of Johannesburg, PO Box 524 Auckland Park 2006, Johannesburg, South Africa

The Main Shear Zone (MSZ) is located in Sør Rondane, East Antarctica, and is characterized by a right lateral sense of movement and high-strain ductile deformation under upper low- to medium grade metamorphic conditions. Structures along this pronounced WSW-ENE trending mostly transpressive shear zone were studied to gain new insights into the tectonic evolution of eastern Dronning Maud Land and contribute to an overall picture with regard to the formation of Gondwana. The MSZ divides south-western Sør Rondane in a northern amphibolite- to granulite facies subterrane and a southern tonalite–trondhjemite–granodiorite subterrane. The structure can be traced over a distance of ca. 100 km and reaches several hundred meters in width. Based on crosscutting relationships with dated magmatic rocks, the activity of the MSZ can broadly be bracketed to Latest Ediacaran to Cambrian times (between ca. 560 and 495 Ma). To provide a more precise age and to reconstruct the thermodynamic evolution of the MSZ, Ar-Ar geochronology on synkinematic minerals and microbrobe analyses are in progress.

Within Dronning Maud Land, the MSZ can be interpreted in terms of bipolar lateral escape tectonics of the East African-Antarctic Orogen as proposed by Jacobs & Thomas (2004).

References:

Jacobs, J., Fanning, C.M., Henjes-Kunst, F., Olesch, M. and Paech, H.J. (1998). Continuation of the Mozambique Belt into East Antarctica: Grenville-age metamorphism and polyphase Pan-African high-grade events in central Dronning Maud Land. The Journal of Geology 106, 385-406.

Jacobs, J. and Thomas, R.J. (2004). Himalayan-type indenter-escape tectonics model for the southern part of the late Neoproterozoic-early Paleozoic East African-Antarctic Orogen. Geology 32, 721-724.

Extension controlled exhumation of the Cenozoic Muskol and Shatput Gneiss domes during orogen-wide contraction (Pamir, Tajikistan)

DANIEL RUTTE[1], LOTHAR RATSCHBACHER[1], SUSANNE SCHNEIDER[1], MICHAEL A. STEARNS[2]

[1] Geologie, TU Bergakademie Freiberg, Freiberg, Germany; d.rutte@gmx.de

[2] Geological Sciences, UCSB, California, USA

We present a structural and thermochronologic study of the Cenozoic gneiss domes and their cover in the eastern Central Pamir based on an improved map of the region. Emphasis is laid on flow along the bounding shear zones, faulting in their hanging walls, and geometric analysis by structural cross-sections.

Cenozoic deformation related to the India-Asia collision dominates the structure of the Central Pamir. Gneiss domes make up about 30 % of the Pamirs surface. The Muskol and Shatput Gneiss domes are asymmetric, elongate (80 km E-W, 15 km N-S), structures, exhibiting up to upper amphibolite facies metamorphic sedimentary rocks of Phanerozoic age (proven by detrital zircon studies). They are bound by E-trending normal sense shear zones with the northern boundary accommodating most of the displacement. Relics of large-scale thrust sheets document the pre-extensional N-S shortening that thickened the crust.

Structural studies—including fault-slip analysis—in the hanging wall of the normal sense shear zones document four major phases of ductile to brittle deformation in the Cenozoic: A first brittle-ductile phase of N-S shortening includes isoclinal folds and deforms Ordovician to Cretaceous strata. This deformation is overprinted by brittle-ductile N-S extension structures that we relate to the normal sense motion along the bounding shear zones of the domes (cooling ages constrain normal shear to 19-14 Ma with cooling rates of 100-180°C; U-Pb, Ar-Ar, AFT geochronology). A third phase - brittle N-S shortening - overprinted the older structures. It was followed by the latest stage, E-W dipping normal faults that we relate to rifting along the Karakul rift. These four phases of deformation can be traced throughout the region.

The normal sense North Muskol Shear Zone (NMSZ) defines the northern boundary of the Muskol and Shatput domes and is among the major structures of the region. The metamorphic gradient across the NMSZ reaches from amphibolite-facies ms+bt+grt+sil+ky-schists and gneisses in the footwall to non-metamorphic to greenschist-facies sedimentary rocks in the hanging wall. High grade ductile fabrics include ms+bt+grt mylonites and hornblende growth in boudin necks. The stretching lineation is defined by quartz, feldspar, and biotite; feldspar deforms mostly brittle. In several outcrops, lower grade fabrics with chlorite and chloritized biotite define the stretching lineation. Normal sense brittle-ductile shear bands and faults indicate that top-to-north extension of the NMSZ continued during cooling. Fault gauge, observed at the basement-cover contact of the NMSZ, documents continuous normal sense deformation until final

exhumation to uppermost crustal conditions. N-plunging lineations along the NMSZ converge to the most deeply exhumed central part of the Muskol dome.

Modeling the basal plane of an andesitic magmatic body for prospection and characterization of the underlying Greywacke-Pelite-Series in the open pit Mammendorf (Germany)

SIMON JOHANNES SACHWITZ

Martin-Luther-Universität, Germany;
    simon.sachwitz@student.uni-halle.de

Introduction
The open pit mine Mammendorf is situated about twelve kilometers west of Magdeburg. Geological it is located on the Flechtingen Basement High. The mine is operated by the "Cronenberger Steinindustrie" which produces aggregates and other products from an andesitic sill.

Due to ongoing mining the underlying unit, the Magdeburg/Flechtingen-Formation, was achieved. Thereby this formation consists of turbiditic sediments and is built up by an intercalation of greywacke and pelite of Namurian age. During this study the basal plane of the andesitic magmatic body was constructed to simplify the production. Besides the footwall rocks were evaluated for their use in aggregate production.

The model
For modeling the basal plane intersecting profiles were constructed. Afterwards these profiles were correlated to each other and, if necessary, were rectified. So the basal plane of the andesitic body was modeled with a very high significance and a good accuracy. The model shows a relatively homogeneous plane which is slightly dipping towards southwest. Looking at a smaller scale the plane shows some inhomogeneous parts that stand 2-3 m above and below the plane, respectively. These differences to the "normal" trend of the basal plane can be explained by a combination of the fold structures in the footwall and the intrusion process of the andesitic sill.

Evaluation of the Greywacke-Pelite-Series
The evaluation of the footwall rocks was performed by different methods. So on one hand, out crops in the open pit mine were studied. On the other hand, drill cores were analyzed, which were obtained during a drilling program on the 5th level of the mine for the purposes of this study. By obtaining these different information the structure and composition of the Greywacke-Pelite-Series was determined and the material could be evaluated.

As a result, the footwall can be described as a very fine intercalation of greywacke and pelite with strongly folded cm- to dm-thick layers. Thereby the amount of pelitic layers is three to four times higher than layers consisting of sand and greywacke, respectively. Furthermore some greywacke layers can achieve thicknesses of some meters but their occasional occurrences can hardly be predicted. Therefore the usage of these rocks for aggregate production is not advisable.

Conclusion
The results of this study yielded a negative evaluation of the footwall rocks in the open pit mine Mammendorf. Besides, the modeling of the contact plane between the andesitic body and its footwall results in a more accurate mining process. So the andesitic body now can be mined much closer to its basal plane, which consequently leads to a higher production of profitable aggregate material.

Configurations of the lithosphere and their expression on the surface – the tectonic evolution of the Namche Barwa Antiform, Tibet

ANDREAS SCHARF[1], MARK HANDY[1], PAOLA CRUPI[1,2]

[1] *Freie Universität Berlin, Germany; scharfa@zedat.fu-berlin.de*
[2] *Gas Survey, Bologna, Italy.*

The eastern part of the India-Asia collisional zone is marked by a N-plunging, non-cylindrical fold, the Namche Barwa Antiform (NBA) with a topographic relief of >7 km. The NBA exposes rapidly exhuming Indian- and parts of the overlying Asian crust. Structural, paleomagnetic and GPS studies reveal clockwise rotation of the crust and mantle around a steep axis located close to the mutual borders of India, China and Myanmar (e.g. Sol et al. 2007; Liebke et al. 2011). Teleseismic tomography beneath the NBA reveals 170km thick Indian lithosphere that is not connected with a slab anomaly to the N beneath the Tibetan Plateau, but that appears laterally continuous with north and E-dipping slab anomalies along strike of the Himalayan chain, respectively, to the W and E of the NBA (Zhang et al. 2012).

A closer look at available structural, geochronological, and petrological data reveals Late Oligocene, N-directed subduction of Indian continental lithosphere followed by two stages of pronounced exhumation during Late Oligocene to Miocene and unroofing in Pliocene time. This history is intimately related to the mantle structure imaged beneath the NBA. Timing of subduction is not constraint in the NBA, but Booth et al. (2009) suggest Paleocene to Eocene ages for age of subduction-related plutonism along strike of the India/Asia suture zone. High-pressure (HP) conditions in granulites in the western NBA at 25-24 Ma preceded decompression beginning no later than 18Ma (Su et al. 2012). These granulites are separated from granulites without HP assemblages by a moderately W-dipping mylonitic fault, indicating that this fault was a thrust (Xu et al. 2012) which accommodated S to E directed exhumation of the HP granulites in its hangingwall. This first stage of exhumation coincided with peak temperatures at ~10 Ma (Booth et al. 2009). The granulites and their intervening thrust fault are folded by the NBA (Geng et al. 2006), indicating that this first stage of exhumation preceded doming of the NBA. The NBA is bounded to the W and E by steep sinistral and dextral transpressional faults, respectively. Based on map-scale relations, we link these faults to the South Tibetan Detachment (STD) which in the NBA area is sited along the Indus-Yarlung Suture Zone and juxtaposes the Late Oligocene granulites in its footwall with Eocene or older amphibolite-facies rocks in its

hangingwall. The STD cuts mylonitic faults in its footwall, including the aforementioned thrust separating the HP and non-HP granulites. Taken together, the STD is interpreted as a system of stretching faults that attenuated the crust in a N-S direction during doming of the NBA. The age of extensional exhumation is poorly constrained, but certainly pre-dated rapid exhumation and cooling (>5mm/a, >50°C/Ma) of the NBA in Pliocene time (4-2 Ma) related to ductile-brittle faulting at ≤300°C of the northern part of the NBA and northerly adjacent Asian units (Stewart et al. 2008).

We attribute Miocene doming and extensional exhumation of the NBA to tearing of the Indian slab. The lateral propagation of this tear allowed Asian asthenosphere to escape clockwise around the front of the subducting Indian plate.

Use of Mobile devices (smartphones, tablets, GPS devices with data storage function) to facilitate mapping in the field

LARS SCHARFENBERG

Geozentrum Nordbayern, Friedrich-Alexander University Erlangen-Nürnberg, Germany; lars.scharfenberg@fau.de

Modern smartphones and tablets, which usually contain built-in GPS sensors, can be used as valuable tools for Geological mapping and orientation in the field in combination with off-line maps, which can be prepared with freely available GIS software. This is especially useful in areas where mobile internet access or mobile phone networks are either too limited or too expensive, which makes the software that is usually bundled with these devices useless.

We want to present a method using the Open-Source GIS-software QGIS, MapTiler and the Android software/app OruxMaps. These programs are mostly available free of charge (in the case of MapTiler a version that's limited to a maximum of 10.000*10.000 Pixels map size (with watermarks)).

Orux Maps can be used to capture GPS points and to take georeferenced pictures in the field. Alternative apps like "Geopaparazzi" can also be used, but their capabilities to display custom maps are more limited.

If the accuracy of the built-in GPS sensor of the devices that are used does not suffice (especially in difficult terrain like forests or inside buildings), it can be enhanced by external GPS-Logging devices, which are connected to the smartphone or tablet via USB or Bluetooth. They transmit a constant geopositioning signal which is automatically picked up by the smartphone or tablet. The data collected in the field can then be transferred to a PC via USB or WiFi in GPX (GPS-Exchange) and KMZ (Google Earth/Google Maps)-format, which can be viewed with GIS software such as Quantum GIS, ArcGIS or Google Earth. It can then be converted to editable formats like the ESRI shape file format, for example in the free GIS software QGIS and therefore it can be used to draft geological maps.

The demonstrated principles can also be applied to GPS devices with data storage capability and the ability to display custom maps, such as many GPS-devices manufactured by Garmin.

Rosetta Marbles in Anatolia – Evidences for multiple polymorphism in a HP–LT metamorphic unit

FRANZISKA SCHEFFLER[1], ROLAND OBERHÄNSLI[1], AMAURY POURTEAU[1], OSMAN CANDAN[2], ADRIAN IMMENHAUSER[3]

[1] *Institute of Earth & Environmental Science, University of Potsdam, Karl-Liebknecht-Str. 24-25, 14476 Potsdam-Golm, Germany; fscheffl@uni-potsdam.de*
[2] *Department of Geological Engineering, Dokuz Eylül Üniversitesi, 35160 Bornova Izmir, Turkey*
[3] *Institute of Geology, Mineralogy and Geophysics, Ruhr Universität Bochum, Universitätsstraße 150, 44801 Bochum, Germany*

Rosetta Marbles have been first described in the Ören Unit (SW Anatolia) as centimetre-to-metre-scaled radial structures consisting of fibrous calcitic pseudomorphs after aragonite. Such structures were reported from a Cretaceous chert-bearing limestone sequence (Figure, left), which was affected by HP–LT metamorphism during the closure of the Neotethys in the latest Cretaceous.

Recent investigations shed light on a large variety of rosetta-type morphologies (e.g. swallowtail (Figure, centre), radiating sabre-crystals (Figure, right), palmate structures) that are typical of giant gypsum (selenite) deposits. Despite HP–LT metamorphism witnesses by the former presence of aragonite (fibrous, Sr-enriched calcite; aragonite inclusions in quartz), high Si-content of phengite, and Fe-Mg-carpholite in the underlying clastic unit, many primary sedimentary features are preserved, such as the macroscopic outlines of typical selenite morphologies.

Figure: Left: Pelagic sequence of alternating chert and marble layers. Middle: Swallowtail textures representing pseudomorphs after selenite. Right: Sabre-like radiating Rosetta structures.

We surveyed similar Cretaceous chert-bearing marble localities in the lateral continuation of this HP–LT unit and could trace rosetta-type structures over 300 km eastwards. Surprisingly, the non-metamorphic equivalents of the Ören Unit do not contain evidence for such structures. Our new field and microscopic observations suggest that fine-laminated gypsum precipitated in alternation with radiolarian beds in a deep-marine environment. Soon after deposition, fluid mobilisation within the gypsum layers led to the growth of large selenite crystals forming intra-sedimentary Rosetta structures. The observed high Sr-contents (>1500 ppm) indicate that aragonite formed directly after gypsum, without an intermediate calcite stage that would not have incorporated Sr (<300 ppm). As no hint for anhydrite was observed, we infer that this sulphate-to-carbonate transformation took place during incipient metamorphic stages, at conditions >3.5 kbar and <80°C.

Despite burial, and the later subduction- and exhumation-related events these spectacular rocks contain detailed information about their early stages of sedimentation. We were able to distinguish mineral growth, recrystallisation and mineral reactions of different time steps with the aim to gather information of the evolution of the northern margin of this Neotethyan domain.

First evidence of subduction-related metamorphism in the most distal European continental margin unit of the Eastern Alps (Modereck Nappe, Tauern Window)

Katharina Schmidt[1], Mark R. Handy[1], Andreas Scharf[1], Ralf Milke[1], Timm John[1], Roland Oberhänsli[2]

[1] Institute of Geological Sciences, Freie Universität Berlin, Germany; k.schmidt2@fu-berlin.de
[2] Institute of Earth & Environmental Science, Potsdam University, Germany

The Tauern Window in the Eastern Alps exposes a subduction-accretion complex that formed during the convergence of Adria and Europe from Late Cretaceous to Neogene time. This is an excellent place to study subduction and exhumation processes that affected the European Margin and parts of the Alpine Tethyan oceanic lithosphere. The most distal part of this margin, represented by the Modereck Nappe, is exposed in the middle of the Tauern Window, where it is isoclinally and recumbently folded with ophiolites of the Glockner Nappe. The sedimentary cover of the Modereck Nappe includes a Permian to Lower Cretaceous sequence of metacarbonate, metaquarzite and metapelite. The samples analysed below (coordinates 47.083478, 12.835894) come from calcareous metapelite with anomalously large amounts of garnet (15%) and white-mica (35%).

The main foliation in this area (local S_2) is a gently to moderately NW dipping schistosity and accommodated top-N shear sense parallel to the stretching lineation. Local S_2 is defined by the alignment of chlorite (chl_2) and both fine- and medium-grained white-mica laths (wm_1, wm_2). This S_2 foliation is overgrown obliquely by white-mica (wm_3). Sub- to euhedral garnets (1.5-3.7 mm in diameter) contain an earlier schistosity (local S_1) that comprises chlorite (chl_1) and is oriented oblique to the main $S2$ foliation in the matrix. S_1 within the garnets is not continuous with S_2 in the matrix, indicating that the garnets

grew after S_1 but before S_2. Blocky pseudomorphs of lawsonite in the garnets comprise muscovite, paragonite, zoisite, white-mica and epidote. Element distribution analyses of the garnets reveal typical growth zonation, with Mn-rich cores grading concentrically to more Mg-rich outer domains. Some garnets have very narrow and irregular Ca-rich rims.

The main foliation (local S_2) is the oldest continuously exposed schistosity in the Tauern Window and forms the axial plane foliation (regional S_3) of a km-scale isoclinal recumbent F_3 sheath fold in the central part of the Tauern Window (Schmid et al. 2013). This fold affects the thrust that emplaced the oceanic Glockner Nappe onto the distal continental Modereck Nappe (regional D_2). The local S_1 foliation preserved in the garnets may represent this regional D_2 thrusting event. The occurrence of pseudomorphs after lawsonite in the garnets indicates that blueshist-facies conditions prevailed during or after regional D_2 but certainly before F_3 sheath folding and $S3$ foliation development. We therefore interpret sheath folding to have occurred in the subduction channel during N-directed exhumation of the previously imbricated and folded D_2 nappe stack. Garnet growth under prograde conditions may have occurred during or just after exhumation.

The age of Cenozoic, high-pressure metamorphism and deformation in the Tauern Window is disputed (Eocene: Ratschbacher et al. 2004, Kurz et al. 2008, Schmid et al. 2013; Oligocene: Nagel et al. 2013). We note that the main foliation in this area is overprinted to the E and W by Barrovian amphibolite-facies metamorphism, which is in turn deformed by large, upright, post-nappe folds. An unanswered question is why the central part of the Tauern Window escaped this late overprinting and was able to preserve earlier subduction-/exhumation-related structures so well.

References:

Kurz, W. Handler, R. & Bertoldi, C. (2008). Tracing the exhumation of the Eclogite Zone (Tauern Window, Eastern Alps) by $^{40}Ar/^{39}Ar$ dating of white mica in eclogites. Swiss J. Geosci. 101, 191–206.

Nagel, T. J. et al. (2013). Lu–Hf dating, petrography, and tectonic implications of the youngest Alpine eclogites (Tauern Window, Austria). Lithos 170, 179–190.

Ratschbacher, L. et al. (2004). Formation, subduction, and exhumation of Penninic oceanic crust in the Eastern Alps: time constraints from $^{40}Ar/^{39}Ar$ geochronology. Tectonophysics 394, 155–170.

Schmid, S. M. et al. (2013). The Tauern Window (Eastern Alps, Austria): a new tectonic map, with cross-sections and a tectonometamorphic synthesis. Swiss J. Geosci. 106, 1–32.

Tektonische Brekzie versus Schlammstromsediment im Variszikum des Westharzes – Gefügeanalysen vom Sparenberg bei Lautenthal

MAIKE SCHMIDT[1], CARL-HEINZ FRIEDEL[2], BERND LEISS[1]

[1] Geowissenschaftliches Zentrum, Universität Göttingen, Goldschmidtstr. 3, D-37077 Göttingen; maike.schmidt@stud.uni-goettingen.de
[2] D-04158 Leipzig, Karl-Marx-Str. 56

Im Westharz treten in den Kalkstein- Tonstein-Wechsellagerungen des Mittel- und Oberdevons mehrfach Horizonte mit ungeordneten Gefügen aus zerbrochenen und verstellten Klasten auf, die von Stoppel & Zscheked (1963) als subaquatische Fließbewegungen unverfestigter Sedimente (Sedifluktion) beschrieben worden sind. Derartige Vorkommen wurden als Beleg für ein beträchtliches Paläorelief angesehen und dienten später wiederholt als Argument für die Etablierung des Olisthostrommodells im Harz (u.a. Reichstein 1965, Lutzens 1972). Dieses Modell wurde auch immer wieder in Frage gestellt und alternativ eine tektonische Genese der Vorkommen vermutet (zuletzt Huckriede et al. 2004). Um zur Klärung der Genese solcher ungeordneter Gefüge beizutragen, wurde ein bereits von Stoppel & Zscheked (1963) bearbeiteter Aufschluss am Sparenberg bei Lautenthal im Juni 2013 erneut aufgenommen und vor allem hinsichtlich der Gefügecharakterisierung detailliert bearbeitet.

Der Aufschluss befindet sich im Grenzbereich Mittel-/Oberdevon, wo obermitteldevonischer Stringocephalenkalk in überkippter Lagerung älteren Tonschiefer überlagert. Der tonige Lagen führende Kalkstein bildet bis dm-mächtige Bänke, die im Aufschluss größtenteils bis in den cm-Bereich zerbrochen sind. Die Klasten schwimmen scheinbar ungeordnet in einer tonig-mergeligen Matrix. In den Kalksteinklasten konnte eine bislang nicht beschriebene Drucklösungsschieferung im Aufschluss makroskopisch beobachtet werden. Lichtmikroskopisch lässt sich diese Drucklösungsschieferung anhand dunkler, teilweise suturierter und toniger Säume, an denen einerseits Fossilien angelöst wurden und andererseits Gänge auskristalliert sind, weiter bestätigen. Eine tektonische Foliation bzw. Schieferung konnte auch innerhalb der tonig-kalkigen Matrix beobachtet werden, die an den in der Matrix eingeregelten Fossilien und durch Drucklösungssäume sichtbar wird. Mikroskopisch wurden außerdem Mikro-Schersinnindikatoren, zerscherte Gänge, abgeschnittene Fossilien sowie Deformationszwillinge nachgewiesen. Drucklösung ist der dominierende Deformationsprozess, wohingegen sich kristallplastische Verformungsmechanismen auf der Basis von Röntgentexturmessungen nicht nachweisen ließen. Im Aufschluss lässt sich zeigen, dass mit den Kalksteinklasten die Drucklösungsschieferung und die Schieferung der schichtparallelen Matrix rotiert sind. Die Schichtflächen der Kalksteinklasten zeigen weiterhin, dass die Klasten nicht regellos verteilt sind, sondern wie bei einer Falte um eine NE-SW streichende und damit variszisch angelegte Faltenachse positioniert sind. Die Übereinstimmung der Großkreisverteilung mit der des regionalen Faltenbaus lässt auf eine gemeinsame Entstehung mit der Großfalte in der Spätphase der variszischen Deformation schließen. Die im unteren Teil des Aufschlusses anstehenden Tonschiefer zeigen einen aufschiebenden Bewegungssinn der Grenzfläche an. Diese schichtparallele Aufschiebung ist im stratigraphisch Hangenden mit komplexen Auf- und Abschiebungen verbunden, die als Reaktion auf die Einengung der Schichten durch die Scherzone entstanden sind.

Die Struktur entstand demnach erst nach Ablagerung der oberdevonischen Schichten als im Zuge der variszischen Deformation die gesamte Schichtenfolge verfaltet und geschiefert wurde. In einer späten Phase der Faltung setzte im überkippten Schenkel der Falte eine schichtparallele Störungstektonik entlang der Grenzfläche zwischen Stringocephalenkalk und Tonschiefer ein, durch die die Kalksteinklasten in die Tonschiefer hineingeschoben, fragmentiert und rotiert wurden. Mit der Aufschiebungstektonik verbunden pull-apart-artige Dehnungsstrukturen schufen den notwendigen Raum für die Klasten. Ausgangsmaterial ist ein Lagengefüge aus massigem Kalkstein im Wechsel mit dünnen tonig-kalkigen Lagen. Dieser lithologische Kontrast ist eine wesentliche Voraussetzung für die Entstehung dieses Gefüges, das als tektonische Brekzie bezeichnet werden kann.

References:
Stoppel, D. and Zscheked, J.G. (1963). Ber. Naturhist. Ges. 107, 5-18.
Reichstein, M. (1965). Geologie 14, 1039-1076.
Lutzens, H. (1972). Geologie, Beiheft 74, 1-105.
Huckriede, H. et al. (2004), Int. J. Earth Sci. (Geol Rundsch) 93, 414-431.
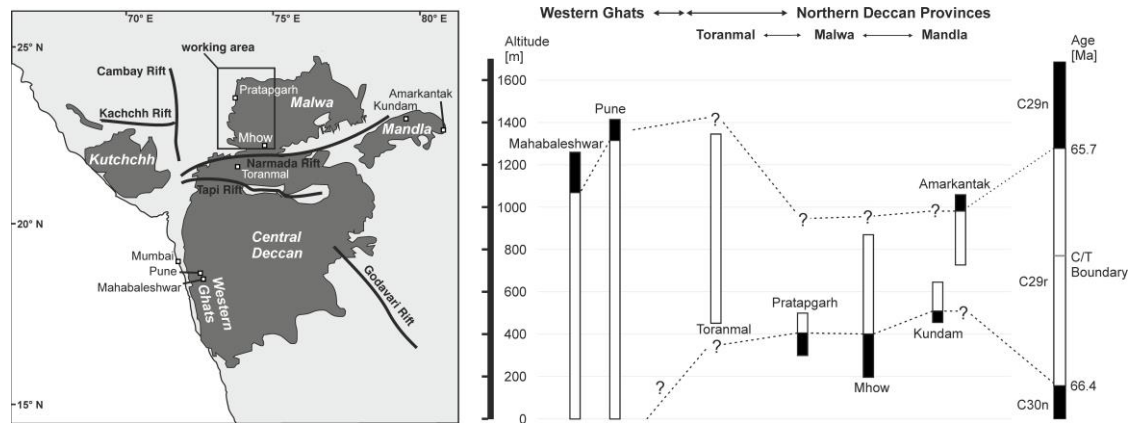
Figure, left: Extent and associated prominent rift zones of the Deccan LIP in central and western India. Right: Magnetostratigraphic correlation of the Northern Deccan Province to the Western Ghats.

The Northern Deccan Traps - A magnetostraphic and ^{40}Ar-^{39}Ar radiometric correlation of the Malwa traps to the main Deccan LIP sequences

STEFAN SCHÖBEL, HELGA DE WALL

GeoZentrum Nordbayern Universität Erlangen, Germany; stefan.schoebel@fau.de

Large Igneous Provinces (LIP) have been extensively studied in the past decades, especially as the awareness raised that large volcanic eruptions can vigorously influence the biosphere and cause mass extinctions. The Deccan LIP, which covers vast parts of the Indian subcontinent is the most prominent and best studied LIP in the world. Despite intense multidisciplinary studies there are still various uncertainties about the origin, the impact on the global climate, the chronology and the eruption mechanism of that massive volcanic event.

The Deccan LIP consists of multiple magmatic Provinces (see Fig. left). The thick (> 2000 m) lava flow pile of the Western Ghats was used to work out the geochemical stratigraphy of Deccan Traps. Most studies on the Deccan Traps were focused on that sequence. The basaltic lava flows of Malwa plateau together with the Mandla area and the Toranmal section constitute the almost unattended Northern Deccan Province. With the present outcrop area of over 80,000 km^2 the Malwa flows form an extensive but relatively thin sequence (~200-500 m).

We sampled Deccan basalts along two 100 km each N-S and E-W transects along the western and southern rims of the Malwa plateau. The ^{40}Ar-^{39}Ar age (67.12 ± 0.44 Ma) obtained for the basal lava flows clearly shows that the eruption of the Malwa flows started during the magnetochron C30n. By mapping the magnetic C30n/C29r transition on the western and southern edge of the plateau, the total volume and eruption rate can be calculated (42,000 km^3; 0.03 km^3/a). Magnetic fabric studies point towards the south situated Narmada-Tapi rift zone as the possible source area for the Malwa lava flows.

The results of this study suggest that the Malwa sequence erupted partly synchronous with the thick sequences of the Western Ghats (see Fig. right). This sets a new time frame for the eruption history of the Deccan LIP, as until now the established models suggested a time gap of 2.5 Ma from the end of the Northern Deccan Volcanism to the start of Southwestern Flows. This implicates, that the eruption rate for the total Deccan LIP during chron C29r was much higher than previously assumed. The eruption rate of a LIP is the most crucial parameter how the volcanic emissions may impact on the global climate. Therefore, the proposed short and synchronous eruption of the Deccan Provinces favor a strong influence of the Deccan flows on the prevalent global climate. The identification of the source area gives furthermore implications for the models dealing with the origin of the Deccan LIP.

AMS and NRM – Watch out for interference!

STEFAN SCHÖBEL, ALEXANDER ZWACK, HELGA DE WALL

Universität Erlangen, Germany; stefan.schoebel@fau.de

Magnetic fabric studies, in particular anisotropy of magnetic susceptibility (AMS) analyses, are established as a state-of-the-art method in many geoscientific disciplines. The acquired magnetic fabric can give important information on the mineral fabric and is therefore readily used for flow direction analysis of volcanic rocks. The magnetic fabric of volcanic rocks, such as basalts, is often dominated by a high fraction of ferrimagnetics, primarily titanomagnetites. However, for interpretation of the magnetic fabric most users reduced the influential parameters on the AMS to the magnetocrystalline anisotropy and the shape anisotropy of those ferrimagnetics. Although the sensitivity of magnetic fabric geometry to a remanent magnetization has been experimentally demonstrated [e.g. Henry et al., 2007; Schöbel et al., 2013] a possible interaction of induced and remanent magnetization has been constantly ignored.

Two case studies on ferrimagnetic basalts will be presented to underline the importance of demagnetization of a natural remanent magnetization (NRM) for reliable AMS interpretations.

Case study A: 900 specimens of subaerial lava flows of the Deccan LIP (NRM shallow)
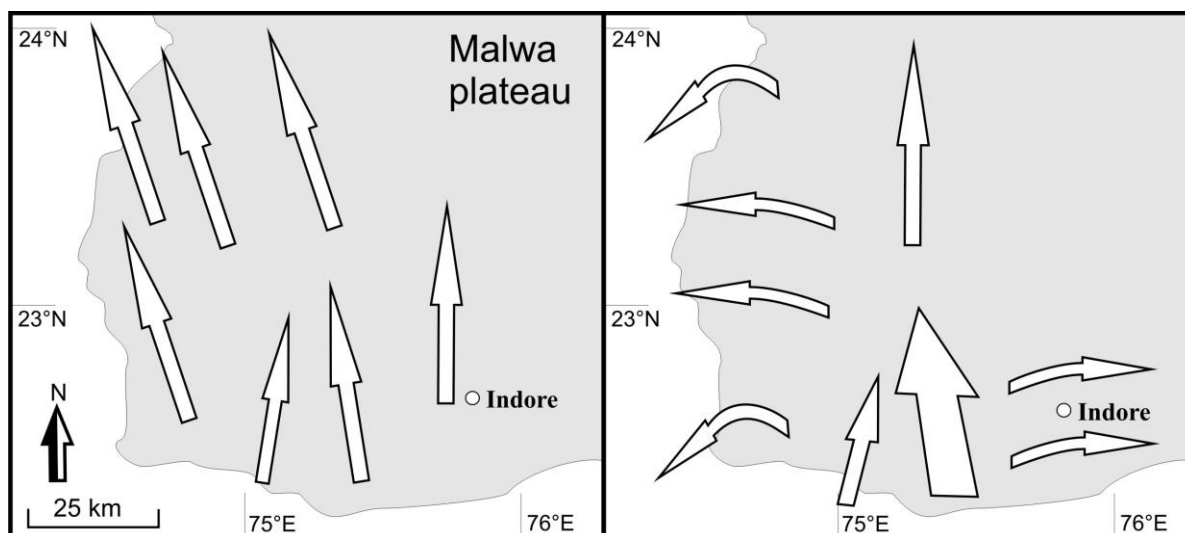
Figure: Evaluated lava flow directions on basis of magnetic fabrics for the Malwa Plateau (Deccan Traps) before (left) and after (right) tumbling demagnetization of the specimens.

Case study B: 120 specimens from a vertical dike swarm within the Jalore granite, Malani Igneous suite, NW India (NRM steep)

The behavior of the magnetic fabrics during the demagnetization experiments shows a complex but systematic pattern. It seems that the changes of the AMS ellipsoid depend on the intensity of the magnetic remanence, the strength of the applied demagnetizing field, the amount of high coercive single-domain titanomagnetites and the geometric relation of the remanence vector to the mineral fabric.

The change of the AMS ellipsoid due to tumbling demagnetization has a crucial influence on the interpretation of the magnetic fabric. After demagnetizing the lava flows give a more differentiated flow pattern of the Malwa Plateau, which fits better to the regional geological setting. The magnetic fabric of the dike samples also show dramatic changes as initial inverse magnetic fabrics can switch to normal after the AF treatment.

The results show that a strong NRM can alter the direction of the AMS principal magnetic axes. Taking such magnetic fabric data as indication for the magma flow directions can result in misleading geological interpretations. AMS measurements on demagnetized specimens give a better reflection of the shape anisotropy of the magnetic carriers. Then the direction of the AMS principal axes will better correlate with the flow fabric. We therefore strongly recommend to clean the remanent field component to get unbiased magnetic fabric results. Demagnetization should occur by use of a tumbling AF-demagnetizer. Thermal and static AF-demagnetization should be avoided.

References:

HENRY, B., JORDANOVA, D., JORDANOVA, N., HUS, J., BASCOU, J., FUNAKI, M., DIMOV D. [2007]. Alternating field-impressed AMS in rocks. Geophysical Journal International, 168, 533-540.

SCHÖBEL, S., DE WALL, H., ROLF C. [2013]. AMS in basalts: is there a need for prior demagnetization?. Geophysical Journal International, 195 (3), 1509-1518.

Local texture analysis of 'High-Temperature-Texture-Type' mylonit marbles from the Alpi Apuane, Italy with EBSD – a first approach

TORBEN SCHULZE, BERND LEISS, KIRSTEN TECHMER

Geowissenschaftliches Zentrum der Universität Göttingen, D-37077 Göttingen; torben.schulz@stud.uni-goettingen.de

Naturally deformed Carrara marbles from the Alpi Apuane, Italy can show 'high-temperature (HT)'-texture types, proven by quantitative neutron texture analysis (Leiss & Molli 2003). High-temperature textures of calcite are characterized by double c-axis maxima, theoretically caused by different simultaneously active intracrystalline slip systems (Wenk et al. 1987). Another cause for the two maxima of global textures, could be the combination of different local textures. In order to identify such domains with locally different directions of preferred c-axis orientations in the microstructure of mylonitic marbles, we applied Electron Backscatter Diffraction Pattern (EBSD) analyses by means of a Scanning Electron Microscope.

The samples originate from the Alpi Apuane in the northwestern Apennines, Italy, of a fold-and-thrust belt which represents a tectonic window that exposes Paleozoic to Mesozoic continental metasediments. The specific sample location is in the inverted limb of the N–S striking, E-vergent, tight to isoclinal Carrara syncline. Stratigraphically, the samples come from Zebrino formation, which are surrounded by Jurassic marbles and siliceous Metalimestones.

Microstructure analyses revealed grain sizes ranging from about 40-500 µm and elongated grains with long/short axis ratios of up to 3:1. All samples show a prolate grain shape with the long axes parallel to the mylonitic foliation and parallel to the macroscopic stretching lineation. In all samples grain shapes are polygonal with inequigranular to seriat grain size distribution. Some samples show small amounts of quartz and mica.

In our first attempt of local texture analyses, we do not find a very good correlation with the global neutron texture. Instead of two distinct c-axis maxima, the local textures show small girdle distributions of the c-axes. It becomes clear, that the global texture related to sample volumes of cylinders with ca. 25 mm of diameter and height cannot be represented by local textures of areas with a size of around 1 x 2 mm. These local areas show a mostly homogenous c-axis distribution with only some domains of 3-6 grains with crystallographic orientations indicating a continuous bending of the lattice, which can be also recognized in the optical microscope with crossed polarizers. This first approach to the characterization of the 'high-temperature' calcite fabrics shows, that more detailed local texture analysis are needed in the sense of a higher local resolution as well as many more additional local areas for representing the global texture.

References:

Leiss, B. and Molli, G. (2003). J. Struct. Geol. 25, 649–658.

Wenk, H.-R., Takeshita, T., Bechler, E., Erskine, B.G. and Matthies, S. (1987). J. Struct. Geol. 9, 731–745.

Possible expression of seismic shaking in the Miocene-Quaternary sediments of the Ili basin (Kazakhstan)

NADINE SEIB[1,2], THOMAS VOIGT[1], KLAUS REICHERTER[2]

[1] Lehr- und Forschungsgebiet Neotektonik und Georisiken, Geowissenschaften, RWTH Aachen, Germany

[2] FSU Jena, IGW, Jena, German,; nadine.seib@uni-jena.de

The Ili basin is an intercontinental basin framed in the north by the Jungar Alatau mountains and in the south by the North Tien Shan mountains. Its development is linked to orogenic processes occurring in the region as a consequence of India-Asia collision.

Cenozoic continental clastic sedimentary rocks fill the syntectonic basin, unconformably overlying a Paleozoic basement. Fluvial and alluvial sands and conglomerates predominate, but interfinger laterally with marly, fossiliferous deposits of a large lake system and associated mudflats at the lake shores. The deposits cover the period from the end of the Mesozoic (same local remains) to the Quaternary. Up to the Middle Miocene sedimentation was accompanied by normal faulting of small magnitude. The main Cenozoic folding in the marginal parts of the basin and thrusting occurred after that time and before deposition of the Pliocene to Pleistocene Chorgos formation. Compression resulted in reactivation of inherited basement structures, a switch to reverse or strike-slip motion on normal faults, and the nucleation of new thrusts. Some of these faults are presently expressed at the surface as fold scarps or flexures, whereas. Some faults were recognized to break Pleistocene - Quaternary sediments. The presence of steep, non-eroded scarps in unconsolidated sediments along some faults, indicate recent activity. Associated geological structures may be interpreted as "soft-sediment deformation structures" (Pisarska-Jamro & Weckwerth, 2013). We hypothesize that they are shear bands developed in the granular sand as a result of lateral compression and shear.

Load cast (sand roller) structures occur in places where there are other structural changes. Often they are accompanied by a change in color of the surrounding sediments that points to oxidative processes. These structures may be interpreted as liquefaction of a sand bed to produce sinking of unliquefied bodies (Mills 1983), or from their structural associations with other soft-sediment deformation structures, as due to lateral movements resulting from horizontal shear. Convex upward sand lenses subparallel to stratification and sand dikes can be interpreted as sandy injections resulting from liquefaction.

The above observations suggest that the sediments had horizons saturated by pore fluids at the time of deformation. Shortening in the basin sediments involves not only folding and thrusting but also translation/shearing and compaction in unconsolidated sediments. Horizons with load casts/sand rollers may be markers of focused deformation.

Earthquakes can cause liquefaction in water-saturated sediment. The scattered intensity of earthquakes can probably be explained by high pore water pressure in the deep part of the Ili basin.

References:

Mills, P. C. (1983). Genesis and diagnostic value of soft-sediment deformation structures: A review. Sedimentary Geology 35(2): 83-104.

Pisarska-Jamrozy M, Weckwerth P (2013) Soft-sediment deformation structures in a Pleistocene glaciolacustrine delta and their implications for the recognition of subenvironments in delta deposits. Sedimentology 60: 637-665.

Oxygen isotope and Ti diffusion in quartz : constraints from the contact-aureole of the Chaltén Plutonic Complex (Fitz Roy, Patagonia)

SUSANNE SEITZ[1], BENITA PUTLITZ[1], LUKAS BAUMGARTNER[1], ANN-SOPHIE BOUVIER[1], STEPHANE ESCRIG[2], TORSTEN VENNEMANN[1], STÉPHANE LERESCHE[1], PETER NESCHER[1]

1 University of Lausanne, Switzerland; susanne.seitz@unil.ch

2 Ecole Polytechnique Féderale de Lausanne

The Chaltén Plutonic Complex (CHPC) is located at the frontier between Chile and Argentina in southern Patagonia. It consists of a suite of calc-alkaline mafic and granitic rocks emplaced in several successive batches. High-precision U/Pb zircon dating yields ages between 16.90 and 16.37 Ma (Ramirez et al. 2012). The host-rocks include a Paleozoic clastic sequence, Jurassic rhyolites and volcanoclastic rocks and a Cretaceous pelitic sequence. The intrusion of the CHPC post-dates the major regional deformation cycle.

The rhyolite and volcanoclastic rocks of the El Quemado Formation are the most common host-rocks in the contact-aureole of the CHPC. Their simple mineralogy provides the opportunity to use the contact-aureole as a well-constrained natural laboratory to investigate trace element thermometry (e.g. Ti in quartz) and stable-isotope exchange kinetics for some key minerals like quartz and zircon. Understanding these mechanisms will in turn help to further constrain intrusion mechanism.

The Jurassic rhyolites show quartz phenocrysts of several millimeter-size. Pre- and syn-intrusive deformation has produced a variety of textures in these phenocrysts: from undeformed to undulose up to heavily recrystallized quartz Cathodoluminescence (CL) images suggest that quartz phenocrysts from weakly deformed samples (from the low-grade aureole) preserved the magmatic zonation. CL images of recrystallized quartz (from the high grade aureole) show a complex pattern of dark CL bands, which partly mimics the shape of subgrains. In quartz dominated systems where other geothermometers are rare, Ti-in-quartz (Wark and Watson 2006) is a potentially powerful thermometer. In combination with diffusion modeling of Ti and oxygen isotopes we want to establish the relative timing and duration of heating events.

Analyses by high resolution NanoSIMS confirm that the zonation and the dark bands observed in the CL images correlates perfectly to varying Ti-concentration. The ^{48}Ti/^{29}Si-ratio changes about 10% over a distance of 5 μm in quartz phenocrysts with preserved magmatic zonation. In the partially recrystallized quartz phenocrysts the ^{48}Ti/^{29}Si-ratio changes about 32% over a distance of only 2 μm. We also could show that changes of the ^{48}Ti/^{29}Si-ratio are correlated to changes in Ti-concentration.

Oxygen isotope values obtained by laser fluorination show relatively high δ^{18}O values between 11-13 ‰ for both whole rocks and quartz phenocrysts. Quartz-phenocrysts and their whole rocks seem to be in (near) magmatic equilibrium outside the contact aureole i.e., show small high-temperature fractionations. Ion-probe data by SwissSIMS from phenocrysts of the low-grade aureole confirms the high δ^{18}O-value obtained by laser fluorination. The δ^{18}O-composition of individual phenocrysts is relatively homogenous, and shows no indication of isotope exchange along cracks. This is in contrast to the observations of King et al. (1997), and suggests that these quartz phenocrysts preserved their

magmatic values. Oxygen isotope profiles across deformed and partially recrystallized quartz crystals from the high-grade aureole show a more complex pattern. Both profiles show sharp, local changes in the oxygen isotope value of more than 1‰.

References:
King et al. (1979). Geology 25, 1079-1082.
Ramírez et al. (2012). Tectonics 31, 1-18.
Wark and Watson (2006). Contrib. Mineral. Petrol. 152, 743-754.

Large-scale fluid flow and fault zone activity: repeated silicification and fragmentation along the Fountain Range Fault (Mt. Isa Inlier, Australia)

LINA SEYBOLD[1], JÖRN H. KRUHL[2], SORAYA HEUSS[1], ALISON ORD[3]

[1] Dept. for Earth and Environmental Sciences, Ludwig Maximilians University Munich, D-80333 Munich Germany; linaseybold@gmx.de
[2] Tectonics and Material Fabrics Section, Technical University Munich, D-80333 Munich
[3] Centre for Exploration Targeting, Earth and Environment, The University of Western Australia, Crawley, WA 6102, Australia

In large-scale fault zones fracture networks are commonly generated by large volumes of pressurized fluids (Sibson, 2004), followed by quartz precipitation and, consequently, formation of large amounts of quartz in extended vein systems and as fine-grained masses. Various generations of quartz may show highly different textures, based on different formation processes (Yilmaz et al., subm.). Quantification of vein patterns and quartz microstructures allow investigation of the various fragmentation and quartz formation processes. Quartz precipitated during activity of the Fountain Range Fault and formed up to ca. 100 m high, 70 m wide and km-long ridges with numerous vein systems and variable microfabrics. This silicified fault zone represents an excellent example of repeated quartz formation during fluid
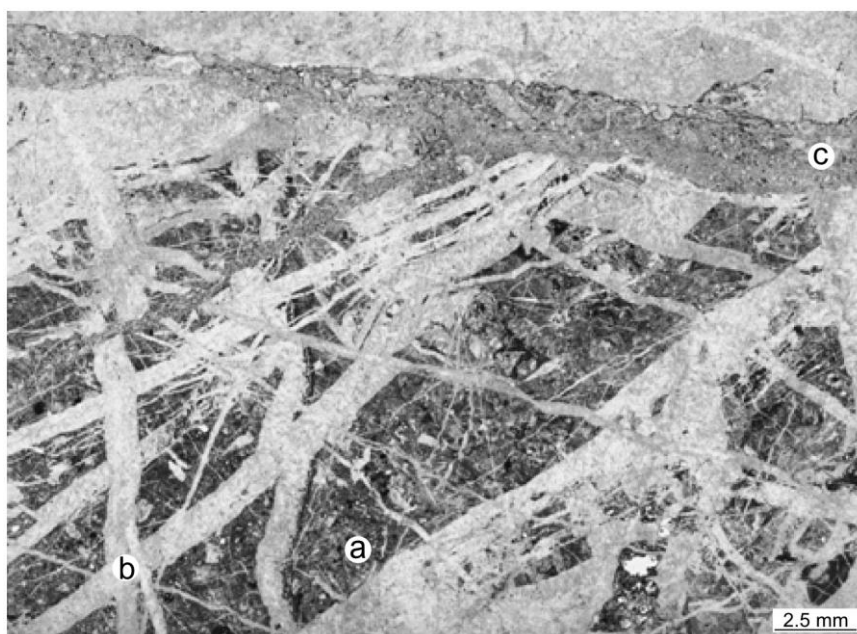

Figure: Fine-grained dark quartz mass (a), transected by sets of quartz veins (b) and late veins with fine-grained quartz matrix (c). Thin-section scan, // polarizers; sample KR5172X2, Fountain Springs.

flow and fragmentation.

In detail, fine-grained reddish to dark and pigment-rich quartz mass builds the matrix of the silicified fault zone (a), transected by numerous generations of typically µm-cm thick quartz veins (b), which form a locally anisotropic network. The early fine-grained quartz mass contains numerous angular fragments of quartz, partly again with internal fragmentation structures indicating earlier fracturing and silicification events. Within the veins, quartz forms geodes, locally filled with fine-grained reddish quartz, and palisade structures with feathery textures and fluid-inclusion zoning. Millimeter- to rarely up to 10 cm-thick veins (c) transect the earlier quartz phases. The vein filling is dark-reddish, contains µm-sized quartz and, again, angular quartz fragments.

Preliminary macro- and micro-scale investigations reveal a multiphase fragmentation and quartz precipitation history of the Fountain Range Fault. Intense fragmentation, together with fluid infiltration and quartz crystallization in pore space, led to fine-grained cataclastic and silicified masses, followed by numerous events of quartz-vein formation and, again, cataclasis probably leading to flow of particle-fluid suspensions. In general, macro- and microstructures reflect repeated processes of fragmentation, fluid flux, quartz precipitation and cataclastic flow during the long-lasting history of a crustal-scale shear zone.

References:
Sibson, R.H., 2004. J. Struct. Geol. 26, 1127-1136.
Yilmaz, T.I., Prosser, G., Liotta, D., Kruhl, J.H., Gilg, H.A., (subm). J. Struct. Geol.

Kinematic link between late Oligocene - Miocene deformation in the Northern Pamir and the Western Tien Shan

EDWARD SOBEL[1], ALEJANDRO BANDE[1], ALEXANDER MIKOLAICHUK[2]

[1] *Universitaet Potsdam, Germany; edsobel@googlemail.com*
[2] *Geological Institute National Academy of Sciences, Kyrgyzstan*

The northern part of the Pamir orogen is the preeminent example of an active intracontinental subduction zone in the early stages of continent-continent collision. The Pamir orogen as a whole is an integral part of the overriding plate in a subduction system, while the Alai basin to the north constitutes the downgoing plate, with the bulk of the convergence accommodated by underthrusting. We suggest that the curvature of the North Pamir is genetically linked to the rollback of the narrow, south-dipping Alai slab. Our model (Sobel et al., 2013) relates late Oligocene - early Miocene deformation, erosion and prograde metamorphism within the Pamir, Alai - western Tarim Basins, and Tien Shan to increased compression following break-off of the north-dipping Indian slab; subsequent subduction (underthrusting) and rollback of the Alai slab partially released this stress, enabling rapid exhumation of the Central Pamir domes above excessively thickened Pamir crust and allowing a hiatus of deformation farther north in the Alai.

Indentation of the Pamir was underway by ~20 Ma based on AFT ages along the Kashgar Yecheng Transfer System (KYTS) as a consequence of the south-dipping subduction at the northern margin of the Pamir (Sobel et al., 2013). The northward indentation of the Pamir salient was accommodated not only by the right-lateral KYTS but also by the Shache-Yangdaman Fault (SYF) (Wei et al., 2013). The latter structure lies in the subsurface of the Western Tarim basin. These authors propose that a right stepover between these two faults formed the 6 km thick Yecheng pull-apart basin. The basal age of this basin fill is apparently contemporaneous with the basal Massaget Formation, which we describe as a syn-rotational unit deposited in the Fergana Basin. Therefore, both units are syn-tectonic units genetically-related by the same tectonic driver. Based on the map pattern and timing, the Talas-Fergana Fault (TFF) can be connected to the newly described SYF, representing the southernmost portion of a major right-lateral strike-slip system. This interpretation explains how the regional strike-slip system was able to transfer shortening driven by Pamir indentation to the NW Tien Shan.

We propose that the observed $20 \pm 11°$ counter-clockwise rotation of the Fergana basin, coupled with the dextral slip TFF (Thomas et al., 1993), was driven by Pamir indentation to the south. Magnetostratigraphy shows that shortening in the Kokshal range propagated rapidly southward into the Tarim basin between 16.3 and 13.5 Ma (Heermance et al., 2008). Therefore, relatively rapid slip along the TFF persisted from ca. 25 Ma until at least 13.5 Ma. This timing appears to agree well with the formation of the transtensional Yecheng depression in the SW Tarim basin, supporting our contention that the SYF and TFF are kinematically linked.

References:
Sobel, E.R., Chen, J., Schoenbohm, L.M., Thiede, R., Stockli, D.F., Sudo, M. and M.R. Strecker (2013). Earth Planet. Sci. Let., 363, 204-218.
Thomas, J., Perroud, H., Cobbold, P.R., Bazhenov, M.L,. Burtman, V.S., Chauvin, A. and Sadybakasov, E. (1993). J. Geophys. Res. 98, 9571-9589.
Wei, H.H., Meng, Q.R., Ding, L. and Li, Z.Y. (2013). Tectonics, 32, 558–575.

Deformation and microfabric development of UHP rocks: Quantification of brittle fabrics and indications for clinopyroxene-quartz phase boundary mobility

CHRISTIAN STÄB, JÖRN H. KRUHL

Tectonics and Material Fabrics Section, Technical University Munich, 80333 Munich, Germany; c.staeb@tum.de

Ultrahigh-pressure (UHP) metamorphic conditions are defined by the stability of coesite and allocated rocks formed in convergent tectonic settings at depth > 90 km. Jadeite-quartzite and eclogite samples from the Shuanghe UHP slab of the Dabie Shan (central China) were investigated. The rocks underwent UHP metamorphism at c. 220-230 Ma due to a N-subduction of the Yangtze craton beneath the Sino-Korean craton and experienced peak metamorphic conditions of ~ 650-700 °C at pressures of 3.5 – 4 GPa. However, peak temperatures of ~ 800 °C were reached during subsequent exhumation at pressures of

~ 1.5 – 2 GPa (Liu et al., 2013). Various generations of symplectites formed during retrogression at amphibolite- to greenschist-facies metamorphic conditions along phase boundaries and fractures. High temperature quartz microfabrics are indicated by (i) prism-, basal-, and rhombehedral-parallel subgrain boundaries, (ii) coarsely sutured grain boundaries, and (iii) concentration of quartz c-axes parallel to the lineation. In the jadeite-quartzites the morphology of jadeite crystals points to mobility of the Cpx-Qtz phase boundary at high temperatures prior to the formation of symplectic coronas at amphibolite-facies conditions (Fig. 1). Preliminary results indicate possible diffusional creep, i.e. dissolution precipitation creep, shown by (i) cuspate structures of the Cpx-Qtz phase boundary, (ii) pinch and swell structures, and (iii) boudinage of clinopyroxenes.
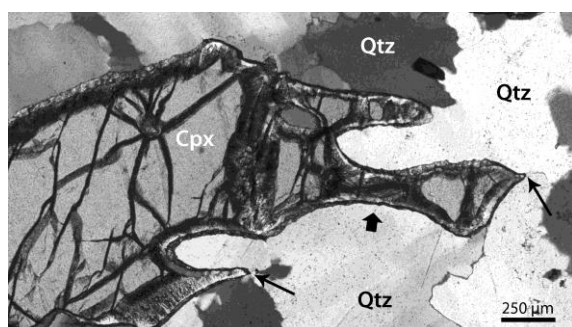

Fig. 1: Photomicrograph of one single clinopyroxene grain within a recrystallized quartz matrix. A thin layer of symplectic aegirine defines the original grain shape prior to marginal retrogression to plagioclase-amphibole symplectite. Thin arrows indicate cuspate structures, bold arrow pinching (volume diffusion) of the clinopyroxene. Quartz recrystallized by grain-boundary migration, which led to coarse suturing.

Fractures are abundant in both clinopyroxene and garnet and, as sub-parallel fracture sets, are mostly oriented at high angle to the foliation plane. Their common orientation in neighbouring garnet as well as pyroxene grains indicates an initially complete fracture network which, consequently, was also present in the quartz groundmass. Analysis of the fracture pattern with MORFA (Peternell et al., 2011) reveals a high homogeneity of anisotropy over the entire pattern. In addition, the fractures are absent in both the recrystallized and crystallographically oriented quartz and in symplectic coronas around clinopyroxenes. This argues for a high-temperature formation of the fracture network, subsequently to deformation of garnet and pyroxene but prior to plastic deformation of quartz. This possibly indicates seismic events during an early stage of uplift preceding the late amphiblite-greenschist facies overprint.

References:
Liu, Q., Hermann, J. and Zhang, J., 2013. Lithos 177, 91-109.
Peternell, M., Bitencourt, M.F. and Kruhl, J.H., 2011. Journal of Structural Geology 33, 609-623.

Fold/Cleavage Relationships as Indicator for Sinistral Transpression in the Rheno-Hercynian – Saxo-Thuringian Boundary Zone, Central European Variscides

TOBIAS STEPHAN[1], UWE KRONER[1], TORSTEN HAHN[2], PETER HALLAS[1], THOMAS HEUSE[3]

[1] TU Bergakademie Freiberg, Institut für Geologie, B. v. Cotta Str. 2, D-09596 Freiberg, Germany; tobiste@googlemail.com
[2] Bayerisches Landesamt für Umwelt, Dienststelle Hof, Hans-Högn-Straße 12, D-95030 Hof/Saale, Germany
[3] Thüringer Landesanstalt für Umwelt und Geologie (TLUG), Göschwitzer Straße 41, D-07745 Jena, Germany

Transpressional tectonics is manifested in oblate strain geometry. In multiply deformed regions, the finite strain ellipsoid may be the expression of different deformational episodes. As demonstrated from the Rheno-Hercynian–Saxo-Thuringian boundary of the Central European Variscides, particularly in the Saxo-Thuringian Zone, there is ample evidence for the superposition of older structures by younger deformation events. Because this fact precludes that the geometry of the finite strain ellipsoid of any deformed sample is the exclusive result of a single deformation event, 3D-strain analysis is not sufficient to demonstrate transpression. Nevertheless, in metasedimentary rocks the youngest fold/cleavage relationship clearly constitutes the latest strain increment. Despite tectonic differences of the investigated units, we show that the dominant ENE-strike of the youngest cleavage is a consistent feature of the Rheno-Hercynian–Saxo-Thuringian boundary zone. Regarding fold/cleavage relationships, our structural observations and statistical analyses of the dihedral angle between the mean cleavage plane and the mean fold axis reveal different fold geometries. Beside domains with cylindrical folds, we observe domains with a significant deviation of the cleavage with respect to the fold axial plane (Fig. 1a). Here the existence of a transecting cleavage [sensu 1] as the latest ductile strain increment provides strong evidence for transpressional tectonics in the multiply deformed region. As consequence of transpression, the cleavage intersects the fold axial plane at an acute angle. Such transected folds are either initiated during an earlier deformation event, or formed oblique to the shortening direction, i.e. the cleavage plane tracks the xy-plane of the finite strain ellipsoid, and thus crosscuts the folds [2, 3]. We use the sense of axial transection as an indicator for the sense of transpression revealing a consistent pattern of clockwise transection, and hence, sinistral transpression (Fig 1b).
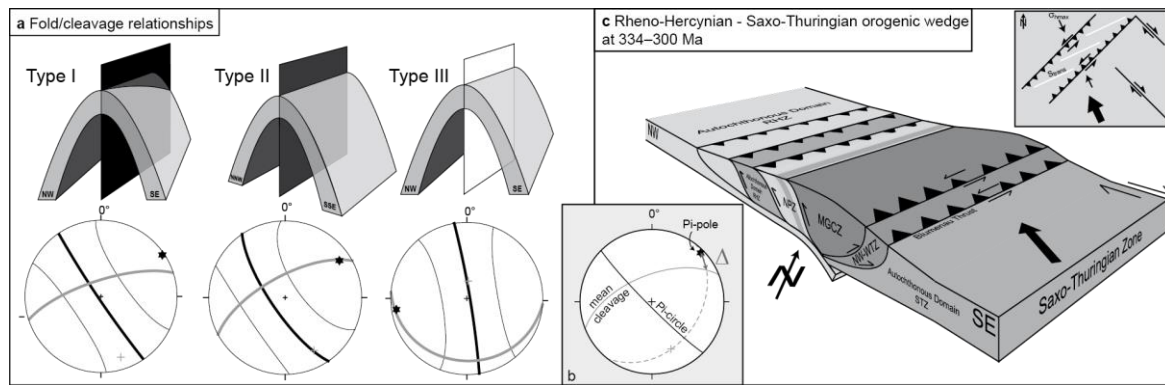
Fig. 1 a Different fold/cleavage relationships and related stereographic projection (equal area, lower hemisphere) Type I is characterized by a transecting cleavage. b Determination of the dihedral angle Δ between fold axial plane and cleavage c Late-Variscan Rheno-Hercynian – Saxo-Thuringian orogenic wedge as result of NNW-SSE shortening under sinistral transpression. Sketch map displays principal orientation of faults and cleavage in relation to the relation to the maximum horizontal compressive stress axis (σ_{hmax}) and plate-convergence vector.

Based on the assumption that the youngest cleavage represents the xy-plane of the finite strain ellipsoid instead of the fold axial plane, our statistical analysis of all youngest cleavage planes reveals NNW-SSE-directed shortening for the entire investigated area (Fig. 1c). Moreover, we demonstrate that the direction of shortening is fully compatible with all different fold/cleavage relationships. Because transpression occurs when stress is applied oblique to pre-existing mechanical anisotropies [4], we interpret the entire NE-trending Rheno-Hercynian–Saxo-Thuringian boundary as a deeply dipping mechanical anisotropy, which is a result of an earlier stage of the Variscan orogeny affecting both sides of the Rheic suture.

References:
[1] Treagus, S.H. and J.E. Treagus, Transected folds and transpression: how are they associated? Journal of Structural Geology, 1992. 14(3): p. 361-367.
[2] Soper, N., Geometry of transecting, anastomosing solution cleavage in transpression zones. Journal of Structural Geology, 1986. 8(8): p. 937-940.
[3] Soper, N., B. Webb, and N. Woodcock, Late Caledonian (Acadian) transpression in north-west England: timing, geometry and geotectonic significance. Proceedings of the Yorkshire Geological Society, 1987. 46(3): p. 175-192.
[4] Jones, R.R. and G.P.W. Tanner, Strain partitioning in transpression zones. Journal of Structural Geology, 1995. 17(6): p. 793-802.

Tsunamigenic sea-floor breakage and slope destabilization controlled by weak sediment fabrics in the Nankai accretionary prism (SW-Japan)

MICHAEL STIPP[1], KAI SCHUMANN[1], BERND LEISS[2], JAN H. BEHRMANN[1], KLAUS ULLEMEYER[3]

[1] GEOMAR, Helmholtz-Zentrum für Ozeanforschung Kiel, Wischhofstr. 1-3, D-24148 Kiel; mstipp@geomar.de
[2] Geowissenschaftliches Zentrum, Universität Göttingen, Goldschmidtstr. 3, D-37077 Göttingen
[3] Institut für Geowissenschaften, Universität Kiel, Otto-Hahn-Platz 1, D-24118 Kiel

Subduction and seismogenesis are currently explored by the International Ocean Discovery Program (IODP) offshore SW-Japan, where earthquakes of magnitude 8.0 to 8.5 and related tsunamis recur every 80-100 years. For assessing the tsunamigenic potential, the mechanical strength, composition and fabric of the forearc slope and accreted sediments have been investigated. 19 drill core samples were experimentally deformed in a triaxial cell under consolidated and undrained conditions at confining pressures of 400-1000 kPa, room temperature, axial shortening rates of 0.01-9.0 mm/min, and up to 64% axial strain (Stipp et al., 2013). Mechanically weak samples from the upper and middle forearc slope of the accretionary prism show a deviatoric peak stress after only a few percent strain (< 10%) and a continuous stress decrease after this maximum combined with a continuous increase in pore pressure. Strong samples from the accretionary prism toe display a constant residual stress at maximum level or even a continuous stress increase together with a decrease in pore pressure towards high strain (Stipp et al., 2013).

Synchrotron texture and composition analysis of the experimentally deformed and undeformed samples using the Rietveld refinement program MAUD indicates an increasing strength of the illite and kaolinite textures with increasing depth down to 523 m below sea floor corresponding to a shape preferred mineral alignment due to compaction. Experimentally deformed samples have generally stronger textures than related undeformed core samples, and they show increasing strength of the illite and kaolinite textures with increasing axial strain. Mechanically weak samples have a bulk clay plus calcite content of 31-65 vol.-% and most of their illite, kaolinite, smectite and calcite (001)-pole figures have maxima >1.5 mrd (multiples of a random distribution). Mechanically strong samples, which were deformed to approximately the same amount of strain (up to 40%) have no calcite and a bulk clay content of 24-36 vol.-%. Illite, kaolinite and smectite (001)-pole figure maxima are mostly <1.5 mrd, except for one sample which was deformed to a considerably higher strain (64%).

The synchrotron textures indicate that the mineral fabric as a whole (clay and also calcite grains) becomes preferentially oriented in the mechanically weak samples. Re-orientation of the mineral grains is an important cause of strain weakening and contraction, persisting to high compressive strains. In contrast, the strong samples from the accretionary prism toe keep their microfabric up to fairly high compressive strain, allowing for strain hardening and dilation. This soft sediment hardening tends

to involve increasingly large volumes of sediment into the imposed deformation, permitting strain dissipation as long as the sediments are homogeneous. Deformation will tend to localize into structurally weak sediments if they occur within the lithological sequence. Such weak sediments, which soften further with increasing strain, predominate in the cover units of the forearc slope and around the existing megasplay fault. They may either provoke mechanical runaway situations allowing for earthquake rupture, surface breakage and tsunami generation, or slope destabilization and resulting submarine mass wasting.

References:

Stipp, M., Rolfs, M., Kitamura, Y., Behrmann, J.H., Schumann, K., Schulte-Kortnack, D. and Feeser, V. 2013. Strong sediments at the deformation front, and weak sediments at the rear of the Nankai accretionary prism, revealed by triaxial deformation experiments. - Geochem. Geophys. Geosys.14/11, doi: 10.1002/ggge.20290.

H$_2$O weakening in experimentally deformed quartz single crystals

HOLGER STÜNITZ[1], ANJA THUST[2], RÜDIGER KILIAN[3], RENÉE HEILBRONNER[3]

[1] *Department of Geology, University of Tromsø, Norway;*
[2] *Institute of Geosciences, University Frankfurt, Germany;*
[3] *Department of Geosciences, Basel University, Switzerland;*
   ruediger.kilian@unibas.ch

The "H$_2$O-weakening" effect, which reduces the strength of quartz dramatically, is still not understood. While lowering the Peierls stress seems likely, it still is not demonstrated. Dislocation generation and multiplication mechanisms have been demonstrated in synthetic quartz (McLaren et al. 1989).

We have carried out experiments on milky quartz in a Griggs deformation apparatus. Cylinders (6.4 mm in diameter, 12-13 mm in length) from the milky zone of a natural quartz single crystal have been cored in orientations (1) normal to one of the prism planes and (2) 45° to <a> and 45 ° to [c](O+ orientation).

The flow strength in most samples in both orientations at 1 GPa confining pressure, 900°C and 10^{-6} s^{-1} is ~150 MPa.

FTIR measurements on double-polished thick sections (200-500 μm) in the undeformed material yield an average H$_2$O content of 250 H/106 Si. The H$_2$O is heterogeneously distributed in the samples. Next to fluid inclusions, the qtz contains less than 150 H/106 Si. Thus, the water in the undeformed material is only present in fluid inclusions of a size of tens to hundreds of microns in size. Microthermometric measurements at low temperature indicate an average salinity of 10.5 wt% NaCl. There is a discrete absorption band at 3585 cm^{-1}, which only forms in deformed regions of the samples and disappears during annealing. The band is unfreezable at -150°C and results from very small fluid inclusions and regions of high dislocation density.

After deformation the distribution of H$_2$O is more homogeneous throughout the sample. The majority of the big inclusions have disappeared and very small inclusions of several microns and usually sub-micron size have

formed. FTIR measurements show an average H$_2$O content in zones of undulatory extinction and shear bands of approximately 3000 H/106Si. These zones are also characterized by a higher salinity.

Deformed samples show deformation lamellae which show a high dislocation density. These zones also show undulatory extinction. Frequently we can observe micro cracks connected with fluid inclusions. Recrystallized grains are rare in deformed samples because of the low strain acquired. The weakening is is attributed to crack healing and distribution of fluid inclusions into regions with a high density of very small inclusions. Both, crack healing and very small inclusions, act as dislocation sources, similar to the effects described by McLaren et al. (1989) for synthetic quartz.

In-situ Ar isotope, ^{40}Ar/^{39}Ar analysis and mineral chemistry of nosean in the phonolite from Olbrück volcano, East Eifel volcanic field, Germany: Implication for status of excess ^{40}Ar in nosean

MASAFUMI SUDO, UWE ALTENBERGER, CHRISTINA GÜNTER

Universität Potsdam, Germany; msudo@geo.uni-potsdam.de

Since the report by Lippolt et al. (1990), it has been known that the hauyne and nosean phenocrysts in certain phonolites in the northwestern side of Quaternary East Eifel volcanic field contain significant amounts of excess ^{40}Ar and show apparent older ages than those of other phenocrysts and groundmass. However, its petrographic meaning has not been well known. In order to measure the accurate eruption ages of very young Quaternary volcanoes by K-Ar decay system, it is quite essential to know where the excess ^{40}Ar locates in the rocks and how it was brought. We have therefore started investigation about the excess ^{40}Ar in the phonolite from Quaternary Ease Eifel volcanic field by combination of in-situ laser Ar isotope and ^{40}Ar/^{39}Ar analyses and mineral chemistry information, considering the study by Sumino et al. (2008), which clarified the source of excess ^{40}Ar in the plagioclase phenocrysts from historic dacite lava flows of Unzen, Japan, as the melt inclusions developed parallel along the plagioclase rim by in-situ laser Ar isotope analysis.

We have collected phonolite from Olbrück volcano in East Eifel. Petrographically, nosean contains fine melt and/or gas inclusions of less than 5 micrometer, which mostly distribute linearly and are relatively enriched in chlorine than the includsion-free area. Similar sizes of solid inclusions are found in some cases and contain CaO and fluorine. In nosean, typically around 5 wt% of sulfur is contained.

In-situ Ar isotopic analyses of the rock section sample have been conducted with the UV pulse laser (wavelength 266 nm) at the ^{40}Ar/^{39}Ar geochronology laboratory in University of Potsdam. The Ar isotopic analyses of nosean and leucite clearly showed significantly different slopes of their isochrons and implied apparent older age of nosean. In-situ ^{40}Ar/^{39}Ar dating was performed to nosean, leucite, sanidine and groundmass within the same rock section. By

the significant decay of short lived [37]Ar (half life: 35.1 days) derived from Ca, contents of Ca and K in nosean and groundmass separately measured by SEM-EDS were applied to the Ar analytical results. Three [40]Ar/[39]Ar ages of nosean ranged variously from 6.86 ± 2.77 Ma to 41.57 ± 11.58 Ma, and were clearly older than those of other minerals and groundmass of around 0.5 Ma. This time beam sizes of UV laser required for Ar analysis did not have enough spatial resolution to distinguish areas with or without inclusions. Presently the excess [40]Ar seems to be accompanied with volcanic volatile elements as sulfur or chlorine which could be separated from magmas and trapped during or after the formation of nosean.

References:

Lippolt, H.J., Troesch, M. and Hess, J.C. (1990) Earth Planet. Sci. Lett. 101, 19-33.

Sumino, H., Ikehata, K., Shimizu, A., Nagao, K. and Nakada, S. (2008) J. Volcanol. Geotherm. Res. 175, 189-207.

Weibull-distributed dyke thickness reflects probabilistic character of host-rock strength

DAVID C. TANNER[1], MICHAEL KRUMBHOLZ[2,3], CHRISTOPH F. HIEROYMUS[3], STEFFI BURCHARDT[2,3], VALENTIN R. TROLL[3], NADINE FRIESE[4]

[1] Leibniz Institute for Applied Geophysics, Stilleweg 2, D-30655 Hannover, Germany; DavidColin.Tanner@liag-hannover.de

[2] Geoscience Center Göttingen, Georg-August Universität, Goldschmidtstraße 1-3, 37077 Göttingen, Germany

[3] Department of Earth Sciences, Uppsala University, Villavägen 16, 75236 Uppsala, Sweden

[4] Wintershall Norge AS, Kanalpiren, Laberget 28, 4020 Stavanger, Norway

Magmatic sheet intrusions (dykes) are the main transport channels for magma through the Earth´s crust, and form large parts of volcanic edifices and the oceanic crust. Their dimension is one parameter controlling the size of eruptions and of surface deformation associated with dyke emplacement.

Thus knowing and interpreting dyke thickness distributions allows deeper insight into crustal growth, magma transport rates, dyke emplacement mechanisms, and can improve eruption forecasting.

We present statistical analyses of 3,767 dyke thickness measurements. The results show that the dyke thickness distribution, independent of tectonic setting, dyke type, and lithology, is best described by the Weibull distribution. The Weibull distribution is used in materials science to describe material strengths and results from randomly-distributed weaknesses in brittle materials, leading to different failure stresses.

We present a dynamic model based on variable magma pressure and the fact that material strength is not a constant, but a random scale-dependent sample from a probability distribution. Our model identifies that the host-rock strength, rather than other factors, exerts the dominant control on dyke emplacement.

Kinematic analysis of normal faults in an extensional passive margin setting, the Otway Basin, Australia

DAVID C. TANNER, JENNIFER ZIESCH, THIES BEILECKE, CHARLOTTE M. KRAWCZYK

Leibniz Institute for Applied Geophysics, Stilleweg 2, D-30655 Hannover, Germany; DavidColin.Tanner@liag-hannover.de

The CO2CRC Otway Project is Australia's first geological carbon sequestration demonstration project, located in the onshore part of the Otway Basin, Australia. To better understand the geological evolution of the area, we analysed a portion (approx. 8 km x 7 km x 4 km) of a large baseline 3-D reflection seismic dataset, and interpreted the faults and eight stratigraphic horizons within it. The faults were interpreted in fault plane-normal and custom-line sections, at 40-60 m intervals. Some faults extend from the lowest recognizable stratigraphic horizons at 2.4 km depth up to the highest seismically-visible horizons at ca. 400 m depth.

All analysed faults have normal displacements; they are partly listric in the south of the area, but planar in the northern part. The major faults dip by 60° southwest on average; some minor antithetic faults are apparent, particularly in the south. Thickness maps of the stratigraphic horizons show that all the faults were active during the deposition of all the strata.

We performed two kinds of fault analysis: fault plane attributes, such as cylindricity and curvature, were calculated and juxtaposition throw maps were constructed to show the lateral change in throw along fault strike for each horizon. The former demonstrate that long axes of the fault plane curvature maxima are not always parallel to the dip direction, rather a number are oblique with a clockwise rotation of ca. 15° with regards to the dip direction. The juxtaposition maps from different faults have some similarities; for instance vertical displacement and fault strike length always decreases stratigraphically upwards. However, there exist two different groups of faults with different tip-line migration: symmetrical and asymmetrical. The juxtaposition maps support the attribute analysis of the faults in that the symmetrical convergence is due to pure dip-slip movement on the faults, whereas the asymmetrical tip-line convergence is due to normal and right-lateral movement of the faults. There is no particular distribution pattern of the different faults; rather their mixture suggests strain partitioning occurred during the geological development of this area.

Strain-partitioning at the eastern Pamir-Alai revealed through SAR data analysis of the 2008 Nura earthquake

KANAYIM TESHEBAEVA[1], HENRIETTE SUDHAUS[2], HELMUT ECHTLER[1], BERND SCHURR[3], SIGRID ROESSNER[1]

[1] GFZ German Research Center for Geosciences, Section 1.4 – Remote Sensing; kanayim@gfz-potsdam.de
[2] University of Potsdam, Inst. of Earth- and Enviromental Sciences
[3] GFZ German Research Center for Geosciences, Section 3.1 - Lithosphere Dynamics

On October 5th, 2008, a magnitude 6.6 earthquake struck the eastern termination of the intermontane Alai valley between the southern Tien Shan and the northern Pamir of Kyrgyzstan. The shallow thrust earthquake occurred in the footwall of the Main Pamir thrust, where the Pamir orogen is colliding with the southern Tien-Shan mountains. We analyze the coseismic surface displacements with InSAR (Interferometric Synthetic Aperture RADAR); the results show clear gradients in the vertical and horizontal directions along a complex pattern of surface ruptures and active faults deforming the fluvial network. To integrate and to interpret these observations in the context of the regional tectonics, we complement the SAR data analysis with seismological data and geological field observations. While the main moment release of the Nura earthquake appears to occurred on the Pamir Frontal thrust, the main surface displacements and ruptures occurred in the footwall along the NE-SW striking Irkeshtam fault. With InSAR data from ascending and descending tracks along with pixel offset measurements, we model the Nura earthquake source as a segmented rupture. One fault segment corresponds to high-angle brittle faulting at the Pamir Frontal thrust and two more fault segments show moderate-angle and low-friction thrusting at the Irkeshtam fault. Our integrated analysis of coseismic deformation argues for rupture segmentation and strain partitioning associated to the earthquake. We suggest that uplift, active strain partitioning and frontal footwall segmentation in the orogenic wedge of the easternmost segment of the Pamir-Alai collision zone may be associated with the presence of Paleogene evaporites.

Uplift and River Incision of the western Pamir Plateau - New insights from river-profile analysis and thermochronology

RASMUS THIEDE[1], EDWARD SOBEL[1], PAOLO BALLATO[1], MUSTAFO GADOEV[2], ILHOMJON OIMAHMADOV[2], MANFRED STRECKER[1]

[1] Potsdam University, Erd- und Umweltwissenschaften, Potsdam-Golm, Germany (thiede@geo.uni-potsdam.de),
[2] Academy of Science of Republic of Tajikistan, Inst. of Geology, Seismology, Dushanbe, Tajikistan

The mechanisms responsible for driving the growth and destruction of orogenic plateaus are subject of ongoing international debate. In addition to thermo-mechanical and structural models, a third class of models emphasizes the pivotal role of surface processes in concert with tectonic processes. The Pamir forms the NW extension of the Tibetan Plateau. Crustal shortening along its western and northern flanks continues until today. In contrast to other Cenozoic plateaus, major climatic gradients in the Pamir are oriented E-W, perpendicular to N-S oriented crustal shortening. The tectonic growth, uplift and incision history of both marginal and interior parts of the Western Pamir are poorly constrained.

To assess the impact of the surface-process system on the geomorphic evolution of the plateau, we performed several standard morphometric analyses. In detail, we analyzed local topographic relief, the overall character of the drainage network, knickpoints, river concavities, and CHI-values. We have also begun measuring apatite He/U-Th data (AHe) to obtain the timing of incision. Combined, the geomorphic observations and the thermochronology data provide proxies for the uplift history of the orogeny, which may ultimately provide data to infer the nature of deep-seated processes that caused uplift and the formation of a plateau in this region. We focus on the western margin of the Pamir, where we observe three zones with different geomorphic characteristics of fluvial network. First, along a 50-km-wide swath across the W-NW flank of the orogen, we find low-relief landscapes with gentle, concave river profiles which are interrupted by major knick points and steep segments in the downstream longitudinal river profile draining towards the deeply incised trunk river, the Panj River. These areas may correspond to pre-uplift relict landscape sectors. Second, beyond this western to northwestern frontal zone lies the Panj River, which has confluences with rivers from five major watersheds which drain the internal parts of the western plateau margin. All of these tributaries are deeply incised (2-3 km) and U-shaped in the vicinity of the mouth, and rise continuously until they reach the plateau realm. In turn, riverprofiles of tributary valleys are all steep in lower parts. In many cases, these valleys have the typical morphology of glacial hanging valleys. Three preliminary AHe cooling ages between 5 and 3 Ma provide valuable estimates on the timing of valley incision, indicating that incision started not earlier than latest Miocene. Third, the central and eastern parts of the Pamir are predominantly characterized by wide, sediment filled basins at elevations >3km and gentle stream gradients.

Based on our preliminary observations we suggest that (1) the frontal segment of the western flank of the Pamir has been rapidly uplifted on the order of 2 to 3 km since late Miocene; (2) the internal portion of the western Pamir constitutes an important orographic barrier for westerly moisture sources, which has facilitated deep glacial/fluvial incision during late Cenozoic. The topographic growth of the western flank is recorded by the deeply incised hydrologic system draining the plateau interior and its margins. Our preliminary AHe data indicate that this process started during the late Miocene.

40Ar/39Ar mica cooling ages for the Saxon Granulite Massif and Frankenberg Complex, Germany

Martin J. Timmerman, Masafumi Sudo

Institut für Erd- und Umweltwissenschaften, Universität Potsdam, D-14476 Potsdam, Germany

The Saxon Granulite Massif (SGM) of predominantly metagranitoids and smaller amounts of intermediate to basic granulites was metamorphosed at ultra-high temperatures (c. 1000°C) under eclogite-facies conditions (c. 22 GPa) in the mid-Carboniferous (c. 340 Ma) (Romer & Rötzler 2001; O'Brien & Rötzler 2003). Intercalated amphibolite-facies, restite-like (cordierite-) biotite schists shown no evidence for granulite-facies metamorphism and had a different metamorphic evolution. Geophysical data indicate that the ellipse-shaped, exposed part of the SGM is the apex of a NE-trending antiform surrounded by, and on all sides plunging below, a tectonically disrupted country rock sequence of variably metamorphosed sediments and volcanics with late Neoproterozoic to Devonian protolith ages. The grade of metamorphism in the country rocks increases from regional anchi-/epizone to upper amphibolite-facies Bt ± Ms schists at the contact with the granulites (the so-called schist mantle), whereby the isograds follow the shape of SGM (Rötzler 1992). The contact metamorphism was caused by the tectonic juxtaposition of an ascending, still hot SGM with very low-grade to unmetamorphosed sediments at high crustal levels. Granulite ascent from peak pressure mantle depths to mid-/upper crustal levels occurred within 2-4 Ma at very high rates (Romer & Rötzler 2001). The heat driving the metamorphism of the country rocks was advected during SGM ascent. Dehydration reactions during amphibolite-facies, prograde metamorphism of the surrounding sediments by the SGM produced hydrous fluids that invaded the granulites and triggered widespread formation of retrograde biotite replacing granulite-facies garnet and orthopyroxene. Subsequently, granulites, schist mantle and sediments were intruded by 331-338 Ma largely undeformed granites. To the south of the SGM, the structurally higher Frankenberg Complex (FC) forms an allochthonous thrust unit of orthogneisses, metavolcanic and metasedimentary rocks with late Neoproterozoic to early Ordovician protolith ages that were metamorphosed under amphibolite-facies conditions in mid-Devonian times (Rötzler et al. 1999).

40Ar/39Ar step-wise heating dating of retrograde Bt in SGM granulites, peak metamorphic Bt in biotite (± cordierite or corundum) schist, Ms from the schist mantle, and magmatic Bt from granite yields Carboniferous cooling ages in the narrow range c. 327 to c. 335 Ma. The mica ages indicate joint cooling of SGM, schist mantle and granites following juxtaposition, prograde metamorphism of the country rocks and retrogression of the granulites, and granite emplacement. In contrast, white mica from granitic orthogneisses of the FC yields 375 and 386 Ma, Devonian cooling ages. This shows that the amphibolite-facies metamorphism of the FC is older that of the SGC and that thermal overprinting by ascending SGM granulites did not occur.

Published U-Pb zircon ages indicate that the granulites have Cambro-Ordovician protolith ages that overlap or are even younger than the deposition ages of the oldest country rocks. This suggests that the SGM is not re-activated local lower crustal basement, but must be of exotic provenance. The argon ages prove the presence of a thermal discontinuity between the structurally deeper SGM and its schist mantle and the structurally higher FC. The latter is a remnant of a nappe that was emplaced in the upper crust in the late Devonian, an event that predated granulite ascent by c. 50 Ma.
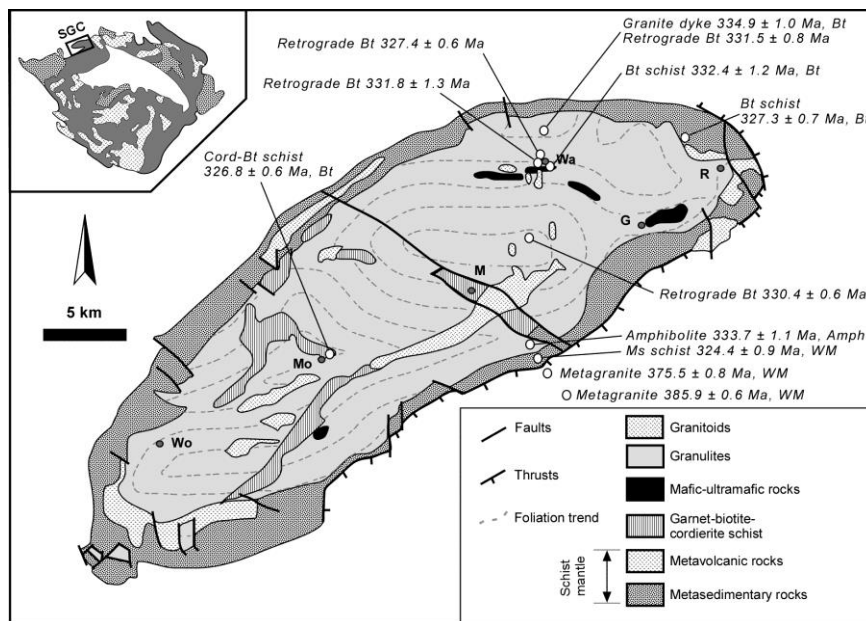

Figure: Geological sketch map of the Saxon Granulite Massif (SGM) (after Rötzler et al. 2008) with obtained 40Ar/39Ar step-wise heating mineral ages. Inset: Bohemian Massif with location of SGM. Abbreviations: Amph = amphibole, Bt = biotite, Cord = cordierite, MS = muscovite, WM = white mica. Towns: G = Greifendorf; M = Mittweida; Mo = Mohsdorf; R = Rosswein; Wa = Waldheim; Wo = Wolkenburg.

References:
O'Brien, P.J. & Rötzler, J. (2003). Journal of Metamorphic Geology 21, 3–20.
Romer, R.L. & Rötzler, J. (2001). Journal of Petrology 42, 2015-2032.
Rötzler, J. (1992). Geotektonische Forschungen 77, 1-100.
Rötzler, J. et al. (1999). Journal of Metamorphic Geology 16, 109–125.
Rötzler, J. et al. (2008).. European Journal of Mineralogy 20, 1097-1115.

Quantifying the Experimental Deformation and Recrystallisation Path at POWTEX Neutron Diffractometer, FRM II Garching, Germany

JENS M. WALTER[1], CHRISTIAN RANDAU[1], MICHAEL STIPP[2], BERND LEISS[1], KLAUS ULLEMEYER[3], HELMUT KLEIN[1], BENT T. HANSEN[1], WERNER F. KUHS[1]

[1] Geowissenschaftliches Zentrum der Universität Göttingen, Göttingen, Germany; jwalter@gwdg.de
[2] Marine Geodynamik, GEOMAR, Kiel, Germany
[3] Institut für Geowissenschaften, Universität Kiel, Kiel, Germany

The quantitative analysis of the crystallographic preferred orientation (CPO) is a common tool for the investigation of fabric developments in mono- and polyphase rocks and their deformation kinematics. Furthermore, bulk texture measurements also allow the quantitative characterisation of the anisotropic physical properties of rocks. To study rock deformation or recrystallisation processes not only from finite samples, but also in time-resolved mode, in-situ experiments during 'continuous' texture measurements are necessary. As neutrons have large penetration capabilities of several cm in geological sample materials neutron diffraction is a strong tool for these kind of investigations.

The new POWTEX (POWder and TEXture) Diffractometer at the neutron research reactor FRM II in Garching, Germany is designed as a high-intensity (~1 x 10^7 n/cm^{2}s) time-of-flight diffractometer. The combination of high flux, the utilization of wavelength frames (TOF) and the large detector coverage (9.8 sr) allow fast and effective texture measurements. As the cylindrical detector provides sufficient angular resolution also for sharp recrystallisation textures, POWTEX offers unique possibilities for in-situ time-resolved texture measurements during deformation and recrystallisation experiments on rock materials as large sample environments can be placed inside the detector system.

The in-situ deformation apparatus is a new design adapted to minimize shadowing effects inside the cylindrical neutron detector. It is operated by a uniaxial spindle drive with a maximum axial load of 200 kN. The HT deformation experiments will be carried out in uniaxial compression or extension and an upgrade to triaxial deformation conditions is envisaged in the near future. The apparatus can alternatively be used for ice deformation by inserting a cryostat cell for temperatures down to 77 K with a triaxial apparatus allowing also simple shear experiments. Strain rates range between 10^{-8} and 10^{-3} s^{-1} reaching to at least 50 % axial strain. The deformation apparatus is designed for continuous long-term deformation experiments and can be exchanged between in-situ and ex-situ placements during continuous operation inside and outside the neutron detector. For the in-situ

recrystallisation analysis the specially designed rotatable furnace reaches temperatures of up to 1800° C and allows a quantitative 3D analysis of the recrystallisation by the stereological calculation of the measured textures as shown by Klein et al. 2009 for synchrotron experiments.

References:
Klein, H. (2009). Principles of highly resolved determination of texture and microstructure using high-energy synchrotron radiation. Adv. Eng. Mat. 11, 452-458.

A new 1:10,000 geological map of the Skutari-Pec Fault and surroundings, northern Albania – evidence of orogen-parallel extension

DSCHAMILJA WANNEK[1], PHILIP GROß[1], SEBASTIAN CIONOIU[1], CORNELIUS DEUTSCH[1], SERGEJ EVSEEV[1], SASCHA ZERTANI[1], JÖRG GIESE[1], ELINE LE BRETON[1], MARK R. HANDY[1], KUJTIM ONUZI[2], JAN PLEUGER[3], KAMIL USTASZEWSKI[3]

[1] Freie Universität Berlin, Institut für Geologische Wissenschaften, Malteserstr. 74-100, 12249 Berlin, Germany
[2] Polytechnic University of Tirana, Institute of GeoSciences, Energy, Water and Environment, Rr. Don Bosko, 60, Tiranë, Albania
[3] Friedrich-Schiller-Universität Jena, Institut für Geowissenschaften, Burgweg 11, 07749 Jena, Germany

The NW-SE trending Dinarides-Hellenides fold-and-thrust belt has accommodated subduction of the Adriatic plate beneath the European plate since Mesozoic time. This belt is discontinuous in northern Albania, where it appears to be offset along the Skutari-Pec Fault (SPF) which trends NE-SW, oblique to the trend of the belt (see Zertani et al., this volume).

Several anomalous features in the vicinity of the SPF motivated our mapping project: (1) paleogeographic units of the Adriatic margin are discontinuous across the SPF (High-Karst and Pre-Karst Units); (2) SE of the SPF, Neogene to recent basins indicate back-arc extension, whereas to the NW such basins are absent; (3) the kinematics of the SPF are debated extensively; recent studies interpret it as a hinge zone that accommodated post-Eocene clockwise rotation of the Hellenic-Aegean arc with respect to the Dinaric orogen.

A new 1:10,000 scale geological and tectonic map of the western end of the SPF reveals cross-cutting relationships between key structures that constrain the following sequence of deformational events:

D1 – the occurrence of mélange s.str. with components of oceanic lithosphere (serpentinite, altered basalts, pelagic sediments) within the West Vardar (Mirdita) ophiolite nappe as well as relics of metamorphic sole (amphibolites) document a first phase of intra-oceanic obduction. NE-plunging stretching lineation on the mylonitic foliation of the amphibolitic metamorphic sole is consistent with NE-SW transport during obduction.

D2 – imbrication of the sequence above with siliciclastic shale containing lenses of sandstone, chert, altered basalt and massive limestone is interpreted as a mélange s.l. This imbricated sequence overlies (partly carbonatic) flysch of the Budva-Krasta-Cukali nappe of presumed Maastrichtian (?) to late Eocene age. Shear bands

in this flysch indicate top-W to -SW nappe transport during Adria-Europe collision.

D3 – the NE-SW trending SPF dips c. 35° to the SSE and overprints D2 nappe contacts. Fault striae indicate top-SE motion of the hangingwall block. Other variously striking, steeply dipping faults offset D2 nappe contacts, but we do not know their age with respect to the SPF. Interestingly, one of these faults trending E-W near Shkoder city induced downthrow of the Shkoder ophiolite klippe with respect to the Budva-Krasta-Cukali Unit. This relative motion is opposite to that along the SPF.

D4 – a NNE-SSW trending pop-up structure ("Bardhaj conjugate fault system") cuts the basal thrust of the Shkoder ophiolite klippe, but is itself dextrally offset by an E-W trending fault of unknown age. We speculate that the pop-up may have formed during a late phase of shortening. However, its age relative to D3 is not constrained by cross-cutting relationships.

In summary, our mapping reveals the first evidence of orogen-parallel extension along the SPF at the junction of the Dinarides and Hellenides. Cross-cutting structural relationships indicate that this extension (D3) clearly post-dated intra-oceanic obduction (D1) and Cenozoic nappe stacking (D2). We propose that extension along the SPF accommodated radial expansion of the Hellenic-Aegean arc. Late shortening (D4) may still be ongoing in external parts of the thrust-and-fold belt and is possibly contemporaneous with orogen-parallel extension.

Interplay of fluid-rock interaction, deformation mechanisms and the U-Th-Pb system in monazite: dating crustal deformation episodes

NICOLE WAWRZENITZ [HOYMANN][1,4], ALEXANDER KROHE[2], ANDREW R.C. KYLANDER-CLARK[3], ROLF L. ROMER[4], DIETER RHEDE[4], BERNHARD GRASEMANN[5]

[1] Universität Potsdam, Germany; nhoymann@uni-potsdam.de
[2] Universität Münster, Germany;
[3] University of California, Santa Barbara, USA;
[4] Helmholtz-Zentrum Deutsches Geoforschungszentrum Potsdam, Germany;
[5] Universität Wien, Austria

Dating the duration and the age of different stages of deformation of crustal rocks is essential for establishing quantitative geodynamic models. This study combines U–Th–Pb dating of monazite and microfabric data of quartzo-feldspathic rocks that make up large parts of the continental crust. Depending on strain rate and fluid availability, deformation of these rocks is accomplished by the mechanisms dislocation creep (DC) or dissolution precipitation creep (DPC). The behavior of the U–Th–Pb system of monazite, however, depends on the deformation mechanism activated in the hosting metamorphic rocks. In quartzo-feldspathic rocks deformed by DC, old predeformative monazite grains may survive high temperatures, intense mylonitization, and high strain. Such predeformative monazite grains commonly show a patchy appearance of compositional domains, reflecting intra-grain transport of material and coupled dissolution–reprecipitation replacement processes. The various patchy zones may show a wide range of apparent, geologically inaccurate Th/Pb and U/Pb ages that are the result of incomplete removal of in-situ grown radiogenic Pb from the patchy domains and the redistribution of Th and U among the domains.

During DPC, mineral reactions - particular the dissolution of feldspar and apatite - increase the alkali- and F-content and, thus, the reactivity of a fluid with monazite. Pre-deformative monazite is dissolved and in its place new syn-deformative monazite grains form, reflecting inter-grain transport of material. This process efficiently leads to complete resetting of the monazite U–Th–Pb system, even at temperatures prevailing during greenschist-facies metamorphism. The new monazite incorporates Eu released from the dissolved feldspar into the fluid. This results in a less pronounced negative Eu anomaly of the new relative to the old monazite. The shape of the monazite grains that precipitated during creep indicates the sense of shear in the shear zone, thus linking the obtained ages directly to the map-scale tectonic transport. We present examples of mylonitic rocks, subsequently deformed by DC and DPC. Monazite growth pulses in layers deformed by DPC allow accurate dating of successive pulses of deformation.

Consequently, rocks pervasively deformed by DPC should be used to obtain monazite most suitable for precise dating of creep episodes linked to shear deformation and for the determination of deformation rates. In contrast, rocks that are deformed by dislocation creep may preserve pre-deformative monazite that is a promising archive for earlier metamorphic histories. Hence, microtectonic studies of the deformed host rocks are a prerequisite for the optimal sample selection and the interpretation of the geochronological data.

Petrography, petrology and REE-geochemistry of a coesite-bearing eclogite, Tso Morari, western Himalaya

FRANZISKA D.H. WILKE[1,2], PATRICK J. O'BRIEN[1], ALEXANDER SCHMIDT[1], MARTIN A. ZIEMANN[1]

[1] Institute for Earth and Environmental Sciences, University of Potsdam, Karl-Liebknecht Str. 24-25, 14476 Potsdam/Golm;
[2] German Research Centre for Geosciences (GFZ), Inorganic and Isotope Geochemistry, Telegrafenberg, 14473 Potsdam; Franziska.Wilke@geo.uni-potsdam.de

Ultrahigh-pressure (UHP), coesite-bearing eclogites in the Himalaya have been documented from the Kaghan Valley in Pakistan and from Tso Morari area in northwest India (O'Brien et al., 2001; Sachan et al., 2004). In both metamorphic complexes two main units can be identified: a Proterozoic basement complex and Phanerozoic meta-sedimentary cover sequences. These units are part of the northern edge of the Indian plate that have been subducted to, and metamorphosed at, mantle depths of 90 km or more before being exhumed to shallow levels. Both UHP complexes are located directly adjacent to the suture zone that separates them from Kohistan-Ladakh arc sequences. The age of UHP metamorphism in eclogites and host rocks is dated at around 45-50 Ma (e.g. Donaldson et al., 2013; Wilke et al., 2010). Exhumation to shallow crustal levels was already completed within 10 Ma after peak

metamorphism as is clear from Ar-Ar, apatite fission track and zircon U-He-Th ages as well as from diffusion modelling of zoning in garnet (e.g. Wilke et al., 2010, 2012). Further east, to Nepal and Bhutan, the metamorphic series of the central Himalaya do not appear directly adjacent to the suture zone with Asia. Instead, these sequences are of Miocene age and underwent amphibolite to granulite-facies metamorphism, reflecting crustal thickening, melting processes and decompression. They show a style of metamorphism that is remarkably different to the subduction-related UHP rocks in the western Himalaya. To understand the tectono-metamorphic evolution of the Himalaya, the sequential and spatial development of both types of processes must be integrated and the prograde, peak and retrograde metamorphic history of the rock sequences need to be understood. Herein, we present new data of a fresh coesite-bearing eclogite from the Tso Morari Crystalline.

Garnet, omphacite, white mica, epidote minerals, amphiboles, carbonates, talc and minor zircon, apatite and titanium ± iron oxides were petrographically identified in the eclogite. Garnets are optically and chemically zoned with Ca and Mn in the core, Fe in the mantle and Mg in the rim, having an outermost Ca-rich margin. Inclusions can be directly correlated with the compositional zoning. Using Laser ICP-MS, rare earth element concentrations (REE) were obtained for garnets, their inclusions and for matrix minerals. We identified a central peak for HREE and parts of the MREE in garnet. HREE concentrations drop by almost 1000 ppm before rising again towards the outermost rim. Some of the MREE and Sm form a central plateau. The concentrations drop by ca. 20 ppm before rising again to the same level as found in the garnet core. The outermost rim is characterized by a significant drop of the MREE and Sm. In particular for white micas, but also for epidote minerals and amphiboles, REE slopes depend on their occurring as inclusions in garnet or as matrix phases. Hence, REE slopes of these minerals may be used to establish the presence or absence of certain minerals during this stage of the prograde metamorphic history. In conjunction with major and trace element phase diagram modelling, the prograde conditions of this UHP eclogite in particular and of the subduction-related UHP rocks in the western Himalaya in general will be analysed, and the peak and retrograde path validated.

References:

Donaldson, G.D., Webb, A.A.G., Menold, C.A., Kylander-Clark A.R.C., Hacker, B.R., 2013. Petrochronolgy of Himalyan ultrahigh-pressure eclogite. Geology, 41, 835-838.

O'Brien, P.J., Zotov, N., Law, R., Ahmed Khan, M., Quasim Jan M., 2001. Coesite in Himalayan eclogite and implications for models of India-Asia collision. Geology, 29, 435-438.

Sachan, H.K., Mukhrjee, B.K., Ogasawara, Y., Maruyama, S., Ishida, H., Muko, A., Yoshioka, N., 2004. Discovery of coesite from the Indus Suture Zone (ISZ), Ladakh, India: Evidence for deep subduction. European Journal of Mineralogy, 16, 235-240.

Wilke F.D.H, O'Brien P.J., Gerdes A., Timmerman M.J., Sudo M., Khan M.A., 2010. The multistage exhumation history of the Kaghan Valley UHP series, NW Himalaya, Pakistan from U-Pb and 40Ar/39Ar ages. European Journal of Mineralogy, 22, 703-719.

Wilke F.D.H, O'Brien P.J., Sobel, E.R., Stockli, D.F., 2012. Apatite fission track and (U-Th)/He ages from the Higher Himalayan Crystallines, Kaghan Valley, Pakistan: implications for an Eocene Plateau and Miocene to Pliocene exhumation. Journal of Asian Earth Sciences, 59, 14-23.

Quartz formation during hydrothermal fluid flow and repeated fragmentation: fluidization, grain growth and deformation structures in the Pfahl

TIM I. YILMAZ[A*], GIACOMO PROSSER[B], DOMENICO LIOTTA[C], JÖRN H. KRUHL[A], H. ALBERT GILG[D], ALISON ORD[E]

[A*] *Technical University Munich, Tectonics and Material Fabrics Section, Arcisstr. 21, 80333 Munich, Germany, tim.yilmaz@tum.de*

[B] *Università della Basilicata, Dipartimento di Scienze, Via dell'Ateneo Lucano 10, 85100 Potenza, Italy, giacomo.prosser@unibas.it*

[C] *Università degli Studi di Bari, Dipartimento di Scienze della Terra e Geo-Ambientali, Via Orabona 4, 70126 Bari, Italy, domenico.liotta@uniba.it*

[A] *Technical University Munich, Tectonics and Material Fabrics Section, Arcisstr. 21, 80333 Munich, Germany, kruhl@tum.de*

[D] *Technische Universität München, Lehrstuhl für Ingenieurgeologie, Arcisstr. 21, 80333 Munich, Germany, agilg@tum.de*

[E] *The University of Western Australia, Center for Exploration Targeting, Earth and Environment, 35 Stirling Highway, Crawley, WA 6102 Australia, alison.ord@uwa.edu.au*

Based on field and microstructural data, the spatial-temporal connection between fluid flow, quartz crystallization and deformation along the Pfahl shear zone in north-eastern Bavaria (Germany) has been investigated. Various fragmentation and fluid-flow processes and their interaction (Fig. 1) lead to complex-structured quartz units: (i) conjugate sets of early quartz veins, (ii) two main phases of finegrained reddish to grayish quartz masses, (iii) voluminous massive white quartz, and (iv) late crosscutting closely spaced fractures and partly open quartz veins. The fine-grained quartz is formed by cataclasis, fluidization and quartz precipitation. Material transport along the brittle shear zone is at least partly governed by flow of mobile fluid-quartz-particle suspensions (Lin et al., 2013). The complex meso- to microstructures of the massive white quartz are generated by repeated processes of fragmentation, quartz precipitation and grain growth. In general, the brittle Pfahl shear zone represents a zone of multiple fragmentation, fluid flow and quartz dissolution and precipitation, and is regarded as key xample of large-scale cyclic interaction of these processes.
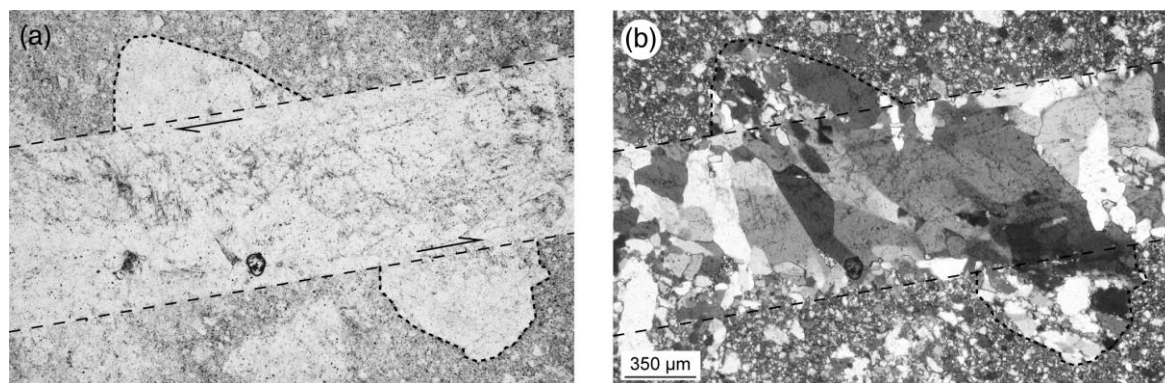
Fig. 1: A quartz vein (broken lines) transects a fragment in quartz mass A; sample KR5179X2, Waschinger Quarry. (a) The two half of the fragment (dotted lines) are displaced by ca. 1 mm (half arrows). Vein and fragment contain less inclusions than quartz mass A. However, the vein center is enriched in inclusions, probably indicating earlier fragmentation; ll pol. (b) Crossed polarizers illustrate that the large fragment consists of quartz grains of highly variable size ranging from ca. 10 to more than 300 μm. In the vein the large blocky and elongate quartz grains are oriented obliquely to the vein boundaries, in the sense of displacement. Along the boundaries, the vein is locally composed of irregular areas of small quartz grains; X pol (from Yilmaz et al., 2014).

Similar meso- and microstructures at the Rusey fault indicate that, again, cyclic interaction of fragmentation, fluid flow and quartz dissolution and precipitation was dominant along this zone.

References:
Lin, A., Yamashita, K. and Tanaka, M. (2013). J. Struct. Geol. 48, 3-13.
Yilmaz, T.I., Prosser, G., Liotta, D., Kruhl, J.H. and Gilg, H.A. (2014). J. Struct. Geol. submitted.

Structure and kinematics of the Skutari-Pec-Fault in northern Albania

SASCHA ZERTANI[1], SEBASTIAN CIONOIU[1], CORNELIUS DEUTSCH[1], SERGEJ EVSEEV[1], PHILIP GROß[1], DSCHAMILJA WANNEK[1], MARK HANDY[1], KAMIL USTASZEWSKI[2], JÖRG GIESE[1], ELINE LE BRETON[1], JAN PLEUGER[2], KUJTIM ONUZI[3]

[1] Freie Universität Berlin, Institut für Geologische Wissenschaften, D-12249 Berlin, Germany; sascha.zertani@fu-berlin.de
[2] Friedrich-Schiller-Universität Jena, Institut für Geowissenschaften, D-07749 Jena, Germany
[3] Polytechnic University of Tirana, Institute of GeoSciences, Energy, Water and Environment, Rr. 'Don Bosko', 60, Tiranë, Albania

The Skutari-Pec Fault (SPF) trends subperpendicular to the Dinarides and Hellenides and is marked by several anomalous features. It coincides with along-strike changes in the Cenozoic nappe structure, e.g., High-Karst and Pre-Karst Units with a combined thickness of 6 km occur NW of the fault, but are missing to the SE in Albania (Cionoiu et al., this volume). There, the West Vardar ophiolites directly overlie the Budva-Krasta-Cukali Unit. Furthermore, the East Bosnian-Durmitor Unit is unmetamorphosed NW of the SPF, but experienced HP metamorphism where exposed to the SE (Most 2003). On the lithospheric scale, the SPF separates a NE-dipping slab anomaly to the SE from a domain to the NW without a lithospheric slab (e.g., Bijwaard & Spakman 2000). The SPF is the northern limit of Neogene clockwise rotation (Kissel et al. 1995) and back-arc extension related to Hellenic rollback subduction (Burchfiel et al. 2008).

Mapping at the western end of the SPF reveals that the fault dips some 35° to the SSE and accommodated top-SE downthrow of the West-Vardar ophiolites in its hangingwall. This is the first direct structural evidence for orogen-parallel extension on the SPF. Three options have been proposed for the western continuation of the SPF near the city of Shkoder: (1) the SPF continues westward, skirting the northern margin of the Shkoder Klippe (map of Schmid et al. 2011); (2) the SPF is linked with an E-W trending fault that downthrows the Shkoder Klippe with respect to the Budva-Krasta-Cukali Unit; (3) the SPF continues to the S along the thrust contact between the West-Vardar Ophiolite Unit above and the Budva-Krasta-Cukali Unit below. Option 2 is unlikely because top-N downthrow on the E-W trending fault is opposite to the observed top-SE downthrow along the SPF. Our mapping supports option 3; contouring of faults at the western end of the SPF indicates that the SPF continues to the S along the base of the West Vardar Ophiolite Unit. This is consistent with SE-plunging striae on joint surfaces arrayed along this gently NE-dipping nappe contact. Thus, we propose that orogen-parallel extension reactivated the basal thrust of the West-Vardar Ophiolite Unit.

Orogen-parallel extension on the SPF provides a possible explanation for the aforementioned omission of the High-Karst, Pre-Karst and East Bosnian-Durmitor Units to the S of the SPF. However, earlier events may also have contributed to this omission: (1) a precursor of the SPF may have segmented the Adriatic continental margin during Triassic-Jurassic rifting, delimiting the High-Karst and Pre-Karst carbonate platforms to the S; (2) the SPF precursor may also have been reactivated as a Cenozoic transfer fault, accommodating subduction and extensional exhumation of HP metamorphic rocks in the East Bosnian-Durmitor Unit S of the SPF; (3) late Miocene orogen-perpendicular extension documented by low-temperature thermochronology (Muceku et al. 2008) affected the Late Cretaceous-to-Paleogene nappe stack south of the SPF. This extension may have been coeval with orogen-parallel extension on the SPF in response to SW-retreat and radial expansion of the Hellenic rollback subduction.

References:
Bijwaard, H. & Spakman, W. (2000). Geophys. J. Int. 141, 71-82.
Burchfiel, B.C., Nakov, R., Dumurdzanov, N., Papanikolaou, D., Tzankov, T., Serafimovski, T., King, R.W., Kotzev, V., Todosov, A. & Nurce, B. (2008). Geosphere 4, 919-938.
Kissel, C., Speranza, F., Islami, I. & Hyseni, A. (1995). Earth and Planetary Science Letters 129, 121-134.
Most, T. (2003). Unpubl. Ph.D. thesis, Univ. of Tübingen, 170 p.

Muceku, B., van der Beek, P., Bernet, M., Reiners, P., Masde, G. and Tashko, A. (2008). Terra Nova 20, 180-187.

Schmid, S.M., Bernoulli, D., Fügenschuh, B., Kounov, A., Matenco, L., Oberhänsli, R., Schefer, S., van Hinsbergen, D. & Ustaszewski, K. (2011). AGU Fall Meeting, T43E-2425, San Francisco, California, USA.

273

2

Pfaueninsel

Sacrow

Havel

Jungfernsee

Conference Dinner
Gasthausbrauerei Meierei
Im Neuen Garten 10

Bornim

Bornstedt

Nauener
Vorstadt

Neuer
Garten

**Campus Golm
TSK15**

Volks-
park

Heiliger
See

Klein
Glienicke

1

605

DB **Golm**

Eiche

Jäger
Vorstadt

273

2

Tiefer
See

Park
Babelsberg

605, 606

Golm

606

Potsdam

Ice-Breaker
WIS im Bildungsforum
Am Kanal 47

Park
Sanssouci

605, 606

Babelsberg
Nord

Griebnitz-
see

Kuhfort

Brandenburger
Vorstadt

Zentrum
Ost

1

DB S

Park
Sanssouci

DB

1

DB

Charlottenhof

DB S

1

S

Babelsberg

Babelsberg
Süd

Potsdam-
West

1

Hermanns-
werder

2

**Potsd.
Hauptbhf.**

Teltower
Vorstadt

Medienstadt
DB Babelsberg

Wildpark

2

Am Stern

Templiner
Vorstadt

Schlaatz

AS
Potsdam-
Babelsberg

E51
115

Pirsch-
heide

Templiner
See

DB

Forst
Potsdam

Waldstadt I

Drewitz

Geltow

Pirsch-
heide

2

Waldstadt II

Gewerbegeb.
Potsdam-
Süd

Rehbrücke DB